

**Large Dense Core Vesicle Exocytosis
in Mouse Chromaffin Cells is Regulated
by Munc13s and Baiap3**

Dissertation

zur Erlangung des Doktorgrades

der Mathematisch-Naturwissenschaftlichen Fakultäten

der Georg-August-Universität zu Göttingen

vorgelegt von

Yong Shin

aus Seoul, Korea

Göttingen 2008

D7

Referent: Prof. Dr. Ernst A. Wimmer

Korreferent: Prof. Dr. Ralf Heinrich

Tag der mündlichen Prüfung:

Dedicated to my family

Abbreviation Index

AMBA	Acrylamide/Bis-Acrylamide-solution
Amp	Ampicillin
APS	Ammoniumpersulfate
A.A	Aminoacid
Bp	Basepair
BSA	Bovine Serum Albumin
C-terminal	at the COOH-terminus of a protein
C-Terminus	COOH-terminus of a protein
cDNA	complementary DNA
CNS	Central Nervous System
dH ₂ O	double distilled water
dCTP	Deoxycytosintriphosphate
DEPC	Diethylpyrocarbonate
DMEM	Dulbecco's Modified Eagle Media
DNA	Deoxyribonucleicacid
DNAse	Deoxyribonuclease
dNTP's	Deoxynucleocidtriphosphate
DTT	Dithiothreitol
<i>E. coli</i>	<i>Escherichia coli</i>
ECL	Enhanced chemoluminescence
EDTA	Ethylene diamine tetraacetic acid
EGTA	Ethylene glycol tetraacetic acid
ES	Embryonic stem cell
et al.	et alteres
GFP	Green fluorescence protein
GST	Glutathion S-Transferase
HEPES	(4-(2-hydroxyethyl)-1-piperazineethanesulfonic acid
IPTG	Isopropyl-b-D-thiogalactopyranosid
Kb	Kilobasepair
kDa	Kilodalton
KO	Knockout, Synonymous for the elimination of a gene in the mouse
$M_r \times 10^3$	relatives Molecularweight in kDa
mRNA	messenger RNA
N-terminal	at NH-Terminus a Protein
N-Terminus	NH-Terminus a Protein

OD	Optical density
ON	Overnight
PAGE	Polyacrylamide gel electrophoresis
PBS	Phosphate Buffered Saline
PCR	Polymerase-chain reaction
pH	per Hydrogen
PMSF	Phenyl-Methylsulfonyl-Fluorid
RNA	Ribonucleicacid
RNAse	Ribonuclease
RT	Room Temperature
SDS	Sodiumdodecylsulfate
SNAPs	soluble NSF attachment proteins
SNARE	SNAP-Receptor
TEMED	N,N,N,N-Tetramethylethan-1,2-diamin
TAQ-Polymerase	Thermostable DNA-Polymerase from <i>Thermus aquaticus</i>
TGN	Trans-Golgi-Network
Tris	Tris-hydroxymethyl-aminomethane
UV	Ultraviolet
WT	Wildtype
X-Gal	5-Brom-4-Chlor-3-Indolyl-b-D-Galactopyranosid

Table of Contents

1	Introduction	8
1.1	Secretory Vesicles Exocytosis	8
1.1.1	Synaptic Vesicles (SVs) Exocytosis	9
1.1.2	Large Dense Core Vesicles (LDCVs) Exocytosis	11
1.1.3	The SNARE Core Complex and SNARE-Regulating Proteins	15
1.2	The Mammalian Unc-13 Protein Family	17
1.3	Munc13-4 and Baiap3/Bap3	20
1.4	The Aim of the Present Study: An Analysis of the Role of Munc13 Proteins and Baiap3/Bap3 in LDCV Exocytosis	23
2	Materials and Methods	24
2.1	Knock Out Mice	24
2.1.1	Munc13-1, Munc13-2, and Munc13-3 KO Mice	24
2.1.2	Baiap3/Bap3 KO Mice	26
2.2	In Vivo Assays	28
2.2.1	Cell Cultures and Transfection	28
2.2.1.1	Cell Line Culture and Transfection	28
2.2.1.2	Mouse Chromaffin Cells Culture	30
2.2.2	SFV Preparation and Infection	31
2.2.3	Protein Extraction from Whole Brain and Adrenal Gland	33
2.3	In Vitro Assays	34
2.3.1	Construct Subcloning	34
2.3.1.1	Restriction Enzyme and Purification	34
2.3.1.2	Dephosphorylation and Ligation and DNA sequencing	35
2.3.2	Western Blotting	35
2.3.2.1	SDS gel Electrophoresis of Proteins	35
2.3.2.2	Coomassie Blue Staining	36
2.3.2.3	Blot Transfer of Protein Gels to Membranes	37
2.3.2.4	Immunoblotting with ECL	38
2.3.3	Northern Blotting	40
2.3.3.1	RNA Extraction	40
2.3.3.2	Blotting	40
2.3.4	Expression of GST Fusion Proteins	42

2.3.5	Co-sedimentation Assays	44
2.3.6	Production of Anti-Baiap3 Antisera	45
2.3.7	Antibodies, Chemicals, Kits and Reagents.	47
2.4	Electrophysiological Analysis	50
2.4.1	Whole Cell Capacitance Measurements	50
2.4.2	Flash Photolysis of Caged Ca^{2+} and Measurements of $[\text{Ca}^{2+}]_i$	52
2.4.3	Data Analysis and Statistics	53
3	Results	54
3.1	Analysis of the Role of the Munc13 Protein Family in LDCV Exocytosis	54
3.1.1	Reduced Exocytosis in Chromaffin Cells from Munc13-1 KO Mice	54
3.1.2	Reduced Exocytosis in Chromaffin Cells from Munc13-2 KO Mice	57
3.1.3	Reduced Exocytosis in Chromaffin Cells from Munc13-1/2 DKO Mice	59
3.1.4	Normal Exocytosis in Chromaffin Cells from Munc13-3 KO and Munc13-1/2/3 TKO mice	63
3.1.5	Enhanced Exocytosis in Chromaffin Cells from Baiap3 KO Mice	66
3.1.6	Depolarization Induced LDCV Exocytosis in Chromaffin Cells from Munc13-1/2 DKO and Baiap3 KO Mice	68
3.1.7	Reduced Exocytosis in Chromaffin Cells Overexpressing Baiap3	70
3.2	Functional Characterizations of Baiap3	73
3.2.1	Basic Characterization of Baiap3 KO Mice	73
3.2.2	Baiap3 Binds to Both Munc13-1 and Syntaxin 1	78
4	Discussion	81
4.1	Munc13s are Positive Regulators of LDCV Exocytosis	81
4.2	Baiap3/Bap3 is a Negative Regulator of LDCV Exocytosis	85
4.3	Munc13s and Baiap3 as Regulators of SNARE-Mediated Exocytosis	89
4.4	Conclusions	92
4.5	Future Studies	93
5	References	94
6	Summary	107

1. Introduction

1.1 Secretory Vesicle Exocytosis

Intercellular communication between neurons or neuroendocrine cells is mediated by secretory vesicle exocytosis. Neurotransmitters can be released from two types of vesicles: Synaptic vesicles (SVs), which typically contain classical neurotransmitters such as glutamate or gamma-aminobutyric acid (GABA) and which mediate fast synaptic transmission, and large dense-core vesicles (LDCVs), which typically contain neuropeptides or monoamines and which usually mediate slower modulatory effects. Several characteristic similarities and differences exist between SVs and LDCVs. Both types of vesicles require a Ca^{2+} trigger in order to fuse, and they share many common proteins that are involved in the control and execution of their membrane fusion. On the other hand, the kinetics of their fusion and its physiological regulation are usually different, indicating the existence of distinct molecular mechanisms in SV- and LDCV-mediated secretion (Speese et al., 2007; Zhou et al., 2007). In the present study, I investigated the role of priming proteins of the Munc13 family in the regulation of LDCV-mediated exocytosis. Studies in *C. elegans* had indicated that the nematode Munc13-homologue Unc-13 specifically regulates SV priming while the CAPS homologue Unc-31 mediates the corresponding regulatory effect in LDCV fusion (Speese et al. 2007), although Unc-13 may also be required in LDCV exocytosis under certain physiological conditions (Zhou et al., 2007). Similarly, a series of earlier studies in mammalian systems had led to the conclusion that CAPS proteins are selectively responsible only for LDCV-mediated exocytosis (e.g. Tandon et al., 1998; Rupnik et al., 2000; Sadakata et al., 2004 and 2007; Speese et al., 2007). However, a recent study in CAPS deficient mice clearly showed that CAPS proteins are absolutely essential for

SV-mediated exocytosis (Jockusch et al., 2007), indicating that a restriction of CASPS/Unc-31-dependent regulatory processes to LDCV-mediated secretion may not exist in mammals. The present study was conducted in order to complement these data by analyzing whether Munc13-function in mammals is specific to SVs, as would be indicated by the *C. elegans* data (Speese et al., 2007; Zhou et al., 2007) or whether they play a more general role in the control of both SV and LDCV fusion.

1.1.1 SV Exocytosis

The exocytosis of SVs is part of a complex trafficking cycle consisting of multiple membrane fusion and fission steps and is restricted to so called active zones, where the final steps of vesicle fusion are tightly coordinated in space and time (Wojcik and Brose, 2007; Figure 1).

Transmitters are filled into SVs by dedicated vesicular carriers, whose activity is driven by a proton electrochemical gradient that is generated by a vacuolar-type ATPase. Transmitter-filled SVs in axon terminals dock to the active zone plasma membrane and undergo a biochemical modification called priming. Only these primed and fusion-competent vesicles are able to fuse with the active zone plasma membrane in response to an action potential and the concomitant influx of Ca^{2+} through voltage-gated Ca^{2+} channels. P/Q- and N-type Ca^{2+} channels are thought to be the main mediators of action potential triggered Ca^{2+} influx in presynaptic terminals while R- and I-type Ca^{2+} channels play a modulatory role (Dietrich et al., 2003). Ca^{2+} influx triggers two different components of release: A fast component of release (synchronous, phasic) is rapidly induced in as little as 50 μs after a Ca^{2+} stimulus, and a second slow component (asynchronous, tonic) often continues for more than 1 s after the action potential (Südhof, 1995; Zucker, 1996). After fusion, SV membrane and protein components are

recycled for reuse. The main recycling pathway involves clathrin-mediated endocytosis. Under certain circumstances however, e.g. during phases of high presynaptic activity, SVs appear to be also recycled in part by a faster pathway, which is termed kiss-and-run, and which is thought to involve direct fission of transiently fusing SVs without a full collapse of the SV into the presynaptic membrane. Endocytosed SVs are reused and refilled with neurotransmitter either directly or after passing through an early endosomal compartment (Wojcik and Brose, 2007; Figure 1).

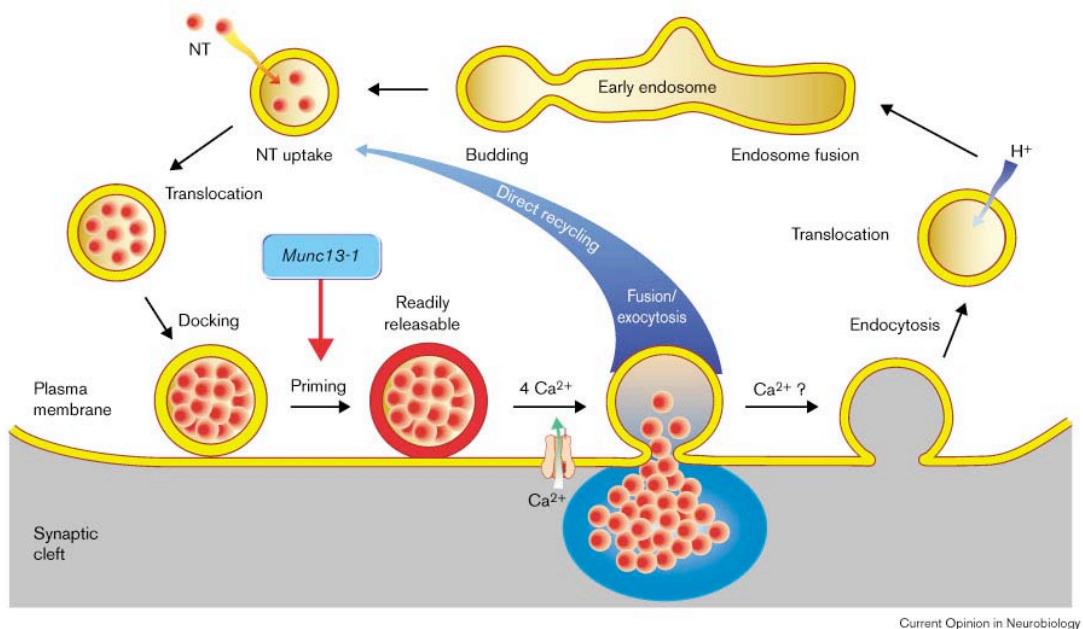


Figure 1. The SV Cycle (image from Brose et al., 2000).

Six large active zone specific proteins - Munc13s, RIMs, Piccolo, Bassoon, ERCs, and α -liprins- are involved in the regulation of active zone function. They engage in multiple protein-protein interactions with each other and thereby form a complex active zone protein network. Munc13s (mammalian Unc-13 proteins) and RIMs (Rab3-interacting molecules) are multidomain proteins that bind to each other and also interact with multiple other presynaptic protein components (Brose et al., 1995; Wang et al., 1997; Wang et al., 2002). Piccolo and Bassoon are very large homologous proteins of

the active zone cytomatrix and thought to act as presynaptic scaffold proteins (Cases-Langhoff et al., 1996; tom Dieck et al., 1998). ERCs (ELKS/Rab3-interacting molecule/CAST) are coiled-coil proteins that bind to RIMs and to RIM-binding proteins (RIMBPs), which are SH2 (Src homology) domain proteins (Wang et al., 2002; Wang et al., 2000). Finally, α -liprins bind to ERCs, RIMs, and several receptor protein tyrosine phosphatases (Ko et al., 2003; Schoch et al., 2002; Serra-Pages et al., 1998).

1.1.2 LDCV Exocytosis

As is the case with SVs, LDCV fusion is triggered by transient rises in the intracellular Ca^{2+} concentration. LDCV fusion has been studied in diverse cell types, including pancreatic exocrine, adrenal chromaffin, and hemopoietic cells, as well as platelets, neutrophils, and mast cells. It appears to share many characteristics and protein components with SV-mediated secretion (Burgoyne and Morgan, 2003; Martin, 1994). Like SV fusion, LDCV fusion is triggered by Ca^{2+} , which typically enters secretory cells after depolarization through voltage-gated Ca^{2+} channels, and executed by SNAREs, which mediate the membrane merger (Figure 2). In addition, several SNARE regulatory proteins such as Munc18 are common to both vesicle systems. On the other hand, the biogenesis of LDCVs and their fate after fusion are different from the corresponding processes governing SV trafficking. Unlike SVs, LDCVs have to be assembled *de novo* at the Golgi apparatus owing to the fact that they need to contain enzymes and secreted peptides/proteins (Kim et al., 2006; Dikeakos and Reudelhuber, 2007). In addition, although involving SNAREs, their cell biological mechanism of fusion (e.g. compound fusion vs. individual vesicle fusion), and their recycling may also be different from SV-related mechanisms (Rutter and Hill, 2006).

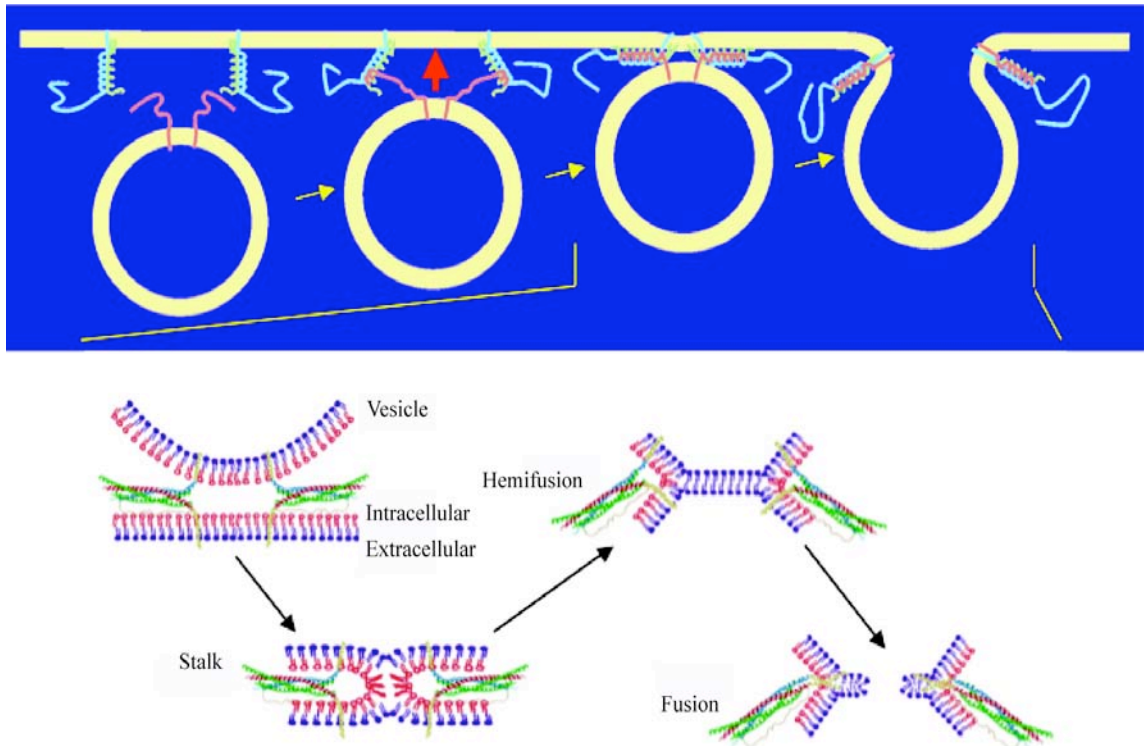


Figure 2. The SNARE Complex.

Vesicular and plasma membrane SNARE proteins assemble into the trimeric SNARE complex. Assembly of this complex is thought to drive the membrane fusion reaction (top), possible via (stalk-like) hemifusion intermediates (bottom). Images are from R. Jahn, Göttingen.

LDCV secretion has been best characterized in adrenal chromaffin cells. These cells are part of the adrenal medulla, which contains three types of chromaffin cells, adranaline- (85 %), noradrenaline- (14-15 %), and dopamine-containing cells (<1 %) (Figure 3). All three types of hormone are synthesized from tyrosine in the adrenal medulla (Trifaro, 2002). A single chromaffin cell contains about 30,000 vesicles or chromaffin granules (Carmichael and Winkler, 1985), which contain a mixture of hormones and neuropeptides.

Due to their spherical shape, chromaffin cells are nicely amenable to electrophysiological recordings of membrane capacitance, membrane characteristics, and ion fluxes. By combining flash-photolysis of caged Ca^{2+} or depolarizing stimuli

with patch-clamp recordings of membrane capacitance and amperometric recordings of released catecholamines, chromaffin cells can be used to study all aspects of LDCV fusion with very high temporal resolution and in highly reliable quantitative terms. This extraordinary experimental accessibility together with the fact that they are derived from the neural crest, i.e. from the same precursors that give rise to sympathetic neurons, have led to the widespread use of chromaffin cells as a model system for the analysis of regulated transmitter release.

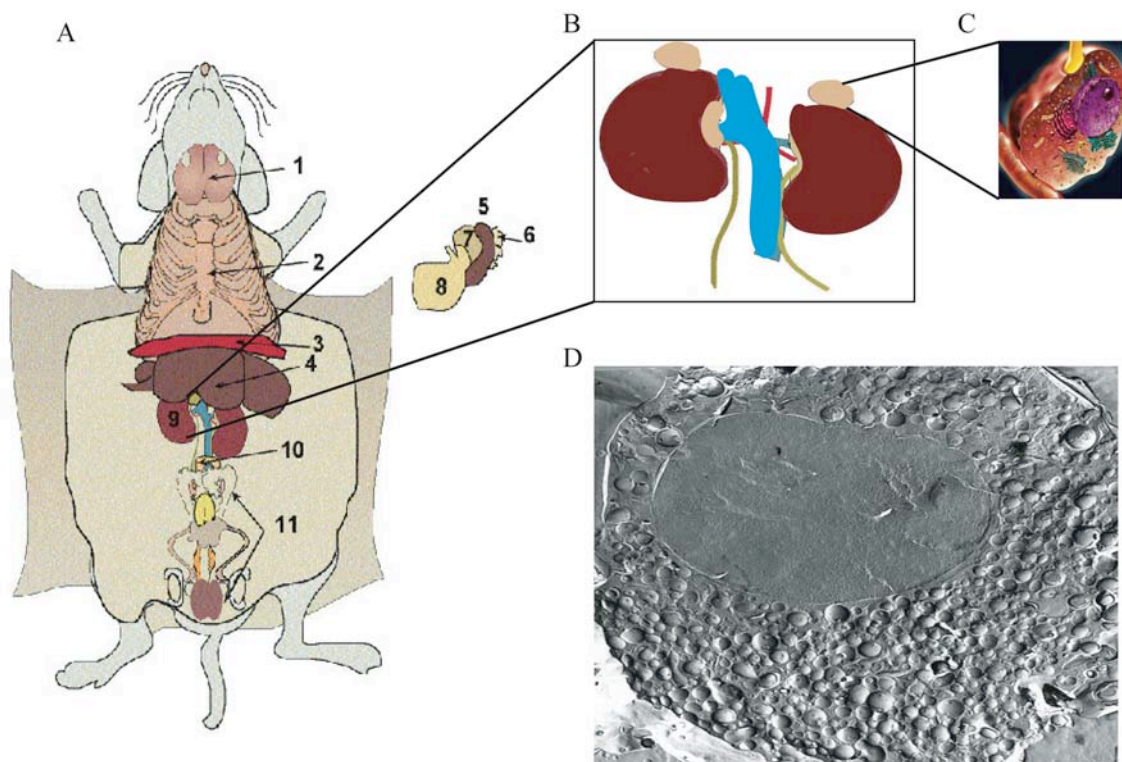


Figure 3. Chromaffin Cells From the Mouse Adrenal Medulla.

(A) Organs in the mouse abdomen (from <http://www3.niaid.nih.gov>). 1. Salivary gland, 2. rib cage, 3. diaphragm, 4. liver, 5. spleen, 6. pancreas, 7. forestomach, 8. glandular stomach, 9. kidney, 10. ascending colon, 11. male urogenital system. (B-C) Adrenal glands lie above both kidneys. (D) Scanning electron micrograph of a chromaffin cell (from <http://webpages.ull.es>).

The LDCVs of adrenal chromaffin cells can be classified functionally into distinct pools. These are distinguished based on their release kinetics, which in turn can be deduced from the shape of the typical membrane capacitance traces measured after

depolarizations or Ca^{2+} release from a previously infused photolabile chelator using UV-flash photolysis (Figure 4). Within the first second after flash photolysis of caged Ca^{2+} , a readily releasable pool (RRP) of vesicles fuses in an exocytotic burst, which consists of a fast and a slow component. The vesicles from the fast burst component of flash photolysis experiments correspond to the RRP released in response to a more physiological depolarization stimulus and fuse with a time constant of about 20-40 ms. Vesicles from the slow burst, which are also referred to as the slowly releasable pool (SRP), fuse with a time constant of about 200 ms (Becherer and Rettig, 2006). These slow burst vesicles are not released by depolarization, but they represent a precursor pool of the fast burst/RRP vesicles (Voets et al., 1999). In addition to these vesicle pools, depolarizing stimuli allow the detection of those vesicles situated closest to Ca^{2+} channels as an immediately releasable vesicle pool (IRP) (Schneggenburger and Neher, 2005). The IRP vesicles are also released during flash photolysis, but due to the global increase in intracellular Ca^{2+} cannot be distinguished as a separate pool.

Unlike SVs, the readily releasable pools of LDCVs in adrenal chromaffin cells are not concentrated at active zones but rather docked and primed at the entire plasma membrane (Allersma et al., 2004; Olofsson et al., 2002; Parsons et al., 1995). Exocytotic delay times and release rates are typically slightly longer in LDCVs than in SVs (Voets et al., 1999 and 2000). The pool of release ready vesicles is refilled from vesicles of the unprimed pool (UPP), which are close to but morphologically detached from the plasma membrane by some 200 nm. The sustained component is the final phase of the capacitance trace after flash photolysis. It is due to docking and priming of vesicles from the UPP and subsequent fusion. Vesicles in the UPP are replenished from a depot pool (DP), which represents the largest pool of LDCVs in adrenal chromaffin cells. The DP is composed of the vesicles that are more than 200 nm away from the plasma membrane (Becherer and Rettig, 2006).

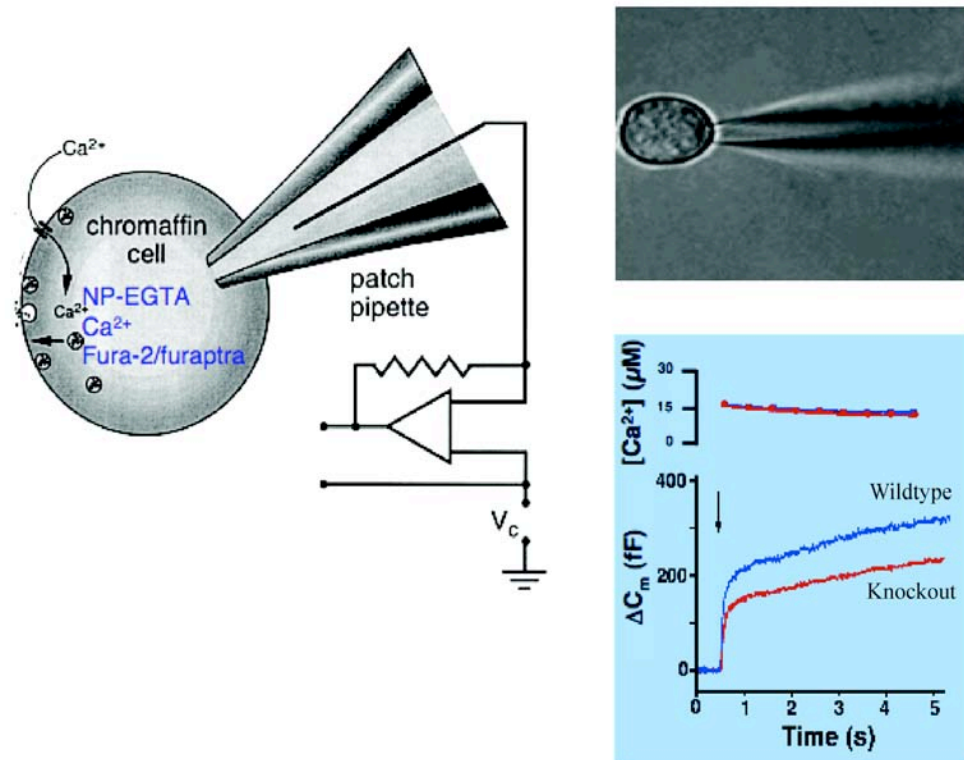


Figure 4. Measuring LDCV Fusion and Exocytosis in Chromaffin Cells.

By UV-flash photolysis of the photolabile Ca^{2+} chelator NP-EGTA- Ca^{2+} in the cell, the intracellular Ca^{2+} concentration can be increased in a step-wise fashion to 15-20 μM (bottom right panel, top trace). Fusion of LDCVs can be measured by a patch-clamp electrode as an increase in the cell membrane capacitance (bottom right panel, bottom trace). Images are modified from J. Rettig and J. Sørensen, Göttingen.

1.1.3 The SNARE Core Complex and SNARE-Regulating Proteins

SNAREs (soluble N-ethylmaleimide sensitive factor attachment protein receptors) are localized to the various intracellular organelles. They comprise a family of mostly membrane-tethered proteins containing a coiled-coil SNARE motif, and they regulate fusion reactions and target specificity in vesicle trafficking. Based on their localization, SNAREs can be classified into vesicle associated v-SNAREs and target-membrane-associated t-SNAREs. The SNARE motifs are homologous 70-amino acid sequences that can be segregated into four distinct classes, R-, Qa-, Qb-, and Qc-SNARE motifs. Four such motifs, typically one of each type, form a stable *trans* SNARE complex, a

four helical bundle that drives the fusion of the resident membranes. Fusion of SVs is mediated by three SNARE core complex component proteins: Syntaxin and SNAP-25 (synaptosome-associated protein of 25 kDa) on the presynaptic plasma membrane, and Synaptobrevin (also called vesicle-associated membrane protein; VAMP) on the vesicle membrane (Söllner et al., 1993). The core of this complex is formed by the R-SNARE motif of Synaptobrevin, the Qa-SNARE motif of Syntaxin 1, and the Qb- and Qc-motifs of SNAP-25. Their association drives the fusion of the SV membrane with the active zone plasma membrane (Figure 2). After fusion, the trimeric complex binds to a complex of the ATPase N-ethylmaleimide-sensitive factor (NSF) and soluble NSF attachment proteins (SNAPs), which disassemble the SNARE complex and make the individual components available for subsequent reuse (Hayashi et al., 1995).

SNARE complexes are essential for fusion of SVs and LDCVs - genetic ablation of synaptic SNAREs in *Drosophila*, *C. elegans*, and *M. Musculus* abolishes evoked neurotransmission (Nonet et al., 1998; Schoch et al., 2001; Schulze et al., 1995; Washbourne et al., 2002). Several proteins are critically involved in the control of SNARE core complex assembly and function. (i) SNARE complex formation is controlled by proteins of the Sec1/Munc18-like (SM) family (Jahn et al., 2003). SM proteins bind to Syntaxin-like SNAREs. Munc18-1, a key SM protein of mammalian that controls synaptic fusion, interacts with a conformation of Syntaxin that is closed and prevented from SNARE complex formation. In addition, Munc18 can bind the Syntaxin N-terminus. One role of Munc18 in neurotransmitter release from SVs and in LDCVs is that of a docking factor that acts prior to SNARE complex assembly. The number of membrane-proximal LDCVs is reduced in chromaffin cells of Munc18-1 deletion mutant mice (Voets et al., 2001). Likewise, docking of SVs at the *C. elegans* neuromuscular junction is impaired in mutants lacking the Munc18-1 orthologue Unc-18 (Weimer et al., 2003). On the other hand, docking of SVs is not altered in

mammalian Munc18-1 deficient central synapses, although these synapses do not release neurotransmitter (Verhage et al., 2000). (ii) Munc13 and CAPS proteins are essential for SV priming (Varoqueaux et al., 2002; Jockusch et al., 2007). Their role will be discussed in further detail below. (iii) The function of Munc13s is counteracted by Tomosyn, which can act as a scavenger of SNAREs, thus limiting SNARE complex assembly (Wojcik and Brose, 2007). (iv) Complexins bind to the assembled SNARE complex and maintain it in a highly fusogenic state (Brose, 2008). (v) Synaptotagmins act as the Ca^{2+} sensors of regulated SV and LDCV secretion (Südhof, 2004). Synaptotagmins form a large family of proteins (Craxton, 2004), which contain an N-terminal transmembrane domain, followed by a linker region and two C-terminal C2 domains that are referred to as C2A and C2B. Synaptotagmin 1 is the family member best characterized. Its C2A and C2B domains bind Ca^{2+} and interact with phospholipid membranes in a Ca^{2+} -dependent manner (Bai et al., 2004; Bai and Chapman, 2004; Brose et al., 1992). Synaptotagmin 1 likely acts as a Ca^{2+} -sensor and trigger of fusion by simultaneously binding in a Ca^{2+} -dependent manner to the assembled SNARE complex and the phospholipids of the fusing membranes (Chapman et al., 1995; Kee and Scheller, 1996; Li et al., 1995; Rickman et al., 2003; Wojcik and Brose, 2007), at the same time displacing Complexin from the complex.

1.2 The Mammalian Unc-13 Protein Family

Munc13 proteins are homologues of *C. elegans* Unc-13, which was initially identified as the product of a gene whose mutation causes uncoordinated movements and reduced transmitter release (Brenner, 1974; Hosono and Kamiya, 1991; Brose et al., 1995). Mammals express three closely related Unc-13 homologues, Munc13-1, -2, -3. (Brose et

al., 1995) and a distantly related variant called Munc13-4 (Koch et al., 2000) (Figure 5). Munc13-1, -2, and -3 are mainly expressed in neurons. In mice and rats, Munc13 expression starts around birth and increases to reach plateau at postnatal days 20-30, when synapse formation is largely complete. Munc13s 1-3 are localized to presynaptic active zones, while Munc13-4 is present mainly in lung and lymphocytes.

Munc13s 1-3 have a complex domain structure with divergent N-termini and conserved C-terminal regions, which contain a C1 domain that binds diacylglycerol and phorbol esters, two C2 domains one of which (C2B) binds Ca^{2+} (Dai et al., 2005; Guan et al., 2008; Lu et al., 2006; Rizo and Rosenmund, 2008), and two Munc13-homology domains that are important for protein function (Stevens et al., 2005; Basu et al., 2005).



Figure 5. Domain Structure of Munc13s and Baiap3.

Munc13s contain a C1 domain, two or three C2 domains and two Munc13-homology domains (MHDs). Baiap3 also contains two C2 domains and two MHDs, but lacks the variable N-terminal region found in Munc13-1, -2, and -3. Based on its sequence, Baiap3 is most similar to Munc13-4.

Munc13-1 is expressed in almost all neurons of the CNS, Munc13-2 is mainly expressed in cortex and hippocampus, and Munc13-3 is mainly found in cerebellum and brainstem (Augustin et al., 1999a). One splice variant of Munc13-2, b-Munc13-2, is brain specific, while a second one, ubMunc13-2, is also found in other tissues (Betz et al., 2001).

Loss of Munc13-1 in mutant mice does not affect synapse, neuron, or brain morphology but causes an almost complete block (90 %) of SV priming in hippocampal glutamatergic neurons and a concomitant almost complete arrest of SV fusion in these cells, while GABAergic neurons are not affected by Munc13-1 deletion (Augustin et al., 1999b). The remaining release in glutamatergic and GABAergic cells of Munc13-1 deficient mice is due to the presence of Munc13-2 and totally eliminated upon the additional deletion of Munc13-2 (Varoqueaux et al., 2002). Similarly, evoked release at cholinergic neuromuscular synapses is almost shut down upon deletion of all three Munc13 genes in mice (Varoqueaux et al., 2005), as is GABAergic and cholinergic transmission at the neuromuscular synapse of *unc-13* null-mutant *C. elegans* (Richmond et al., 1999). Loss of the *Drosophila* homologue Dunc-13 completely abolishes synaptic transmission at the fly glutamatergic neuromuscular junction (Aravamudan et al., 1999).

Munc13s are thought to mediate vesicle priming by binding to the N-terminus of Syntaxin, thereby keeping it in its open conformation which is able to enter SNARE complex formation (Betz et al., 1997; Brose et al., 2000; Richmond et al., 2001). Munc13s are regulated by diacylglycerol through their C1 domains (Betz et al., 1998; Rhee et al., 2002) and by Calmodulin (Junge et al., 2004), and the presynaptic targeting of Munc13-1 and ubMunc13-2 is controlled by the interactions of their respective N-termini with RIM (Betz et al., 2001; Andrews-Zwilling et al., 2006). As mentioned above, the MHDs of Munc13s and their flanking sequences are essential for the Munc13-mediated priming function (Stevens et al., 2005; Basu et al., 2005). The

corresponding minimal priming region, called MUN domain, domain binds to membrane-anchored SNARE complexes and to Syntaxin 1-SNAP-25 heterodimers (Guan et al., 2008).

The role of Munc13 proteins in LDCV secretion is less well understood. Overexpression of Munc13-1 in mouse chromaffin cells leads to an increase in secretion as compared with wild type cells. More specifically, the size of the exocytotic burst is increased 3-4 fold, and the sustained component of release is strongly augmented upon Munc13-1 overexpression. Importantly, the overexpression of Munc13-1 does not affect the rate constants of fusion from releasable pools, indicating that Munc13-1 can drive priming of chromaffin secretory granules from a docked to a fusion competent state, which is apparently rate limiting in adrenal chromaffin cells (Ashery et al., 2000). This gain-of-function effect of Munc13-1 overexpression in chromaffin cells requires the two MHDs with the flanking C2C domain and its ability to bind Syntaxin (Stevens et al., 2005). Munc13 deletion mutant chromaffin cells have not been studied so far. However, in *C. elegans*, Unc-13 does not appear to be necessary for LDCV secretion. Rather, a distant relative of Munc13s, Unc-31/CAPS is necessary for LDCV secretion in *C. elegans* (Speese et al., 2007; Zhou et al., 2007).

1.3 Munc13-4 and Baiap3/Bap3

Munc13-4 was identified as a distant Munc13 homologue in protein profile searches for proteins with MHDs (Koch et al., 2000). Together with Baiap3/Bap3, which was identified in the same profile search, it forms a subfamily of Munc13-like molecules, in which the typical Munc13-like domain structure is conserved (Figure 5). Munc13-4 is mainly expressed in lung where it is localized to goblet cells of the bronchial epithelium

and to alveolar type II cells, which are both cell types with a secretory function, and in lymphocytes (Koch et al., 2000).

Loss-of-function mutations in the human Munc13-4 gene cause familial hemophagocytic lymphohistiocytosis type 3 (FHL3). At the functional level, these mutations appear to cause defective cytolytic granule exocytosis. Further analyses showed that human Munc13-4 is involved in a late step of the cytolytic granule exocytosis pathway, downstream of Rab27a (Feldman et al., 2003). Indeed, Munc13-4 binds directly to Rab27a, whose mutation causes Griscelli Syndrome type 2 (GS2), a genetic disorder involving life-threatening defects of cytotoxic T lymphocytes.

Munc13-4 and Rab27a are highly expressed in cytotoxic T lymphocytes and mast cells, where they colocalize at secretory lysosomes. Overexpression of Munc13-4 enhances degranulation of secretory lysosomes in mast cells, which indicates that it has a positive regulatory role in secretory lysosome fusion (Neeft et al., 2005). Thus, Munc13-4 appears to be essential for the priming of cytolytic granules, much like Munc13s 1-3 mediate priming of SVs.

Baiap3/Bap3 (Brain-specific Angiogenesis Inhibitor 1-Associated Protein 3) is 34% identical to Munc13-4 (Koch et al., 2000). Baiap3/Bap3 was first identified as an interactor of the cytoplasmic region of BAI 1 (Brain-specific Angiogenesis Inhibitor 1), which is the product of a p53 target-gene, which encodes a seven span transmembrane protein, and which is specifically expressed in brain (Shiratsuchi et al., 1998).

The function of Baiap3/Bap3 is currently unknown. It is expressed predominantly in hypothalamus, amygdala, periaqueductal grey, septum and several brainstem nuclei. Analyses of deletion mutant fragments of Baiap3 showed that the interaction between Baiap3/Bap3 and BAI1 is dependent on the MHDs of Baiap3/Bap3 but not on the flanking C2 domains (Shiratsuchi et al., 1998). Interestingly, the Baiap3/Bap3 interactor BAI1 is distantly related to the Ca^{2+} -independent receptor for α -latrotoxin, CIRL)

which regulates synaptic neurotransmitter release (Krasnoperov et al., 1997; Lelianova et al., 1997).

So far, Baiap3/Bap3 has mostly been studied in the context of cancer development. The Baiap3/Bap3 promoter specifically binds the transcription factor EWS (Ewing's sarcoma)-WT1 (Wilms' tumor suppressor 1), which can transactivate a number of genes implicated in cellular differentiation. Baiap3/Bap3 is expressed in secretory syncytiotrophoblast cells of the placenta and in epithelial cells of the breast and prostate, and it is colocalized with a secreted growth factor within cytoplasmic organelles. Ectopic expression of Baiap3/Bap3 in tumor cells dramatically enhances growth in low serum and colony formation in soft agar assays. Interestingly, the Baiap3/Bap3 gene encodes a transcriptional target of an oncogenic fusion protein and regulates the exocytotic pathway in cancer cell proliferation (Palmer et al., 2002). In summary, the role of Baiap3 may be rate limiting for selected steps in the secretory pathway of specific cell types (Chan and Weber, 2002). However, the exact role of Baiap3/Bap3 in the control of SV or LDCV secretion and its relationship with other members of the Munc13 protein family are unknown.

1.4 The Aim of the Present Study: An Analysis of the Role of Munc13 Proteins and Baiap3/Bap3 in LDCV Exocytosis

The present study was performed with the aim to examine the role of Munc13 proteins and their relative Baiap3 in LDCV exocytosis. More specifically, my plan was to study LDCV secretion in mouse chromaffin cells in order to address the following two questions:

1. Do Munc13s regulate LDCV priming? Studies in *C. elegans* indicated that the nematode Munc13-homologue Unc-13 specifically regulates SV priming while the CAPS homologue Unc-31 mediates the corresponding priming effect in LDCV fusion (Zhou et al., 2007). These findings supported earlier studies in mammalian systems, which led to the conclusion that CAPS proteins are selectively responsible only for LDCV-mediated exocytosis (e.g. Tandon et al., 1998; Rupnik et al., 2000; Sadakata et al., 2004 and 2007; Speese et al., 2007). However, a recent study in CAPS deficient mice clearly showed that CAPS proteins are absolutely essential for SV-mediated exocytosis (Jockusch et al., 2007), indicating that a restriction of CASPS/Unc-31-dependent regulatory processes to LDCV-mediated secretion may not exist in mammals. In order to complement these findings, my first aim was to test systematically whether in mammals the SV priming proteins Munc13-1, 2, and -3 are also important for LDCV priming.

2. Does Baiap3/Bap3 play a Munc13-related role in LDCV priming? Baiap3/Bap3 is a distant Munc13 homologue of unknown function. In view of its homology with Munc13s and the published literature indicating that Munc13s may not be involved in LDCV secretion, I set out to examine whether Baiap3/Bap3, instead of Munc13s, controls LDCV priming in chromaffin cells.

2. Materials and Methods

2.1 Knock Out Mice

2.1.1 Munc13-1, Munc13-2 and Munc13-3 KO Mice

The Munc13-1, Munc13-2 and Munc13-3 deficient mice used in this study have been described previously (Augustin et al., 1999b; Varoqueaux et al., 2002; Augustin et al., 2001). Chromaffin cells used in this study were cultured from pups on postnatal day 0 (P0) if the mice were deficient for only one Munc13 isoform, whereas in the case of double and triple Munc13-1, -2 and -3 KO mice, cells were cultured on embryonic day 18 (E18). For each experiment WT or heterozygous littermates were used as controls.

PCR Genotyping for Munc13-1

Primer 1 (#544): 5'-CTTACCCATCTGAGAGCCGGAATTCCA-3'

Primer 2 (#5216): 5'-CTCCGAGGGGAATGCGCTTCCGTTTCCTG-3'

Primer 3 (#428): 5'-GAGCGCGCGCGGCGGAGTTGTTGAC-3'

Munc13-1 WT allele; 250 bp and Munc13-1 KO allele; 230 bp

#: Primer number as designated by the AGCT DNA Core Facility, Max Planck Institute for Experimental Medicine, Germany.

Reaction Mixture		PCR Program	
10X Buffer	2 μ l	94 °C for 3 min	— 1 cycle
dNTPs	1 μ l	94 °C for 30 sec] 30 cycles
Primer 1	2 μ l	60 °C for 30 sec	
Primer 2	1 μ l	72 °C for 1 min	
Primer 3	1 μ l	72 °C for 10 min	— 1 cycle
Red Taq	1 μ l	10 °C for forever	— 1 cycle
dH ₂ O	11 μ l		
Total	19 μ l		
Template DNA	1 μ l		

PCR Genotyping for Munc13-2

Primer 4 (#1125): 5'-TCTCCACTGCCCCCTTTTACTGT-3'

Primer 5 (#1124): 5'-TCAAGGGACTGTTCTAGCAATGTT-3'

Primer 6 (#428): 5'-GAGCGCGCGCGGCGGAGTTGTTGAC-3'

Munc13-2 WT allele; 322 bp and Munc13-2 KO allele; 349 bp

Reaction Mixture		PCR Program	
10X Buffer	2 μ l	94 °C for 3 min	— 1 cycle
dNTPs	1 μ l	94 °C for 30 sec] 30 cycles
Primer 4	2 μ l	60 °C for 30 sec	
Primer 5	1 μ l	72 °C for 1 min	
Primer 6	1 μ l	72 °C for 10 min	— 1 cycle
Red Taq	1 μ l	10 °C for forever	— 1 cycle
dH ₂ O	11 μ l		
Total	19 μ l		
Template DANN	1 μ l		

PCR Genotyping for Munc13-3

Primer 7 (#776): 5'-GGCTAGGAAGCAGGTAGTGATGGCTG-3'

Primer 8 (#775): 5'-GCTTAACTGGAACTCACTGGATGTCAGAG-3'

Primer 9 (#495): 5'-GACGAGTTCTTCTGAGGGGATCGGC-3'

Primer 10 (#494): 5'-TACATTAGAGATGATAATTATCACACCCCAAAG-3'

Munc13-3 WT allele; 395 bp, and Munc13-3 KO allele; 410 bp

Reaction Mixture		PCR Program	
10X Buffer	2 μ l	94 °C for 3 min	— 1 cycle
dNTPs	1 μ l	94 °C for 30 sec] 30 cycles
Primer 7	2 μ l	60 °C for 30 sec	
Primer 8	1 μ l	72 °C for 1min	
Primer 9	1 μ l	72 °C for 10 min	— 1 cycle
Primer 10	1 μ l	10 °C for forever	— 1 cycle
Red Taq	1 μ l		
dH ₂ O	11 μ l		
Total	19 μ l		
Template DNA	1 μ l		

2.1.2 *Baiap3/Bap3* KO Mice

Baiap3 deficient mice were generated by Dr. Iris Augustin by homologous recombination in embryonic stem cells. Briefly, genomic sequences of *Baiap3* were subcloned into the pTK-Neo vector. In the targeting vector a 500 bp genomic fragment containing exon 1-3 was replaced by a neomycin resistance gene. The vector also contained two copies of the herpes simplex virus thymidine kinase for negative selection. Recombinant stem cell clones were identified by Southern blotting. Two positive clones were injected into mouse blastocytes to obtain highly chimeric mice that transmitted the

mutant gene through the germ line. Germ line transmission of the mutant gene was confirmed by southern blotting. Subsequent routine genotyping was performed by PCR. Western blot analyses of adult mouse brain homogenates with a Baiap3 specific antiserum directed against the N-terminus (a.a 9-181) or C-terminus (a.a 330-1150) of Baiap3, demonstrated the total absence of Baiap3 in homozygous mutant brain. Chromaffin cells from Baiap3 KO mice were cultured from P0 pups and WT littermates were used as controls.

PCR Genotyping for Baiap3

Primer 11 (#2862): 5'- CCAGAAATCCGCAGGCAGTCGTCA-3'

Primer 12 (#2863): 5'- CAAGGCAACCACCAGCCGCATCTA-3'

Primer 13 (#2935): 5'- GAACACGGCGGCATCAGAGCAG-3'

Baiap3 WT allele; 546 bp and Baiap3 KO allele; 636 bp

Reaction Mixture		PCR Program	
10X Buffer	2 µl	94 °C for 1 min	— 1 cycle
dNTPs	1 µl	94 °C for 1 sec] 33 cycles
Primer 11	2 µl	60 °C for 30 sec	
Primer 12	1 µl	72 °C for 30 sec	
Primer 13	1 µl	72 °C for 10 min	— 1 cycle
Red Taq	1 µl	10 °C for forever	— 1 cycle
dH ₂ O	11 µl		
Total	19 µl		
Template DNA	1 µl		

2.2 In Vivo Assays

2.2.1 Cell Culture and Transfection

2.2.1.1 Cell Line Culture and Transfection

The HEK (Human Embryonic Kidney) 293FT cell line, an epithelial line derived from human embryonic kidney cells transformed with the large T-antigen, was used for both in vivo and in vitro binding assays. The cell line was maintained in plastic tissue culture dishes with high-glucose Dulbecco's Modified Eagle's Medium (DMEM) supplemented with 10 % fetal calf serum (FCS) in a 37 °C humid incubator with 5 % ambient CO₂. The selection agent G418 (Geneticin) was added to complete DMEM medium of HEK293FT cells at a concentration of 500 µg/ml. Passaging was performed using standard procedures of trypsin mediated dislodgment of confluent cultures.

1. For thawing cells, pre-warm the complete DMEM medium without G418
2. Frozen vial from Liquid Nitrogen Tank, thaw the vial by gently shaking in a 37°C water-bath
3. Transfer the cells into 10 ml pre-warmed complete DMEM medium without Geneticin in a 50 ml falcon tube and mix slowly
4. Centrifuge for 3 min at 800 rpm
5. Carefully discard supernatant
6. Wash the pellet with PBS and centrifuge a second time
7. Resuspend the cells in 10ml of pre-warmed medium
8. Transfer the suspended cells into T75 flask and incubate at 37 °C

9. One day before cells reach 90 % confluency, discard the medium from the T75 flask
10. Add 5 ml 0.05 % Trypsin and incubate for 5 min at 37°C
11. Add 10 ml complete DMEM medium and triturate cells thoroughly
12. Centrifuge for 3 min at 800 rpm
13. Carefully discard supernatant
14. Wash the pellet with PBS and centrifuge again
15. Resuspend cells in 10 ml of pre-warmed medium
16. Transfer suspended cells into 3 X T75 flask and incubate at 37 °C

Transfections were performed using Lipofectamine 2000 by following standard procedures.

1. For transfection of HEK293FT cells with either pMYC-Baiap3 full-length or pCDNA3-Munc13-1 full-length constructs, plate $6-7 \times 10^5$ cells in 15 ml of complete DMEM medium (for 15 cm dish format). Cells will be 85-90 % confluent at the time of transfection
2. For transfection samples, dilute 30 µg of DNA (each construct) in 1.5 ml of Opti-MEM I without serum and gently mix.
3. Mix Lipofectamine 2000 gently before use, dilute 60 µl of Lipofectamine 2000 in 1.5 ml Opti-MEM I and incubate for 5min at RT
4. Combine the diluted DNA with the diluted Lipofectamine 2000. Mix gently and incubate for 20 min at RT
5. Add the DNA-Lipofectamine complexes to each dish
6. Incubate the cells at 37 °C in a CO₂ incubator for 30 hr prior to testing for co-sedimentation

Complete DMEM medium:	DMEM
	10 % FCS
	0.1 mM Non-Essential Amino Acids
	2 mM L-glutamine
	500 µg/ml G418
	1 % Penicillin/Streptomycin

2.2.1.2 Mouse Chromaffin Cells Culture

Embryonic (E18) and/or postnatal (P0) adrenal glands were dissected and chromaffin cells prepared by digestion with Papain solution. The adrenal glands were incubated with 400 µl papain solution at 37 °C for 30 min in Eppendorf Thermocycler (500 rpm), followed by addition of 400 µl stop solution and incubation for 15 min. The solution was then replaced by 500 µl complete NBA (Neurobasal-A) medium. The adrenal glands were gently opened before digestion, and triturated gently through a 10 µl pipette tip. The entire cell suspension obtained from two glands (one animal) was plated on a sterile coverslip in a 6-well plate. The cells were incubated at 37 °C and 5 % CO₂ and used within 2 days after plating.

Complete NBA medium:	500 ml NBA medium
	10 ml B27
	5 ml Glutamax
	1 ml Penicillin/Streptomycin
Papain Solution:	250 ml DMEM medium
	50 mg L-Cystein
	2.5 ml 0.1M CaCl ₂
	2.5 ml 50mM EDTA
	20 units/ml papain
Stop Solution:	225 ml DMEM medium
	25 ml heat inactivated FCS
	625 mg Albumin
	625 mg Trypsin inhibitor

2.2.2 SFV Preparation and Infection

SFV1 constructs expressing a Munc13-1-EGFP fusion protein have been described previously (Ashery et al., 2000). A Baiap3-IRES-EGFP construct was sub-cloned blunt-ended into the SmaI site of the pSFV1 polylinker. Following linearization with SpeI, cDNAs of pSFV-Baiap3-IRES-EGFP, pSFV-Munc13-1-EGFP, and pSFV-helper1 were transcribed in vitro with SP6 RNA polymerase. BHK21 cells, derived from hamster kidney, were then transfected by electroporation (400 V, 975 μ F) with a combination of 10 μ g of each constructs and incubated at 37 °C, 5 % CO₂ for 24 hr. Following this incubation, the supernatant was collected and clarified from cell debris by low speed centrifugation. The supernatant containing the inactivated virus was snap-frozen in 450 μ l aliquots and stored at -80 °C. To test the virus titer, an aliquot was thawed and activated. BHK21 cells were then infected with various dilutions of the activated virus, and the infection efficiency was determined by assessing EGFP fluorescence. Four hundred and fifty microliters of frozen virus were thawed and diluted 1:1 with opti-MEM medium with 2.5 % FCS. To activate the virus, 110 μ l Chymotrypsin was added and incubated for 35 min at RT. In order to inactivate the chymotrypsin, 110 μ l Aprotinin was added, incubation continued for an additional 5 min at RT. Infection was performed on cultured cells 24 hr after preparation according to published protocols (Ashery et al., 1999).

To generate viral RNA for electroporation of BHK21 cells:

1. Linearize DNA with SpeI enzyme
2. Linearized DNA purification using phenol-chloroform extraction
3. Precipitate DNA using 3M sodium acetate after purification
4. In vitro transcription using SP6 transcription Kit

5. RNA purification using phenol-chloroform extraction
6. Precipitate RNA using 3M sodium acetate after purification
7. Check RNA on formaldehyde-agarose gel
8. Quantification of RNA concentration
9. Transfection with BHK21 cells using electroporation
10. Culture BHK21 cells for 2 days and then harvest the inactive virus
11. Make 450 µl aliquots into cryotubes and freeze in liquid nitrogen
12. Store at -80 °C until use

To activate the SFV:

1. Take one 450 µl virus aliquot and thaw
2. Add 450 µl BHK21 cell medium
3. Add 110 µl Chymotrypsin and mix and incubate for 35 min at RT
4. Add 110 µl Aprotinin and mix and incubate for 5 min at RT
5. Store at 4 °C

DEPC-treated distilled water :	0.1 % DEPC (under hood) in dH ₂ O Stir for 2hr under hood and autoclave
5X MOPS Buffer:	0.1 M MOPS 40 mM sodium-acetate 5 mM EDTA (pH 8.0)
3M Sodium Acetate:	20.4 g of Sodium acetate trihydrate Adjust to pH 5.8
RNA gel loading buffer :	1X MOPS 6.5 % Formaldehyde 50 % Formamide 5 % Glycerin 0.1 mM EDTA 0.025 % Bromophenol Blue

BHK Cell Medium :	500 ml DMEM medium
(for growth)	12.5 % FCS
	1 ml Penicillin/Streptomycin
BHK Cell Medium :	500 ml NBA medium
(for electroporation)	10 ml B27
	1 ml Penicillin/Streptomycin
	1 ml Glutamax
Chymotrypsin:	2 mg/ml
Aprotinin:	6 mg/ml

2.2.3 Protein Extraction from Whole Brain and Adrenal Gland

Both whole brain and adrenal gland were taken from WT and Baiap3 KO mice and homogenized with a Glass-Teflon-Homogenizer in 4 °C in Lysis buffer. Total protein concentration was determined by a BCA protein assay and adjusted to 1-2 mg/ml in Sample Buffer (1x Laemmli Buffer). Prepare the samples for loading by heating them to 100 °C for 5 min in Sample Buffer to denature the proteins.

Lysis Buffer:	320 mM Sucrose
	150 mM NaCl
	1 mM EGTA (pH 8.0)
	0.2 mM PMSF
	1 µg/ml Aprotinin
	1 µg/ml Leupeptin
3X Sample Buffer:	10 % SDS
	140 mM Tris/HCl (pH 6.8)
	3 mM EDTA
	30 % Glycerol
	0.1 % Bromophenol Blue
	150 mM DTT before use

2.3 In Vitro Assays

2.3.1 Construct Subcloning

2.3.1.1 Restriction Enzyme and Purification

For the construction of some constructs the gene of interest was amplified by PCR and subsequently digested with the appropriate restriction enzymes. Digested DNA fragments were purified by using phenol-chloroform extraction before subcloning using the following procedures:

1. Amplify DNA and digest with the appropriate restriction enzymes
2. To purify of the DNA, add 200 μ l Phenol-chloroform-isoamylalcohol (25:24:1) (pH 7.5-8 for DNA; pH 4-6 for RNA). Mix by pipetting up and down
3. Add 200 μ l Chloroform and vortex thoroughly
4. Centrifuge at 15000 rpm for 5 min (DNA is in upper phase)
5. Transfer the supernatant into new eppendorf tube
6. Add 200 μ l chloroform and mix with vortexer
7. Centrifuge at 15000 rpm for 2 min
8. Transfer the supernatant into new eppendorf tube
9. Add 1/10 volume of 3M Ammonium-acetate
10. Add 2.5 volume of 100 % cooled EtOH and mix
11. Incubate at -20 °C for ON
12. Centrifuge at 15000 rpm for 30 min
13. Wash the pellet with -70 % cooled EtOH
14. Centrifuge at 15000 rpm for 10 min

15. Carefully remove supernatant and dry the pellet
16. Add 50 μ l dH₂O to resuspend and quantify

2.3.1.2 Dephosphorylation, Ligation and DNA-sequencing

Prior to ligation of insert DNA and vector DNA, the 5' ends of the vector were dephosphorylated by Shrimp Alkaline Phosphatase. Ligation was performed using T4 DNA ligase. After transformation, plasmid DNA was prepared from cultures grown from colonies, analyzed by restriction digests and plasmid DNA from selected clones was sequenced by the Applied Biosystems 373 DNA sequencer by the DNA core facility.

1. For dephosphorylation, add 2.5 μ l dephosphorylation buffer and 2 μ l phosphatase in 20.5 μ l purified DNA
2. Incubate for 10 min (for sticky ended) or 1 hr (for blunt ended) at 37 °C
3. Inactivate the Shrimp Alkaline Phosphatase for 15 min at 65 °C
4. For the ligation reaction, a 1:5 to 3:8 (vector: insert) ratio is usually used and ligations are placed in 4 °C water-bath that warms up to 15°C ON
5. Transformation into *E.coli*

2.3.2 Western Blotting

2.3.2.1 SDS gel Electrophoresis of Proteins

In order to investigate subunit compositions and to verify homogeneity of protein samples, electrophoresis is used to separate complex mixtures of proteins. Proteins

migrate in response to an electrical field through pores in the gel matrix. The combination of gel pore size and protein size and charge determines the migration rate of the proteins. SDS-PAGE is an anionic system due to the negatively charged SDS.

1. Pour gel of appropriate polyacrylamide concentration, depending on molecular weight of the protein of interest
2. Mount the gel in the electrophoresis apparatus and fill with running buffer (1X RB)
3. Load the prepared samples into the wells
4. Attach the electrophoresis apparatus to an electric power supply. Apply a current of 25 mA and 50 mA for one and two gels, respectively
5. After running the gel, place the polyacrylamide gel in a plastic container for either coomassie staining or blot transfer to membranes

Stacking gel:	1 M Tris-HCl (pH 6.8)	Separating gels
Separating gel:	1.5 M Tris-HCl (pH 8.8)	7.5 % gel: > 100 kDa
Acrylamide/Bisacrylamide:	30 % Acrylamide/Bis (37.5:1)	10 % gel: 60~130 kDa
SDS:	10 % Stock solution	13 % gel: 20~80 kDa
APS	10 % Stock solution	15 % gel: < 50 kDa
TEMED:	Solution from SERVA	
10X RB:	250 mM Tris	
	2.5 M Glycine (pH 8.3)	
	1 % SDA	

2.3.2.2 Coomassie Blue Staining

An easy and rapid detection method for proteins in gel is to perform a coomassie blue staining of the polyacrylamide gel. It is based on nonspecific binding of the dye coomassie brilliant blue R250 to proteins. The detection limit is 0.3 to 1 µg/protein band.

1. Place the polyacrylamide gel in a plastic container and cover it with 5 volumes of Coomassie staining solution A.
2. Incubate for 1 min at 100 °C using Microwave
3. Remove solution A and add Coomassie staining solution B. Incubate for 1 min at 100 °C using Microwave
4. Remove solution B and add Coomassie staining solution C. Incubate for 1 min at 100 °C using Microwave
5. Remove solution C and add Coomassie staining solution D. Incubate for 1 min at 100 °C using Microwave
6. Pour out Coomassie staining solution D. Keep the gel at RT

Coomassie staining solution A:	0.15 % Coomassie Brilliant Blue R25 25 % Isopropanol 10 % Acetic Acid
Coomassie staining solution B:	0.015 % Coomassie Brilliant Blue R25 10 % Isopropanol 10 % Acetic Acid
Coomassie staining solution C:	0.006 % Coomassie Brilliant Blue R25 10 % Acetic Acid
Coomassie staining solution D:	10 % Acetic Acid

2.3.2.3 Blot Transfer of Protein Gels to Membranes

The membranes used for the electrophoretic transfer were manufactured from nitrocellulose. In this procedure, blotting is performed in a tank of buffer with the gel in a vertical orientation, completely submerged between two large electrode panels as follows:

1. Assemble transfer sandwich; one plastic support, one porous pad, two pieces of Whatman paper, nitrocellulose, gel, two pieces of Whatman paper, one porous pad, and a plastic support. The transfer cassette should be assembled under buffer to avoid trapping of air bubbles
2. Fill tank with transfer buffer and place the sandwich into electroblotting apparatus. Transfer is achieved by applying a current of 40 mA for 16 hr at 4°C in a cold room

Transfer Buffer:	25 mM tris-HCl (pH 8.3)
	190 mM Glycine
	20 % Methanol

2.3.2.4 Immunoblotting with ECL (Enhanced Chemiluminescence)

ECL uses the HRP (hydrogen peroxide) catalyzed oxidation of luminol in alkaline conditions. Immediately following oxidation, the luminol is in an excited state which then decays to ground state via a light emitting pathway. ECL is achieved by performing the oxidation of luminol by the HRP in the presence of chemical enhancers such as phenols. This increases the light output approximately 1000 fold and extends the time of light emission. The maximum light emission is at a wavelength of 428 nm, which can be detected by a short exposure to blue-light sensitive autoradiography film. The detection limit of the ECL system is less than 1 picogram (pg) of antigen. Procedures used were as follows:

1. Pour 10 ml of Buffer A onto membrane and incubate for 1 hr at RT or for ON at 4 °C on an orbital shaker to block non-specific binding

2. Dilute the primary antibody in Buffer A and incubate the membrane for 1 hr at RT
3. Wash the membrane three times for 15 min in Buffer B at RT
4. Dilute the secondary antibody in Buffer A and incubate the membrane for 1 hr at RT
5. Wash the membrane three times for 15 min in Buffer B at RT
6. Wash the membrane three times for 15 min in Buffer C at RT
7. Wash the membrane three times for 15 min in Buffer D at RT
8. Mix an equal volume of ECL detection solution 1 with detection solution 2 to give sufficient volume in order to cover the membrane
9. Incubate for 1 min at RT with mixed ECL solution
10. Drain off excess detection reagent and cover the filter with a copier transparency
11. Check the signal by exposing the membrane to an autoradiography film in a dark room

10X Transfer Buffer:	1.92 M Glycine 250 mM Tris
10X TBS:	1.37 M NaCl 200 mM Tris-HCl, pH 7.6
Tween 20 stock solution:	10 % Tween 20
Buffer A:	5 % goat serum 5 % milk powder 0.1 % Tween 20 1X TBS
Buffer B:	5 % milk powder 0.1 % Tween 20 1X TBS
Buffer C:	0.1 % Tween 20 1X TBS
Buffer D:	1X TBS

2.3.3 Northern Blotting

2.3.3.1 RNA Extraction

To check the expression level of Baiap3 RNA in WT and Baiap3 KO mice, total RNA was isolated from littermates as follows:

1. Homogenize whole brain from WT and Baiap3 KO mice in Trizol reagent using a Glass-teflon homogenizer
2. Store the homogenate for 10 min at RT
3. Add chloroform and shake vigorously
4. Store the mixture at RT for 15 min and centrifuge at 15000 rpm for 15 min at 4°C
5. RNA remains exclusively in the aqueous phase and is transferred into a new tube
6. Add isopropanol and mix vigorously
7. Store the mixture at RT for 10 min and centrifuge at 15000 rpm for 10 min at 4°C
8. Remove the supernatant and wash the RNA pellet with 75 % EtOH
9. Centrifuge at 15000 rpm for 5 min at 4 °C
10. Briefly dry and resuspend RNA pellet with DEPC-water

2.3.3.2 Blotting

The RNA extracted from whole brain of WT and Baiap3 KO littermates was used to detect Baiap3 RNA using a specific probe corresponding to a region of the gene that is not deleted in the Baiap3 KO (a.a 330-1150). RNA is transferred from an agarose gel to

a Hybond+ (nucleic acid transfer) membrane by capillary transfer. The blots are analyzed by hybridization analysis with a radioactively labeled DNA probe as follows:

1. Prepare RNA samples with 10X MOPS, 12.3 M formaldehyde, and formamide
2. Incubate for 15 min at 55 °C and add formaldehyde loading buffer
3. Load the prepared RNA samples onto a formaldehyde agarose gel
4. Run the gel at 80 V for 4 hr in 1X MOPS
5. Transfer the gel into a new plastic container with 1L 20X SSC and soak for 45min
6. For blot, Cut three pieces of 3 M paper and the Hybond+ (nucleic acid transfer) membrane to cover the exposed surface of the gel
7. Incubate for overnight in 0.4 N NaOH
8. Wash the membrane with 1X SSC until the pH reaches 7.5 and dry the membrane
9. Cross link the RNA to the membrane with UV light (1 J/Cm²)
10. Pre-wet the membrane with 2XSSC and place in hybridization bottle, add hybridization solution and incubate at 65 °C for 30 min
11. Prepare labeled probe with ³²PdCTP

25 ng of DNA	1 µl
dH ₂ O	23 µl
Random primer	10 µl
12. Incubate for 5 min at 100 °C
13. Add 10 µl 5 X buffer and 5 µl ³²PdCTP and 1ul Exo-Klenow and incubate for 10 min at 37 °C

14. Add 2 μ l Stop mix and purify the labeled probe with Bio-Spin 6 column and Incubate for 6 min at 100 °C
15. Store the probe on ice for 10 min
16. Add labeled probe to the membrane and incubate ON at 65 °C
17. Wash the membrane with 2X SSC + 0.1 % SDS at RT for 20 min
18. Wash the membrane with 1X SSC + 0.1 % SDS at 65 °C for 20 min
19. Wash the membrane with 0.5X SSC + 0.1 % SDS at 68 °C for 30 min
20. Check the radioisotope activity and wash until counts are below 100
21. Expose the membrane with film at -80 °C for 3 days

10X MOPS:	0.4 M MOPS (pH7.0)
	0.1 M sodium acetate
	0.01 M EDTA
20X SSC: (pH7.0)	3 M NaCl
	0.3 M Na ₃ citrate.2H ₂ O
Formaldehyde loading buffer:	1 mM EDTA (pH8.0)
	0.25 % bromophenol blue
	0.25 % xylene cyanol
	50 % glycerol
Formaldehyde gel (100ml):	1 g Agarose in 72ml dH ₂ O
	10 ml 10XMOPS
	18 ml 12.3M formaldehyde

2.3.4 Expression of GST Fusion Proteins

In order to express with either Munc13-1 or Syntaxin 1A (a.a 1-256) or Baiap3-MHDs (a.a 330-1150) fusion proteins with GST, *BL21DE3 E.coli* was subjected to electroporation-mediated plasmid transformation with the respective constructs in pGEX-KG. GST-fusion proteins were prepared by follows;

1. Inoculate one colony from LB- ampicillin plates with either GST-Munc13-1 or GST-Syntaxin 1A (a.a 1-256) or Baiap3-MHDs (a.a 330-1150) into individual 5 ml of LB broth containing ampicillin and grow ON at 37 °C with shaking.
2. Inoculate 1 L of LB with 5ml from step 1
3. Grow at 37 °C with shaking for 4 hr
4. Induce expression of the protein by adding 0.3 mM IPTG and incubate for 4 hr at 25 °C with shaking
5. Centrifuge the culture at 3500 g for 20 min at 4 °C
6. Discard the supernatant and resuspend the pellet in 20 ml PBS with protease inhibitors
7. Add Lysozyme and incubate for 10 min at RT
8. Sonicate the bacterial suspension on ice, three times in short 30 sec bursts
9. Add 1 % Sodium cholate and incubate for 10 min at 4 °C with shaking
10. Centrifuge the lysate at 15000 g for 15 min at 4 °C
11. Transfer the supernatant to a fresh tube
12. Add 1 ml of a 50:50 slurry of Glutathione-Sepharose 4B beads in lysis buffer and incubate for ON at 4 °C
13. Centrifuge at 750 g for 5 min at 4 °C to pellet the beads
14. Wash the beads four times in 5 ml of cold wash buffer
15. The fusion protein should be stored on the beads at 4 °C

Ampicillin Solution:	20 mg/ml
Kanamycin Solution:	10 mg/ml
LB-Medium:	10 g NaCl
	10 g Bacto-Trypton
	5 g Bacto-Yeast-Extract
	In 1 L dH ₂ O and Autoclave

LB-Plate:	15 g Bacto-Agar In 1 L LB Medium appropriate antibiotic selection
50X TAE:	242 g Tris Base 57.1 ml Acetic acid 100 ml 0.5M EDTA (pH 8.0)

2.3.5 Co-sedimentation Assays

Recombinant fusion proteins consisting of glutathione S-transferase fused to syntaxin 1A (a.a 1-256), Munc13-1-176/178 (a.a 517-1735), Munc13-1-N1/N2 (a.a 3-317), Munc13-1-13'1 (a.a 1032-1345), or Munc13-1-3'13A (a.a 1399-1622) (Betz et al., 1997) were produced in *E. coli* using the pGEX-KG expression vector. Recombinant proteins were purified on glutathione-sepharose 4B, and immobilized on the resin for co-sedimentation assays. Cell lysate from HEK293FT cells co-transfected with pEGFP-Munc13-1 (full-length) and pMYC-Baiap3 (full-length) or crude whole brain extract from adult WT mice was solubilized at a concentration of 2 mg/ml in lysis buffer. After stirring on ice for 10 min, insoluble material were removed by centrifugation at 15000 rpm for 30 min at 4 °C. The equivalent of 3 mg of total protein was incubated with 50 µg immobilized GST-fusion protein ON at 4 °C on a rotating wheel. Beads were washed 4 times with lysis buffer, resuspended in SDS-PAGE sample buffer, and analyzed by SDS-PAGE and immunoblotting using standard procedures. Immunoreactive proteins were visualized with ECL. The following primary antibodies were used for immunodetection: two monoclonal antibodies to MYC for Baiap3, to Syntaxin 1A/B, and a polyclonal antibody to Munc13-1.

2.3.6 Production of Anti-Baiap3 Antisera

Polyclonal antibodies directed against Baiap3 were generated with a GST fusion protein as the antigen. Recombinant GST-Baiap3-MHDs fusion protein was generated by using the expression plasmid pGEX-Baiap3-MHDs, which expresses the residues 330-1150 of Baiap3 in the pGEX-KG vector. A polyclonal antibody that recognizes the N-terminus of Baiap3 (a.a 9-181) had previously been generated by Dr. Iris Augustin. Since the antibody produces a rather high background in immunofluorescence staining, we generate an antibody to a.a 330-1150 of Baiap3. We subcloned the regions spanning the MHDs to up to C2C domain of Baiap3 into the pGEX-KG construct. The host immunization and bleeding of rabbits and guinea pigs was performed by Eurogentec. The antisera were derived from the final bleeding of the rabbits SA5990 and SA5991 and of the guinea pigs SAC106 and SAC107. Since the recombinant Baiap3 protein proved to be insoluble and furthermore stuck to the beads, the following purification procedures were used:

Subcloning of the Baiap3 MHDs

Primer 14 (#11742): 5'-CCGGAATTCTAATGAACTTAGAGGTGGCCTCGG-3'

Primer 15 (#3417): 5'-TACGCGTCGACTCACCGGTTCTGCTCCAG-3'

Reaction Mixture		PCR Program	
10X Buffer	10 µl	94 °C for 3 min	— 1 cycle
dNTPs	5 µl	94 °C for 30 sec] 35 cycles
Primer 14	4 µl	55 °C for 30 sec	
Primer 15	4 µl	72 °C for 1min	
<i>Pfu</i> Taq	1 µl	72 °C for 10 min	— 1 cycle
dH ₂ O	25 µl	10 °C for forever	— 1 cycle
Total	50 µl		
Template DNA	1 µl		

1. Inoculate one colony from LB-ampicillin plates with GST-Baiap3-MHDs into individual 5 ml of LB broth containing ampicillin and grow ON at 37 °C with shaking incubator
2. Inoculate 1 L of LB with 5 ml from step 1
3. Grow at 37 °C with shaking for 4 hr
4. Induce expression of the protein by adding 0.3 mM IPTG and incubate for 4 hr at 25 °C with shaking
5. Centrifuge the culture at 3500 g for 20 min at 4 °C
6. Discard the supernatant and resuspend the pellet in 20 ml PBS with protease inhibitors
7. Add Lysozyme and incubate for 10 min at RT
8. Sonicate the bacterial suspension on ice, three times in short 30 sec bursts
9. Add 1 % sodium cholate and incubate for 10 min at 4 °C with shaking
10. Centrifuge the lysate at 15000 g for 15min at 4 °C
11. Transfer the supernatant to a fresh tube
12. Add 1 ml of a 50:50 slurry of Glutathione-Sepharose 4B beads in lysis buffer and incubate for ON at 4 °C
13. Centrifuge at 750 g for 5 min at 4 °C to pellet the beads
14. Wash the beads four times in 5 ml of cold wash buffer
15. Cleave between GST and Baiap3 fragment by thrombin digestion for 2 hr at RT
16. Protein purification from the beads by Electro-HPLC (high performance liquid chromatography)
17. The denatured purified Baiap3 fragment was sent to Eurogentec for immunization

2.3.7 Antibodies, Chemicals, Kits and Reagents

Antibodies		
Primary monoclonal	Source	Dilution
Anti-ChromograninA	BD Biosciences	1:1000
Anti-MYC	Abcam	1:3000
Anti-NMDA R1	Synaptic Systems	1:1000
Anti-NSF	Abcam	1:2000
Anti-SNAP 25	Synaptic Systems	1:2000
Anti-Synaptobrevin2	Synaptic Systems	1:2000
Anti-Synaptophysin	Synaptic Systems	1:2000
Anti-Syntaxin1	Synaptic Systems	1:2000
Anti-Tubulin	Sigma	1:10.000
Primary polyclonal	Source	Dilution
Anti-BAI 1	Abcam	1:1000
Anti-Baiap3	Shin et al.	1:500
Anti-Munc13-1 (40.1)	Varoqueaux et al.	1:1000
Anti-bMunc13-2 (44.1)	Varoqueaux et al.	1:1000
Anti-ubMunc13-2 (48.1)	Varoqueaux et al.	1:1000
Anti-Munc13-3 (52.1)	Varoqueaux et al.	1:1000
Anti-Munc18-1	Synaptic Systems	1:2000
Anti-VMAT2	Weihe et al.	1:2000
Secondary	Source	Dilution
Anti-Mouse, HRP-conjugate	Bio-Rad	1:10.000
Anti-Rabbit, HRP- conjugate	Bio-Rad	1:10.000

Chemicals	
Product	Company
Agarose	Gibco-BRL
Ammoniumpersulfate	Sigma-Aldrich

Ampicillin	Sigma-Aldrich
Aprotinin	Roche
Bacto-Yeast-Extract	DIFCO Laboratories
Bacto-Trypton	DIFCO Laboratories
Bacto-Peptone	DIFCO Laboratories
Bacto-Agar	DIFCO Laboratories
BAPTA	Sigma-Aldrich
BCA (Protein Assay)	Bio-Rad
Bromophenol Blue	Sigma-Aldrich
Coomassie Blue R250	BIOMOL
Chymotrypsin	Sigma-Aldrich
[α - ³² P]dCTP	Amersham
DEPC	Sigma-Aldrich
DMSO	Sigma-Aldrich
dNTP's	Pharmacia Biotech
DTT	Sigma-Aldrich
ECL-Reagents	Amersham-Buchler
Films	Kodak
Ethanol	JT Baker
Ethidiumbromide	Sigma-Aldrich
Ficoll 400	Pharmacia Biotech
Fura-4F	Invitrogen
Glutathion Sepharose 4B	Sigma-Aldrich
Glutathion-Agarose Matrix	Sigma-Aldrich
Glycin	Bio-Rad Laboratories
IPTG	BioMol Feinchemikalien
Isopropanol	Merck
Kanamycin	Sigma-Aldrich
Klenow-Fragment	Roche
Leupeptin	Roche
Lysozym	Sigma-Aldrich
Ni-NTA-Agarose-Matrix	Qiagen
NP-EGTA	Synaptic Systems
Mg ²⁺ -Fura-2	Invitrogen
Paraformaldehyde	BIOMOL
PBS	Sigma-Aldrich
Pfu-Polymerase	Stratagene
Phenol-Chloroform	ROTH

PMSF	Roche
Ponceau S	Sigma-Aldrich
Protein Assay	Bio-Rad Laboratories
Proteinase K	Boehringer Mannheim
Rapid-hyb. Buffer	Amersham pharmacia
Rat Quick Clone cDNA, MouseBrain	Clontech
SDS	Roche
Standard Molecular weight marker	Prestained Standards, Bio-Rad
T4-DNA-Ligase	Roche
T4-DNA-Polymerase	Roche
<i>Taq</i> -Polymerase	ABI
Temed	Sigma-Aldrich
2,2,2-Tribromethanol	Sigma-Aldrich
Tris Base	Sigma-Aldrich
Triton X-100	Roche
Dry Milk	Nestle
Tween 20	Sigma-Aldrich
X-Gal	BIOMOL

Kits	
Product	Company
Centricon 10	Amicon GmbH
ECL-film	Amersham
Electroporation Cuvettes	Bio-Rad Laboratories
Hybond-N ⁺ -Membrane	Amersham
Plasmid-Purification Kit	Qiagen
Prime-It II-Random Primer Labelling Kit	Stratagene
Protran (nitrocellulose transfer membrane)	Whatman International
Shrimp Alkaline Phosphatase	Roche
SP6 in vitro transcription Kit	Roche
Topo T/A und Topo XL Cloning Kit	Invitrogen
Qiafilter Plasmid Kit	Qiagen
Qiaquick Gel-Extraction Kit	Qiagen
Qiaquick PCR-Purification Kit	Qiagen
Whatman 3MM paper	Whatman International

Reagents	
Product	Company
β -Mercaptoethanol "cell culture tested"	Sigma-Aldrich
DMEM	Gibco-BRL
Knockout DMEM	Gibco-BRL
Fetal Calf Serum	Hyclone
Fetal Bovine Serum	Hyclone
G418	Invitrogen
L-Cysteine	Gibco-BRL
L-Glutamine (100 x)	Gibco-BRL
Lipofectamin 200	Invitrogen
NEAA (100 x)	Gibco-BRL
Neurobasal Medium	Gibco-BRL
Papain	Worthington
Penicillin/Streptomycin	Gibco-BRL
Opti-MEM	Gibco-BRL
Trypsin-EDTA (0.05x)	Gibco-BRL
Trypsin-EDTA (0.25%)	Gibco-BRL

2.4 Electrophysiological Analysis

2.4.1 Whole Cell Capacitance Measurements

Conventional whole-cell recordings were performed at 30 °C with 3-5 M Ω pipettes (Kimax-51; Kimble/Kontes, Vineland, NJ) (Voets et al., 2000). An EPC-9 patch-clamp amplifier was used together with the Pulse software package (HEKA Electronics, Lambrecht, Germany). Capacitance measurements were performed by using the Lindau-Neher technique implemented as the “sine+ dc” mode of the software lock-in extension

of pulse, which allowed long-duration capacitance measurements in a single sweep. A 1000 Hz, 70 mV peak-to-peak sinusoid voltage stimulus was superimposed onto a DC holding potential of -70 mV. Currents were filtered at 3 kHz and sampled at 12 kHz.

The capacitance traces were exported to Axograph (Axograph Scientific, Sydney, Australia) for analysis. Displayed traces are averages for each condition, with the number of cells given in the figure legends. To control for variation between preparations, we always compared WT or heterozygous and KO chromaffin cells obtained from the same preparation. Kinetic data were obtained by fitting individual capacitance recordings with a sum of three exponential functions.

10X External Solution: (pH 7.2, 310-320 mOsm)	1.4 M NaCl (pH 7.6)
	24 mM KCl
	100 mM HEPES
	100 mM Glucose
	40 mM CaCl ₂
	40 mM MgCl ₂
Intracellular Solution 1: For trains of short depolarizations (pH 7.2, mOsm:310)	120 mM CsCl
	20 mM TEA-Cl
	1 mM CaCl ₂
	2 mM MgCl ₂
	11 mM EGTA
	10 mM HEPES
	2 mM Mg-ATP
	0.5 mM Na-GTP
Intracellular Solution 2: For Flash photolysis (pH 7.2, mOsm:310)	110 mM Cs-glutamate
	8 mM NaCl
	2 mM Mg-ATP
	0.3 mM Na-GTP
	20 mM Cs-HEPES
	4.5 mM CaCl ₂
	5 mM NP-EGTA
	0.3 mM Mg ²⁺ -Fura-2
	0.2 mM Fura-4F

2.4.2 Flash Photolysis of Caged Ca^{2+} and Measurements of $[\text{Ca}^{2+}]_i$

Flashes of UV light were generated by a flash lamp (Rapp Optoelektronik, Hamburg, Germany), and fluorescence excitation light was generated by a monochromator (TILL Photonics, Planegg, Germany) as described previously (Gillis et al., 1996; Xu et al., 1998); these were coupled into the epifluorescence port of an inverted Axiovert 100 microscope with a 40X Fluorobjective (Zeiss, Oberkochen, Germany). Mg^{2+} -Fura-2 was excited at 380/340 nm, and the illumination area was reduced to cover only the diameter of the cell. Emitted light was attenuated with a neutral density filter, detected with an avalanche photodiode (TILL Photonics, Planegg, Germany), filtered at 3 kHz and sampled at 12 kHz by Pulse software (Ashery et al., 2000). The basal $[\text{Ca}^{2+}]_i$ was measured to be 220 nM by fura-2 in vivo using calibration solution 1 (R_{\min}), solution 2 (R_{\max}), solution 3 (K_{eff}), and solution 4 (α -coefficient). The flash photolysis efficiency was also measured as described (Xu et al., 1998). The photolysis efficiency of a 350 V discharge flash for NP-EGTA was determined to be 30 %. Fluorescence excitation light was used to measure $[\text{Ca}^{2+}]_i$ and simultaneously photorelease Ca^{2+} after the flashes in order to keep $[\text{Ca}^{2+}]_i$ approximately constant. $[\text{Ca}^{2+}]_i$ was calculated from the fluorescence ratio (R) according to Grynkiewicz et al (1985) and the flash photolysis efficiency was calculated as according to published protocols (Xu et al., 1998). Fluorescent excitation light was used not only to measure but also to adjust before and after flash. The basal Ca^{2+} concentration before the flash was 500-900 nM.

Each cell was patched under conditions as follows;

1. Access resistance is low, preferably $< 7 \text{ MOhm}$
2. Leak current is low, preferably $< 20 \text{ pA}$

3. Fluorescence ratio is stable before the flash
4. Loading with dye saturates, indicating the cell is not swelling excessively

2X Pipette Solution:	250 mM Cs-glutamate
	80 mM Cs-HEPES (pH 7.2)
10X Nucleotide:	20 mM Mg-ATP
	3 mM Na-GTP
	10 mM HEPES (pH 7.2)
Solution 1:	20 mM BAPTA
	1X Pipette solution
	1X Nucleotide
	0.5 mM Fura-2
Solution 2:	10 mM CaCl ₂
	1X Pipette solution
	1X Nucleotide
	0.5 mM Fura-2
Solution 3:	20 mM BAPTA
	13.33 mM CaCl ₂
	1X Pipette solution
	1X Nucleotide
	0.5 mM Fura-2
Solution 4:	1X Pipette solution
	1X Nucleotide
	0.2 mM Fura-2

2.4.3 Data Analysis and Statistics

Data were analyzed offline using AxoGraph 4.9 or AxoGraph X 1.0 (AxoGraph Scientific, Sydney, Australia) and Kaleidagraph 4.0 (Synergy Software, PA, USA). Statistical significance was tested using Student's *t*-test.

3. Results

3.1 Analysis of the Role of the Munc13 Protein Family in LDCV Exocytosis

3.1.1 Reduced Exocytosis in Chromaffin Cells from Munc13-1 KO Mice

Munc13-1 is expressed in bovine chromaffin cells, which are used as a model for LDCV secretion (Ashery et al., 2000) and is also present in mouse adrenal gland (Figure 16A). The role of Munc13-1 in SV exocytosis has been investigated in individual hippocampal primary neurons cultured on astrocyte feeder islands (microisland culture) (Augustin et al., 1999b). Munc13-1 deficient neurons showed a striking deficit in evoked and spontaneous neurotransmitter release. In present study, we investigated whether the absence of Munc13-1 affects exocytosis of LDCVs in mouse adrenal chromaffin cells (Figure 6F). We performed whole-cell patch clamp recordings combined with flash photolysis of caged Ca^{2+} on chromaffin cells cultured from P0 adrenal glands. Flash photolysis of caged Ca^{2+} typically causes a biphasic increase in membrane capacitance. Upon photolysis of caged Ca^{2+} , release was undetectable at Ca^{2+} concentration of $< 1 \mu\text{M}$, became measurable at $1\text{-}2 \mu\text{M}$ Ca^{2+} , and resembled the release observed during a normal action potential at $> 5 \mu\text{M}$ Ca^{2+} , and saturated at $> 20 \mu\text{M}$ Ca^{2+} (Bollmann et al., 2000).

We found that, in chromaffin cell from Munc13-1 KO mice, both the exocytotic burst and the sustained component were significantly reduced (Burst: by $\sim 40\%$, and Sustained: by $\sim 50\%$; Figure 6A-C; Table 1).

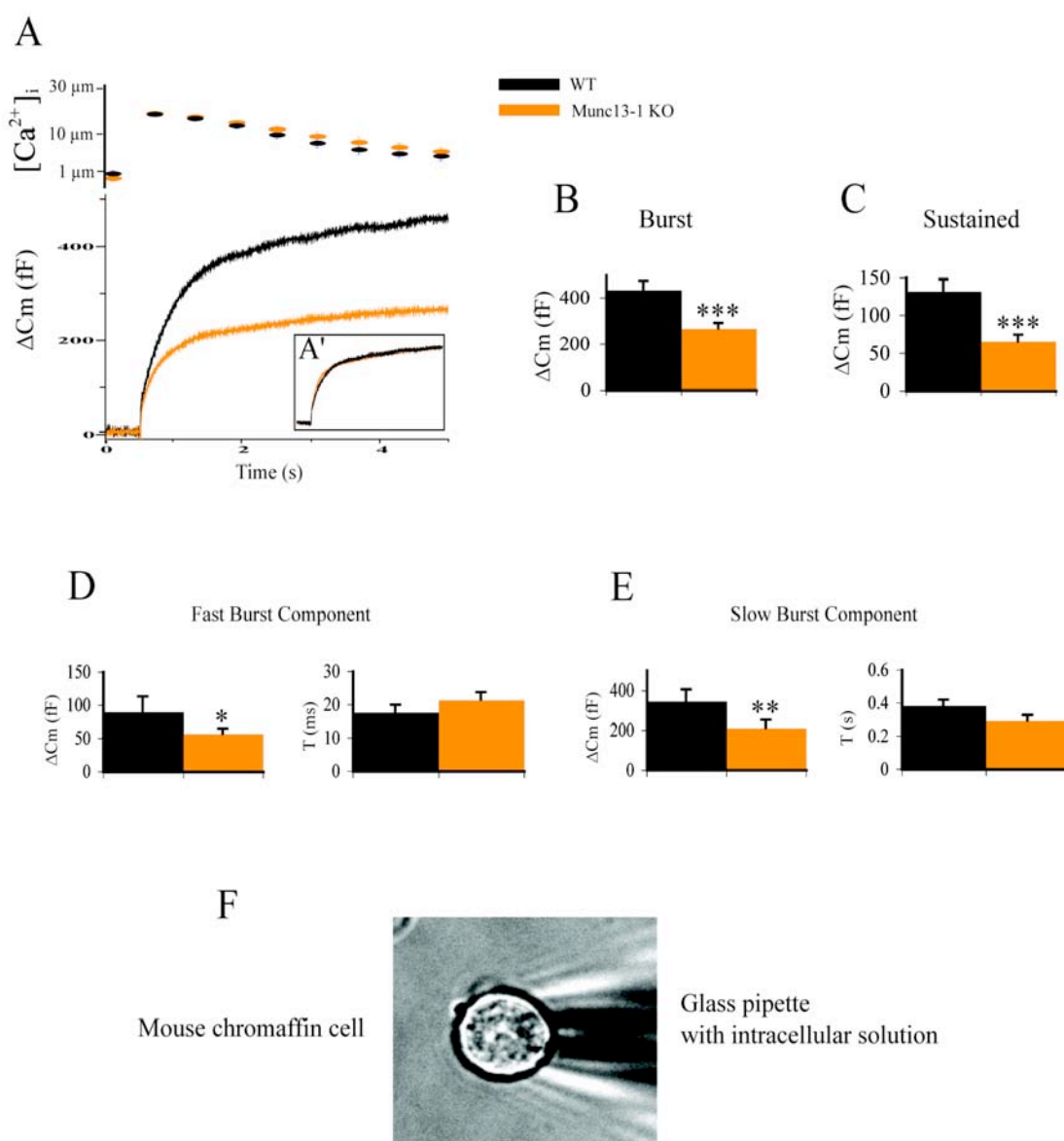


Figure 6. Reduced exocytosis in chromaffin cells from Munc13-1 deficient mice.

(A) Average ΔC_m in response to flash photolysis of NP-EGTA in chromaffin cells cultured at P0 from WT (28 cells from 5 mice, black line) and Munc13-1 KO mice (32 cells from 5 mice, orange line). The intracellular Ca^{2+} concentration following the flash is shown in the upper trace. (A') The Munc13-1 KO trace was normalized to the WT amplitude at 4 s after the flash. (B-C) Comparison of the exocytotic burst ($P=0.0007$) and sustained release ($P=0.0005$) in WT control and Munc13-1 KO cells. The exocytotic burst and sustained release were determined as the ΔC_m 1 s and 2 s to 5 s after the flash, respectively. (D-E) Kinetic analysis of the capacitance traces revealed that the two burst components, fast ($P=0.032$) and slow ($P=0.035$), are both reduced in amplitude, without any change in the time constant. Error bars indicate standard error of the mean. (F) Representative mouse chromaffin cell with attached glass pipette.

*, $P < 0.05$; **, $P < 0.01$; ***, $P < 0.001$.

In order to investigate the release kinetics of exocytosis, we fitted individual capacitance traces with a sum of exponentials within the first second after the flash. The amplitudes of the capacitance traces represent the vesicle pool sizes, whereas the time constants identify their fusion kinetics. The first phase, the exocytotic burst, can be further subdivided into a fast burst (fusion with a time constant of ~20 ms at 20 μ M Ca^{2+}) and a slow burst (fusion with a time constant of > 200 ms at 20 μ M Ca^{2+}) components (Sørensen et al., 2003). These phases represent fusion of two distinct pools of docked and primed vesicles, the RRP and the SRP. The slow component or SRP represents a precursor state to the fast component or RRP and the sustained phase of secretion, which persists for several seconds, is thought to represent refilling of the primed vesicle pools (Voets et al., 1999).

In chromaffin cell from Munc13-1 deficient mice, we found that both the fast and the slow burst components were significantly smaller than in WT chromaffin cells, but that vesicle fusion kinetics were not affected (Figure 6D-E, Table 1). To examine whether the reduction in Munc13-1 KO exocytosis obscures a difference in the kinetics of the sustained phase, we normalized the traces to the sustained phase of release at 4 s (Figure 6A'). However, no change in the kinetics of the sustained phase or the relative amplitudes of burst and sustained component were detected, indicating that the Munc13-1 deficiency impairs the docking/priming reactions necessary for the release of all vesicles, rather than affecting the burst phase or sustained phase selectively. Postflash $[\text{Ca}^{2+}]_i$ was closely matched between KO and WT cells (Figure 6A, top), which shows that the release deficit in Munc13-1 KO chromaffin cells is not due to altered Ca^{2+} levels. These findings demonstrate that loss of Munc13-1 leads to a reduction of both the pool of fusion-competent LDCVs and to a reduction of

recruitment of new LDCVs into this pool, without affecting the kinetics of the fusion step.

3.1.2 Reduced Exocytosis in Chromaffin Cells from Munc13-2 KO Mice

Munc13-2 is expressed in bovine chromaffin cells (Zikich et al., 2008) and also in mouse adrenal gland (Figure 17A). To test whether Munc13-2 is required for exocytosis of LDCVs, we stimulated chromaffin cells obtained from P0 WT and Munc13-2 KO littermates using flash photolysis of caged Ca^{2+} . We found that in chromaffin cells from Munc13-2 deficient mice, both the exocytotic burst and the sustained component were reduced (Burst: by ~30 %, and Sustained: by ~40 %; Figure 7A-C; Table 1), however, the reduction was statistically not significant (Figure 7).

When we investigated the release kinetics of exocytosis by fitting individual capacitance traces within the first 1 s after the flash with a sum of exponentials, we found that in chromaffin cell from Munc13-2 KO mice, both the fast and slow burst were reduced, but the reduction was statistically not significant (Figure 7D-E, Table 1). Like the loss of Munc13-1, loss of Munc13-2 also had no effect on the vesicular release kinetics during the exocytotic burst (Figure 7D-E, Table 1), nor did normalization of the traces to the sustained component reveal a selective alteration of the kinetics of the sustained component (Figure 7A'). Postflash $[\text{Ca}^{2+}]_i$ was closely matched between KO and WT cells (Figure 7A, top). In cultured hippocampal neurons obtained from Munc13-2 KO mice, SV exocytosis was not affected, suggesting a compensatory effect of Munc13-1 in Munc13-2 KO neurons (Varoqueaux et al., 2002).

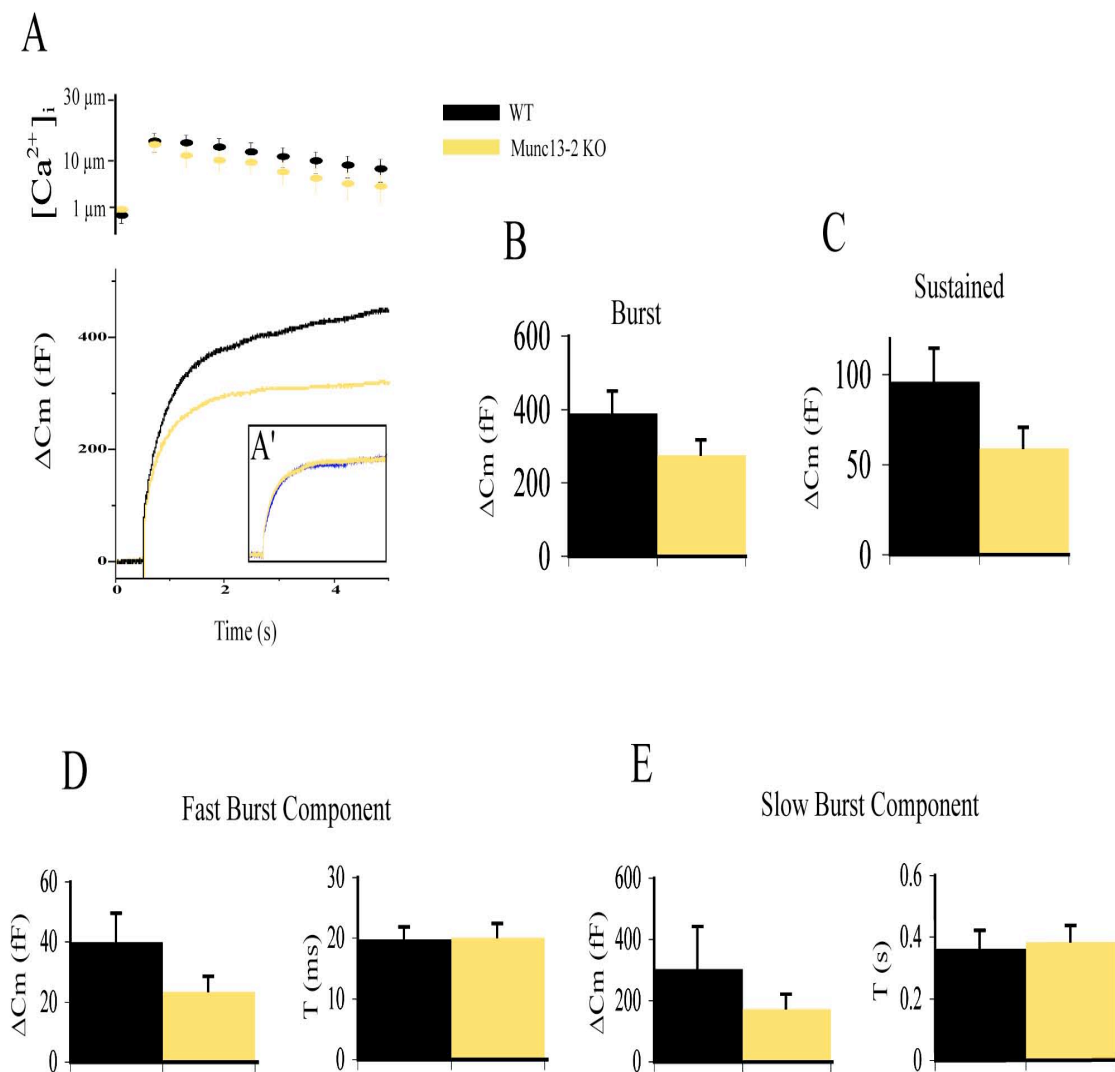


Figure 7. Reduced exocytosis in chromaffin cells from Munc13-2 deficient mice.

(A) Average ΔC_m in response to flash photolysis of NP-EGTA in P0 WT control (21 cells from 4 mice, black line) and Munc13-2 KO (22 cells from 4 mice, vanilla line). The intracellular Ca^{2+} concentration following the flash is shown in the upper trace. (A') The Munc13-2 KO trace was normalized to the WT amplitude at 4 s after the flash. (B-C) Comparison of the exocytotic burst ($P=0.096$) and sustained release ($P=0.080$) in WT control and Munc13-2 KO cells. The exocytotic burst and sustained release were determined as the ΔC_m 1 s and 2 s to 5 s after the flash, respectively. (D-E) Kinetic analysis of the capacitance traces revealed that the two burst components, fast ($P=0.13$) and slow ($P=0.95$), are both reduced in amplitude, without any change in the time constant. Error bars indicate standard error of the mean. *, $P < 0.05$; **, $P < 0.01$; ***, $P < 0.001$.

Although the release deficit in Munc13-2 KO LDCV exocytosis was statistically not significant, our data indicate that in the regulation of LDCV exocytosis in mouse chromaffin cells, Munc13-1 may not be able to fully compensate for the loss of Munc13-2.

3.1.3 Reduced Exocytosis in Chromaffin Cells from Munc13-1/2DKO Mice

In this study, we found that both the exocytotic burst and the sustained phase component were reduced in chromaffin cells deficient for either Munc13-1 or Munc13-2 (Figure 6A-E, 7A-E). Next, we investigated LDCV secretion in chromaffin cells lacking both Munc13-1 and -2. Munc13-1/2 DKO mice are completely paralyzed, die immediately after birth and neurotransmitter secretion from both GABAergic and glutamatergic hippocampal neurons is completely abolished in Munc13-1/2 DKO mice (Varoqueaux et al., 2002). Thus we expected that LDCV exocytosis (both the exocytotic burst and the sustained component) might be abolished in Munc13-1/2 deficient chromaffin cells. We analyzed adrenal chromaffin cells from E18 (Embryonic day 18) embryos that were obtained by caesarean section of pregnant females from Munc13-1 heterozygous and Munc13-2 homozygous KO background matings. Munc13-2 KO chromaffin cells were used as controls and compared with Munc13-1/2 DKO chromaffin cells. Interestingly, we found that the adrenal glands from Munc13-1/2 DKO mice were about 50% smaller than those of Munc13-2 KOs, which were indistinguishable from WT adrenal glands (data not shown).

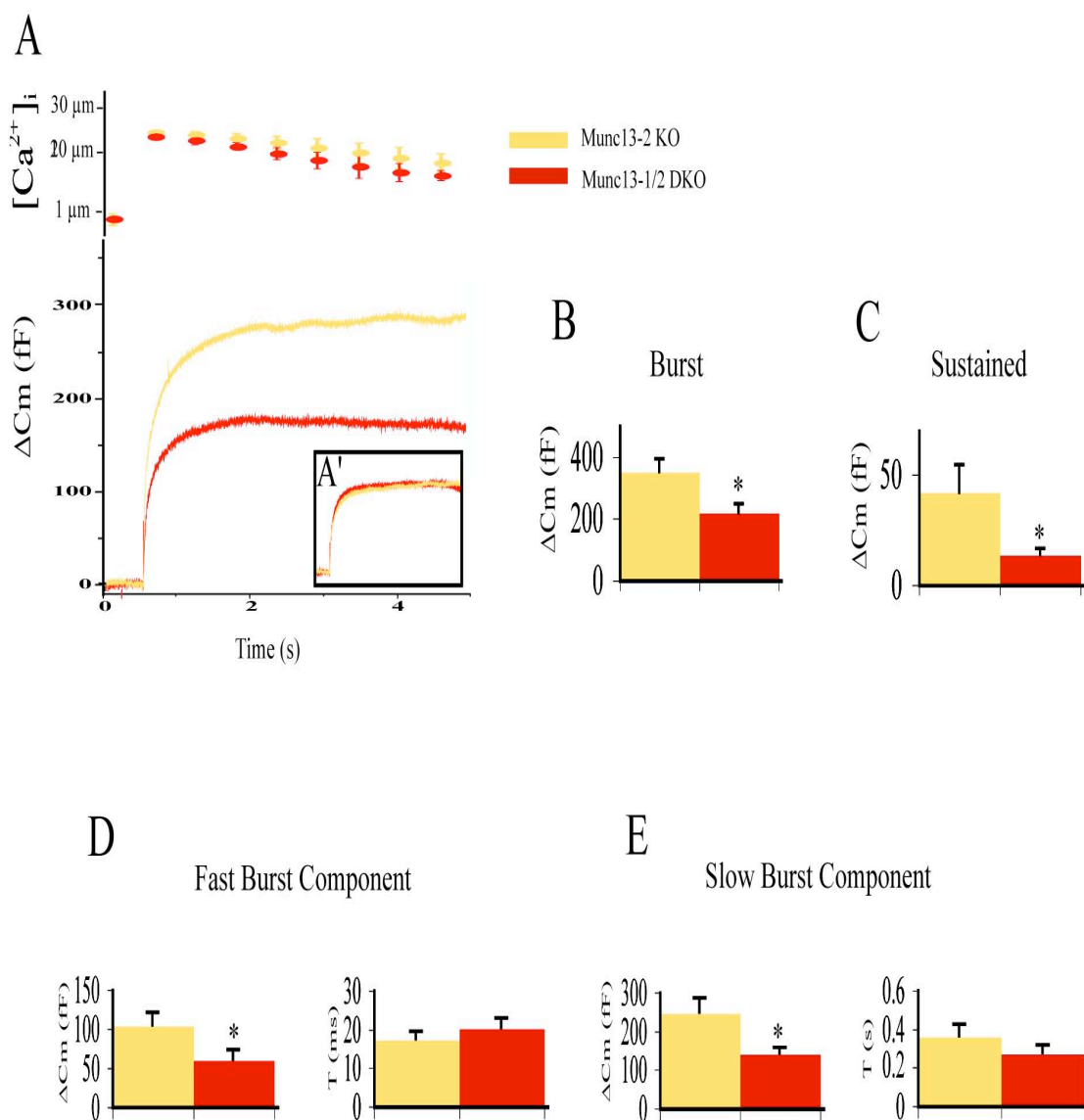


Figure 8. Reduced exocytosis in chromaffin cells from Munc13-1/2 DKO mice.

(A) Exocytosis in mouse chromaffin cells from Munc13-2 KO and Munc13-1/2 DKO mice after flash photolysis of caged Ca^{2+} . Average ΔC_m in response to flash photolysis of NP-EGTA in Munc13-2 KO (12 cells from 3 mice) and Munc13-1/2 DKO (14 cells from 3 mice). The intracellular Ca^{2+} concentration following the flash is shown in the upper trace. (A') The Munc13-1/2 DKO trace was normalized to the Munc13-2 KO amplitude at 4 s after the flash. (B-C) Comparison of the exocytotic burst ($P=0.0014$) and sustained release ($P=0.024$) in control and Munc13-1/2 DKO cells. The exocytotic burst and sustained release were determined as the ΔC_m 1 s and 2 s to 5 s after the flash, respectively. (D-E) Kinetic analysis of the capacitance traces revealed that the two burst components, fast ($P=0.040$) and slow ($P=0.011$), are both changed. Error bars indicate standard error of the mean. *, $P<0.05$; **, $P<0.01$; ***, $P<0.001$.

To test whether secretion is completely abolished in Munc13-1/2 DKO cells, we stimulated the chromaffin cells obtained from Munc13-2 KO and Munc13-1/2 DKO littermates using flash photolysis of caged Ca^{2+} . We found that in chromaffin cell from the Munc13-1/2 DKO mice, both the exocytotic burst (by ~40%, Figure 8B, Table 1) and the sustained component (by ~70%, Figure 8C, Table 1) were reduced significantly compared to Munc13-2 KO cells (Figure 8A).

However, in contrast to the complete shutdown of SV exocytosis from Munc13-1/2 DKO hippocampal neurons (Varoqueaux et al., 2002), exocytosis from chromaffin cells, although drastically reduced, was not abolished entirely in the absence of both Munc13-1 and -2.

In order to investigate the release kinetics of exocytosis we fitted individual capacitance traces within the first 1 s after the flash with a sum of exponentials. We found that compared to chromaffin cells from Munc13-2 KO littermates, cells from Munc13-1/2 DKO mice showed a reduction of 40% in the fast and of 75% in the slow burst amplitude (Figure 8D-E, Table 1). Taking into account that, compared to WT, Munc13-2 KO cells already have a 30%-40% reduction of exocytosis, both the exocytotic burst and the sustained component were reduced more drastically in the Munc13-1/2 DKOs than in either single KO (Figure 20). Furthermore, like the loss of Munc13-1 or Munc13-2 alone, the absence of both isoforms had no effect on the vesicular release kinetics during the exocytotic burst (Figure 8D-E, Table 1), nor did normalization of the traces to the sustained component reveal a selective alteration of the kinetics of the sustained component (Figure 8A'). Taken together, these findings indicate that the presence of Munc13-1 suffices for the establishment of an almost WT-sized pool of LDCVs released in the initial burst, but recruitment of new vesicles into

the releasable pool during ongoing release is severely impaired in the absence of both isoforms. As in the previous experiments, no effect on $[Ca^{2+}]_i$ was detected in the absence of Munc13-1 and Munc13-2 (Figure 8A, top). Thus, both Munc13-1 and -2 are positive regulators in LDCV exocytosis in mouse chromaffin cells.

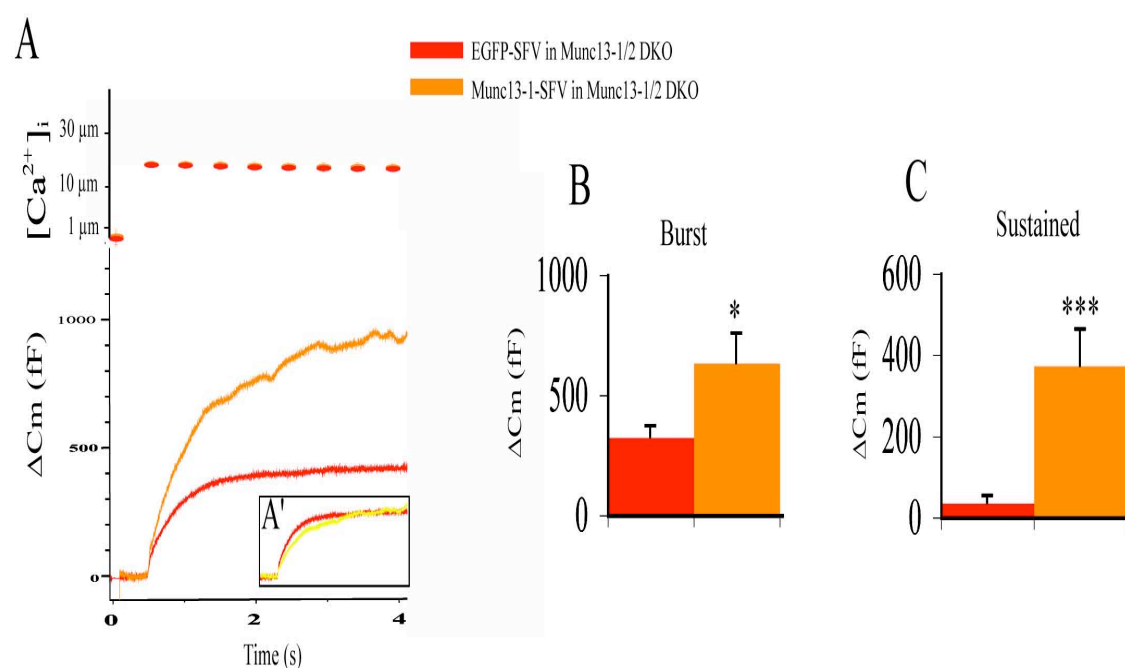


Figure 9. Rescue of exocytosis in Munc13-1/2DKO chromaffin cells by overexpression of Munc13-1

(A) Average ΔC_m in response to flash photolysis of NP-EGTA in E18 Munc13-1/2 DKO cells overexpressing either EGFP (9 cells from 3 mice) or Munc13-1 (7 cells from 3 mice). The intracellular Ca^{2+} concentration following the flash is shown in the upper trace. (A') The Munc13-1-SFV trace was normalized to the EGFP-SFV amplitude at 4 s after the flash. (B-C) Comparison of the exocytotic burst ($P=0.019$) and sustained release ($P=0.0009$) in cells overexpressing EGFP and cells overexpressing Munc13-1. The exocytotic burst and sustained release were determined as the ΔC_m 1 s and 2 s to 5 s after the flash, respectively. Error bars indicate standard error of the mean. *, $P<0.05$; **, $P<0.01$; ***, $P<0.001$.

To confirm these results, we tested whether Munc13-1-SFV overexpression in Munc13-1/2 DKO chromaffin cells would rescue secretion. Using the SFV expression system, we infected mouse chromaffin cells obtained from Munc13-1/2 DKO mice with the RNA coding for Munc13-1 tagged with EGFP (Enhanced Green Fluorescent Protein) (Ashery et al., 1999). The average capacitance after flash photolysis of caged Ca^{2+} was larger in Munc13-1 overexpressing cells than in EGFP overexpressing cells (Figure 9A). Both the exocytotic burst (Figure 9B, 633.72 ± 121.3 fF, $P=0.019$) and the sustained component (Figure 9C, 372.57 ± 88.56 fF, $P=0.0009$) were increased significantly. Normalization of the Munc13-1-SFV trace to the trace of EGFP-SFV control cells revealed no significant changes in the kinetics of the sustained component (Figure 9A'). Thus, in agreement with previous studies that showed that overexpression of Munc13-1 in WT chromaffin cells boosted LDCV release (Ashery et al., 2000), overexpression of Munc13-1 in Munc13-1/2 DKO chromaffin cells leads to both a larger amount of fusion-competent vesicles and a more rapid vesicle supply.

3.1.4 Exocytosis in Chromaffin Cells from Munc13-3 KO and Munc13-1/2/3 TKO Mice

In addition to Munc13-1 and -2, a third Munc13 isoform, Munc13-3, is also expressed in bovine chromaffin cells (Ashery et al., 2000) and mouse adrenal gland (Figure 17A). To test whether Munc13-3 also contributes to the regulation of LDCV exocytosis, we stimulated chromaffin cells obtained from P0 WT and Munc13-3 KO littermate mice using flash photolysis of caged Ca^{2+} .

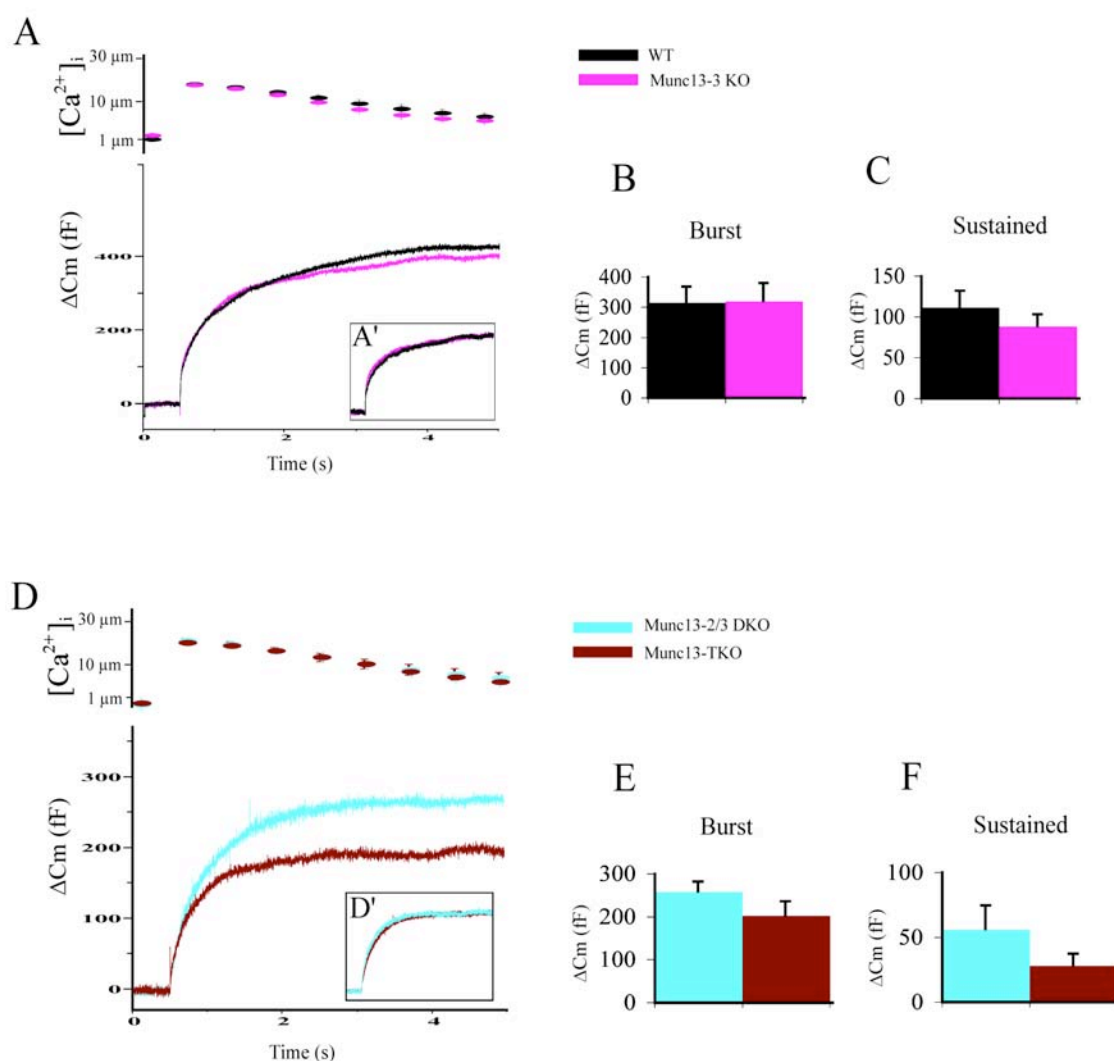


Figure 10. Exocytosis in chromaffin cells from Munc13-3KO and Munc13-1/2/3 Triple knockout (TKO) mice.

(A) Average ΔC_m in response to flash photolysis of NP-EGTA in chromaffin cells cultured at P0 from WT (15 cells from 3 mice, black line) and Munc13-3 KO mice (12 cells from 3 mice, magenta line). The intracellular Ca^{2+} concentration following the flash is shown in the upper trace. (A') The Munc13-3 KO trace was normalized to the WT amplitude at 4 s after the flash. (B-C) Comparison of the exocytotic burst and sustained release in WT control and Munc13-3 KO cells. The exocytotic burst and sustained release were determined as the ΔC_m 1 s and 2 s to 5 s after the flash, respectively. (D) Average ΔC_m in response to flash photolysis of NP-EGTA in chromaffin cells cultured at E18 from Munc13-2/3 DKO (17 cells from 3 mice, blue line) and Munc13-1/2/3 TKO mice (13 cells from 3 mice, purple-red line). The intracellular Ca^{2+} concentration following the flash is shown in the upper trace. (D') The Munc13-1/2/3 TKO trace was normalized to Munc13-2/3 DKO amplitude at 4 s after the flash. (E-F) Comparison of the exocytotic burst and sustained release in Munc13-2/3 DKO and Munc13-1/2/3 TKO cells. The exocytotic burst and sustained release were determined as the ΔC_m 1 s and 2 s to 5 s after the flash, respectively. Error bars indicate standard error of the mean.

We found that the exocytotic burst and the sustained component were not reduced compared to WT, nor were the release kinetics altered (Figure 10A-C, Table 1), most likely because Munc13-1 and Munc13-2 are able to compensate for the absence of Munc13-3. The postflash $[Ca^{2+}]_i$ did not differ between WT and Munc13-3 KO cells (Figure 10A, top).

Lastly, to investigate whether the secretion is completely abolished in cells lacking all three Munc13 isoforms (Munc13-1, -2, and -3), we obtained chromaffin cells from Munc13-1 heterozygous and Munc13-2/3 double homozygous KO background matings. Munc13-1/2/3 TKOs are completely paralyzed, die immediately after birth and look rather similar to Munc13-1/2 DKO mice (Varoqueaux et al., 2002). For the Munc13-1/2/3 TKO experiments control chromaffin cells were cultured from Munc13-2/3 DKO littermates, which were viable and fertile. We analyzed adrenal chromaffin cells from E18 embryos that were obtained by caesarean section of pregnant females. Compared to Munc13-2/3 double deficient cells, Munc13-1/2/3 triple deficient chromaffin cells showed no significant changes in the exocytotic burst, the sustained component, or in the kinetics of release (Figure 10D-F, Table 1, Figure 10A').

Based on our data, the sustained component in both the Munc13-2/3 DKO and Munc13-1/2/3 TKO cells was reduced by at least 50 % (Figure 20, Figure 10F). Since it is not possible to obtain WT and Munc13-1/2/3 triple deficient mice in the same litter at a frequency that is experimentally feasible, we were unable to accurately assess the contribution of Munc13-3 to LDCV exocytosis. However, taken together, the our data imply that the absence of Munc13-3 seemed to have the smallest effect on LDCV exocytosis, and furthermore, that residual LDCV exocytosis persists in the absence of the three Munc13 isoforms known to regulate neuronal SV exocytosis.

3.1.5 Enhanced Exocytosis in Chromaffin Cells from Baiap3 KO Mice

We first investigated basic properties of exocytosis in mouse adrenal chromaffin cells obtained from P0 Baiap3 KO and WT littermates.

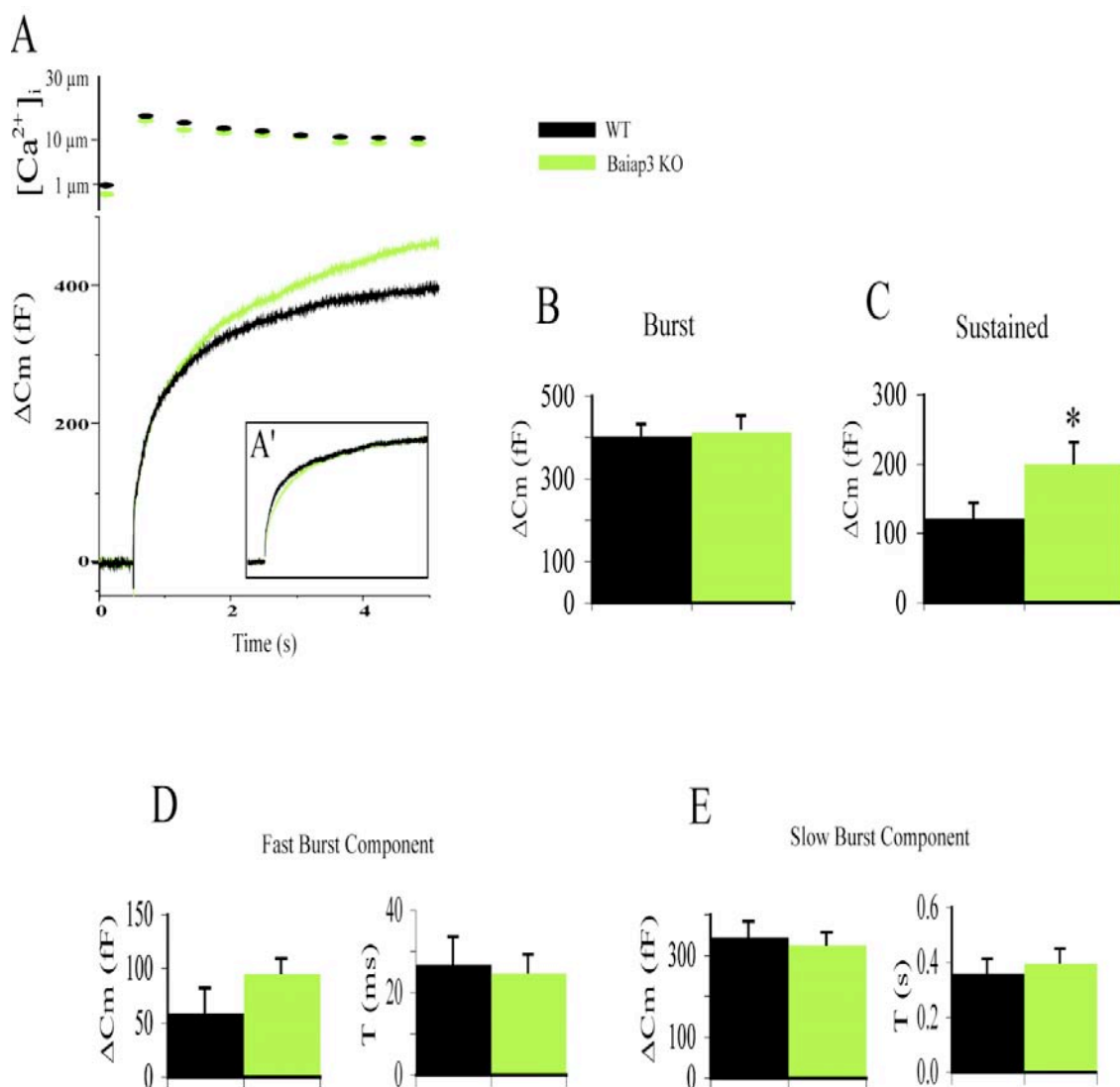


Figure 11. Increased exocytosis in chromaffin cells from Baiap3 deficient mice.

(A) Average ΔC_m in response to flash photolysis of NP-EGTA in WT control (27 cells from 6 mice) and Baiap3 KO (28 cells from 6 mice). The intracellular Ca^{2+} concentration following the flash is shown in the upper trace. (A') The Baiap3 KO trace was normalized to WT amplitude at 4 s after the flash. (B-C) Comparison of the exocytosis burst and sustained release ($P=0.031$) in control and Baiap3 KO cells. The exocytotic burst and sustained release were determined as the ΔC_m 1 s and 2 s to 5 s after the flash, respectively. (D-E) Kinetic analysis of the capacitance traces revealed that the two burst components, fast and slow components, are unchanged. Error bars indicate standard error of the mean. *, $P < 0.05$; **, $P < 0.01$; ***, $P < 0.001$.

To test whether LDCV exocytosis is regulated by Baiap3, we stimulated chromaffin cells obtained from Baiap3 KO mice by flash photolysis of caged Ca^{2+} . We found that the sustained component of release was significantly increased by 30% in Baiap3 deficient cells ($P=0.031$, Figure 11C), whereas the exocytotic burst was unchanged (Figure 11B,D-E). However, normalization of the traces to the sustained component revealed no significant differences in the kinetics of the sustained phase (Figure 11A'), which argues against an effect that is specific to the sustained phase. Postflash $[\text{Ca}^{2+}]_i$ values were similar in WT and KO cells, indicating that the increase in sustained exocytosis was not due to differences in $[\text{Ca}^{2+}]_i$ (Figure 11A, top).

Mouse lines	Genotype	Burst fF	Fast Burst Component		Slow Burst Component		Sustained fF	No. of cells
Munc13-1	WT	432.9 ± 41	89.2 ± 8	17.5 ± 2	343.7 ± 59	0.38 ± 0.03	131.4 ± 16	28
	KO	267.3 ± 23	56.7 ± 7	21.3 ± 2	210.7 ± 38	0.28 ± 0.04	64.9 ± 9	32
Munc13-2	WT	389.4 ± 57	39.8 ± 9	19.7 ± 1	303.4 ± 135	0.36 ± 0.05	96.1 ± 17	21
	KO	275.7 ± 37	23.3 ± 4	20.0 ± 2	172.2 ± 44	0.38 ± 0.05	59.0 ± 11	22
Munc13-3	WT	314.2 ± 52					111.1 ± 20	15
	KO	318.9 ± 59					88.1 ± 14	12
Munc13-1/2	CTL*	358.2 ± 42	103.1 ± 16	17 ± 1	247 ± 36	0.35 ± 0.06	42 ± 12	12
	DKO	218.1 ± 28	60.1 ± 11	20 ± 2	140.1 ± 14	0.26 ± 0.04	10 ± 2	14
Munc13-1/2/3	CTL**	257.9 ± 22					55.7 ± 18	17
	TKO	201.7 ± 33					27.9 ± 9	13
Baiap3	WT	402.6 ± 27	58.4 ± 8	26.8 ± 5	344.2 ± 38	0.41 ± 0.04	121.3 ± 21	25
	KO	420.1 ± 31	95.2 ± 15	25 ± 5	324.8 ± 32	0.40 ± 0.04	200.8 ± 29	22

* Munc13-2 KO as a control for Munc13-1/2 DKO

** Munc13-2/3 DKO as a control for Munc13-1/2/3 TKO

Table 1. Comparison of LDCV exocytosis in all KO mouse lines analyzed

3.1.6 Depolarization Induced LDCV Exocytosis in Chromaffin Cells from Munc13-1/2 DKO and Baiap3 KO Mice

We have shown that LDCV exocytosis induced by uncaging Ca^{2+} in Munc13-1/2 DKO cells was drastically reduced in both the exocytotic burst and the sustained component of release. To investigate the effect of Munc13-1 and -2 deletion on LDCV exocytosis in response to a more physiological stimulus, chromaffin cells were stimulated with a voltage protocol consisting of six 10 ms depolarizations followed by four 100 ms depolarizations (Figure 12A top). The 10 ms depolarizations cause the fusion of the IRP, which corresponds to the fraction of the readily releasable vesicles that are closely associated with Ca^{2+} channels. The subsequent 100ms depolarizations elicit fusion of the remainder of the readily releasable pool (RRP), and the IRP and RRP together correspond to the fast component of flash photolysis experiments (Voets et al., 1999). Munc13-2 KO chromaffin cells responded the train of depolarizing stimuli with robust increases in membrane capacitance. In contrast to this, the secretory response was drastically reduced in chromaffin cells from Munc13-1/2 DKO cells. In chromaffin cells deficient for Munc13-1, and -2, exocytosis in response depolarization was significantly reduced. Both the IRP (Figure 12B, 7.7 ± 2 fF, $P=0.0009$) and the RRP (Figure 12C, 55.9 ± 7 fF, $P=0.0005$) in Munc13-1/2 DKO cells were reduced compared to Munc13-2 KO cells (Figure 12B, IRP: 33.8 ± 7 fF; Figure 12C, RRP: 108.7 ± 11 fF). Measurement of Ca^{2+} currents did not reveal significant differences between the Munc13-1/2 DKO and Munc13-2 KO chromaffin cells (Figure 12D). The reduction in both the IRP and the RRP is consistent with the reduction in the fast component seen in flash photolysis experiments (Figure 8D).

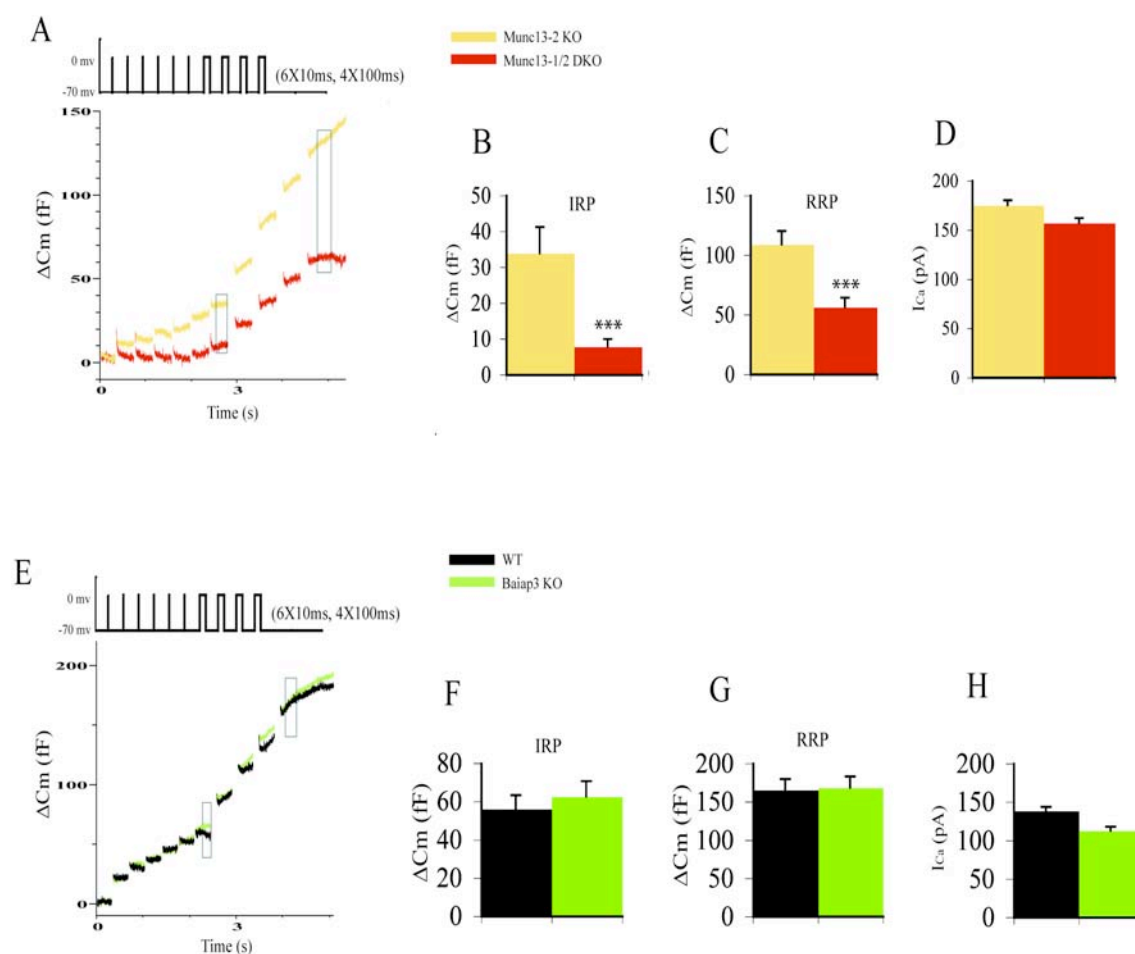


Figure 12. Depolarization induced exocytosis in chromaffin cells from Munc13-1/2 DKO and Baiap3 KO mice.

(A) Voltage protocol (top) and the resulting average capacitance increase in E18 chromaffin cells from Munc13-2 KO (15 cells from 3 mice, black line) and Munc13-1/2 DKO mice (17 cells from 3 mice, red line). Chromaffin cells were stimulated with trains of short depolarizations, and the Ca^{2+} current and membrane capacitance were monitored simultaneously before and after stimulation. (B) IRP ($P=0.0009$), determined as the average capacitance during the time period indicated by the left dashed rectangle in A. (C) RRP ($P=0.0005$), determined as the average capacitance during the time period indicated by the right dashed rectangle in A. (D) The average Ca^{2+} current was identical in the Munc13-2 KO and Munc13-1/2 DKO cells shown in A. (E) Voltage protocol (top) and resulting average capacitance increase in P0 chromaffin cells from WT (20 cells from 4 mice, Black line) and Baiap3 KO (32 cells from 4 mice, lime line) mice. Chromaffin cells were stimulated with trains of short depolarizations, and the Ca^{2+} current and membrane capacitance were monitored simultaneously before and after stimulation. (F) IRP, determined as the average capacitance during the time period indicated by the left dashed rectangle in E. (G) RRP, determined as the average capacitance during the time period indicated by the right dashed rectangle in E. (H) The average Ca^{2+} current was identical in the WT and Baiap3 KO cells shown in A. Error bars indicate standard error of the mean. *, $P < 0.05$; **, $P < 0.01$; ***, $P < 0.001$.

Since there was no selective reduction of the IRP, Munc13-1 and -2 do not appear to control the docking and priming of vesicles near Ca^{2+} , and our data consistently point to a general role for Munc13-1 and -2 in the docking/priming of vesicles in all release pools.

We also analyzed the response of Baiap3 KO cells to the depolarization protocol (Figure 12E top). Consistent with the previous finding that after flash photolysis the sustained component, but not the exocytotic burst was increased in Baiap3 KO cells (Figure 11), the voltage protocol consisting of six 10 ms depolarizations followed by four 100 ms depolarizations did not reveal any significant differences in the IRP (Figure 12F, 62.4 ± 7 fF) and RRP (Figure 12G, 167.9 ± 14 fF) of Baiap3 KO cells compared to WT cells (IRP; 55.6 ± 7 fF, RRP; 164.5 ± 14 fF). The Ca^{2+} currents of Baiap3 KO cells did not differ from those of WT cells (Figure 12E-H).

3.1.7 Reduced Exocytosis in Chromaffin Cells Overexpressing Baiap3

To confirm the finding that loss of Baiap3 leads to an increase in the sustained component of release, we examined whether the opposite situation, overexpression of Baiap3, would reduce the LDCV exocytosis. We overexpressed either EGFP or Baiap3 as an IRES (internal ribosome entry site)-EGFP construct with SFV in WT chromaffin cells. Expression of Baiap3 from the viral construct was confirmed by Western blot analysis of Baiap3-SFV infected BHK cells (Figure 13A). Complementary to the increase in exocytosis seen in the absence of Baiap3 (Figure 11), overexpression of Baiap3 resulted in a smaller capacitance change after flash photolysis of caged Ca^{2+} than overexpression of the EGFP control construct (Figure 13B).

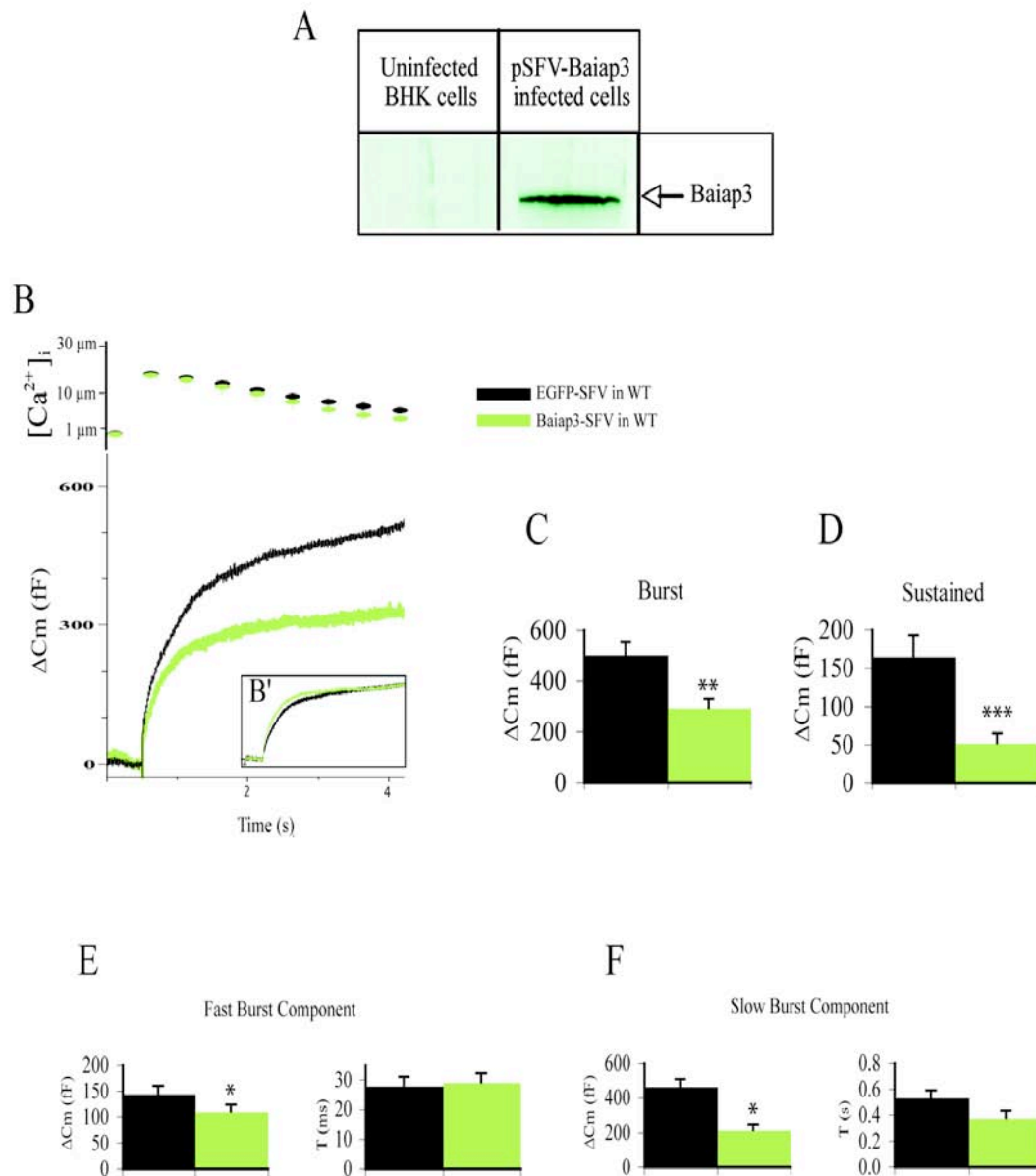


Figure 13. Reduced exocytosis in chromaffin cells overexpressing Baiap3.

(A) Overexpression of Baiap3-SFV in BHK cells. (B) Average ΔC_m in response to flash photolysis of NP-EGTA in P0 EGFP overexpressing WT cells (23 cells from 5 mice) and Baiap3 overexpressing WT cells (24 cells from 5 mice). The intracellular Ca^{2+} concentration following the flash is shown in the upper trace. (B') The Baiap3 KO trace was normalized to the WT amplitude at 4 s after the flash. (C-D) Comparison of the exocytotic burst ($P=0.008$) and sustained release ($P=0.0004$) in cells overexpressing EGFP and cells overexpressing Baiap3. The exocytotic burst and sustained release were determined as the ΔC_m 1 s and 2 s to 5 s after the flash, respectively. (E-F) Kinetic analysis of the capacitance traces revealed that the two burst components, fast ($P=0.014$) and slow ($P=0.025$), are both changed. Error bars indicate standard error of the mean. *, $P < 0.05$; **, $P < 0.01$; ***, $P < 0.001$.

Overexpression of Baiap3 significantly depressed both the exocytotic burst (Figure 13C, 293.3 ± 34.17 fF, $P=0.008$) and the sustained component (Figure 13D, 51.1 ± 12.8 fF, $P=0.0004$) in comparison to EGFP overexpressing cells (Figure 13C-D, 500.23 ± 51 fF (Burst), 165.1 ± 27.2 fF (Sustained)). We found that in the exocytotic burst of Baiap3 overexpressing cells both the fast (Figure 13E, 109.2 ± 12.1 fF, $P=0.014$) and the slow burst (Figure 13F, 209 ± 34 fF, $P=0.025$) were significantly smaller than in EGFP overexpressing cells (Figure 13E-F, 143.4 ± 16 fF (fast), 463.1 ± 40 fF (slow)).

The overpexpression of Baiap3 thus has the opposite effect of overexpressing Munc13-1 (Figure 9). However, like Munc13-1, Baiap3 does not appear to affect the kinetics of the exocytotic burst (Figure 13E-F) or the kinetics of the sustained component (Figure 13B'). Postflash $[Ca^{2+}]_i$ was also closely matched between EGFP- and Baiap3 overexpressing cells (Figure 13B, top).

In summary, our data indicate that Baiap3 reduces the number of fusion-competent vesicles and inhibits vesicle recruitment and priming during ongoing release while Ca^{2+} levels remain high.

3.2 Functional Characterizations of *Baiap3*

3.2.1 Basic Characterization of *Baiap3* KO Mice

Baiap3 deficient mice were generated by homologous recombination in mouse embryonic stem cell (Figure 14A). Targeting vector construction and gene targeting in ES cells was done by Dr. Iris Augustin.

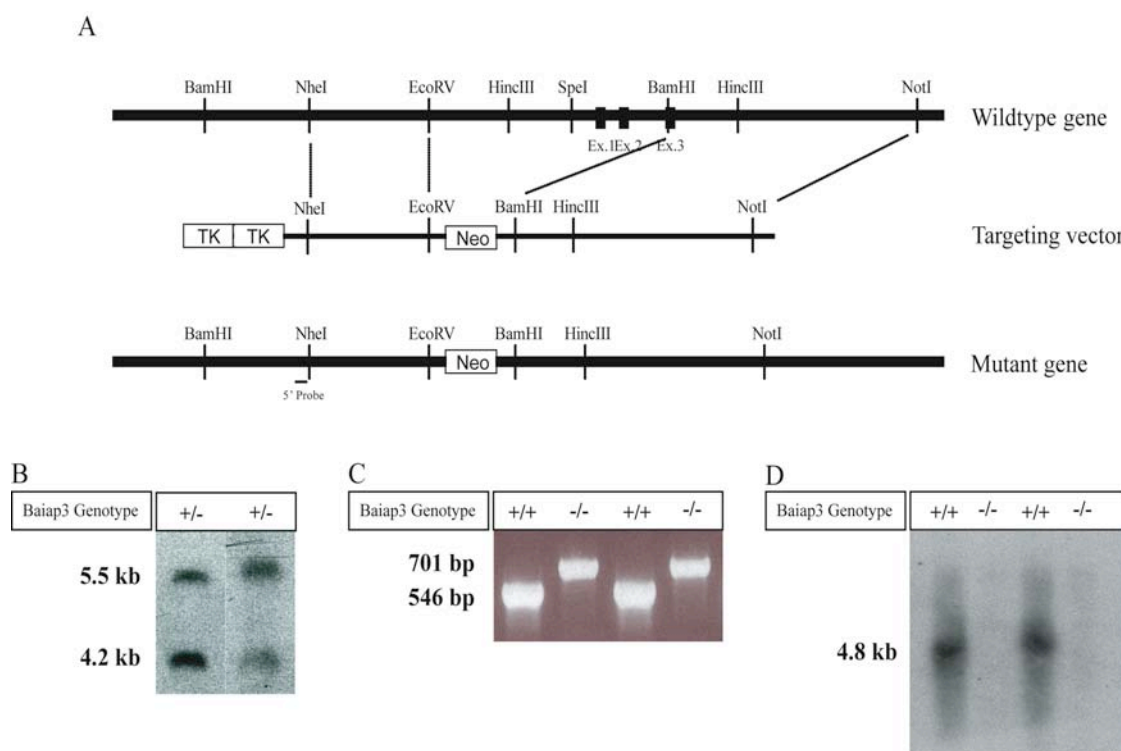


Figure 14. Gene targeting strategy to generate *Baiap3* KO mice.

(A) Targeting vector and *Baiap3* locus before and after homologous recombination. (B) Genomic Southern blot with an external 5' probe after BamHI digestion of stem cell DNA. Homologous recombination of the *Baiap3* targeting vector results in a shift of a WT 5.5 kb BamHI fragment to 4.2 kb. (C) Genomic PCR used for genotyping *Baiap3* litters with 546 bp for WT and 636 bp for the KO. (D) Northern blot analysis with a 3' probe that lies outside the deleted region shows that *Baiap3* mRNA is not expressed from the targeted locus.

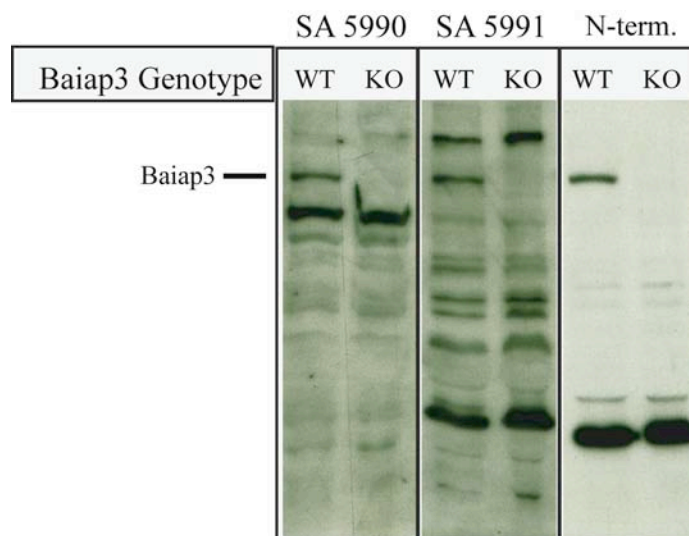


Figure 15. Specificity of Baiap3 antisera.

Specificity of Baiap3 antisera in mouse whole brain from WT and Baiap3 KO mice. SA5990 and SA5991 were generated in rabbit against the MHD to C-terminal region of Baiap3. The antibody against the N-terminus (Dr. Iris Augustin) was also generated in rabbit. All of antisera recognize Baiap3 in WT mice.

Baiap3 KO mice were obtained at the predicted Mendelian frequency. The respective genotypes were initially detected by Southern blotting (Figure 14B), by PCR for routine genotyping (Figure 14C), and by Northern blotting to check for mRNA expression (Figure 14D). Baiap3 KO mice are viable and fertile and show no obvious phenotypic changes in the cage environment. Litter sizes resulting from interbreeding of homozygous Baiap3 deficient animals were indistinguishable from those obtained with WT controls.

To verify Baiap3 protein expression level in WT and Baiap3 KO mice, we generated three polyclonal anti-Baiap3 antisera, which were raised to either the N-terminus or a region of Baiap3 encompassing the MHDs and C-terminus (Figure 15). Western blot analysis of homogenates from whole brain and other tissues showed that Baiap3 protein expression was completely abolished in homozygous Baiap3 KOs (Figure 16B).

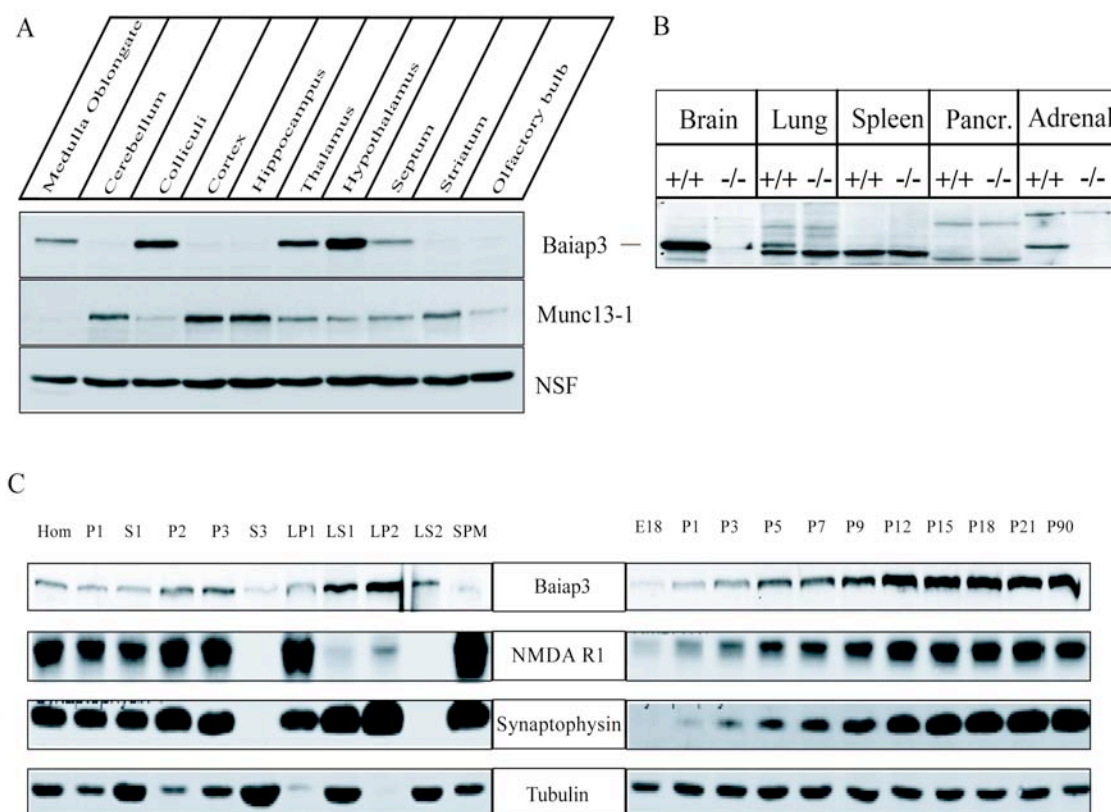


Figure 16. Protein Expression of Baiap3.

(A) Expression of Baiap3 in sub-regions of the brain and (B) brain, lung and adrenal gland. Baiap3 is not expressed in the pancreas and, in contrast to Munc13-4, is absent from spleen. Tissues were homogenized, and the proteins were separated by SDS-PAGE and analyzed by immunoblotting with antibodies to the indicated proteins. (C) Panels on the left show the distribution of Baiap3 in subcellular fractions of brain homogenate. Fractions (10 μ g protein per lane) were analyzed by SDS-PAGE and immunoblotting with antibodies to the indicated proteins. Hom, Homogenate; P1, nuclear pellet; P2, crude synaptosomal pellet; P3, light membrane pellet; LP1, lysed synaptosomal membranes; LP2, crude synaptic vesicle fraction; SPM, synaptic plasma membranes; S1, supernatant after synaptosome sedimentation; S3, cytosolic fraction; LS1, supernatant after LP1 sedimentation; LS2, cytosolic synaptosomal fraction. Panels on the right show the expression of Baiap3 during development from E18 to P90 (Dr. Iris Augustin). Immunoblotting was done with antibodies to the indicated proteins.

The absence of Baiap3 expression did not affect the protein levels of any of the proteins involved in vesicle exocytosis that we investigated (Figure 17A). These included other members of the Munc13 protein family (Munc13-1, -2, and -3), SNARE

core complex components (Syntaxin, SNAP-25, and Synaptobrevin), and the SNARE regulatory protein Munc18 (Figure 17A). In order to determine where in the brain Baiap3 is expressed, we performed Western blot analysis on sub-regions of the brain. Baiap3 expression is most prominent in the hypothalamus, thalamus, colliculi, septum and in the brain stem. Unlike Munc13-1 and Munc13-2, Baiap3 is not strongly expressed in hippocampus (Figure 16A). To study developmental regulation and subcellular distribution of Baiap3 protein in WT mice, we analyzed the expression level by Western blotting. The expression level of Baiap3 was very low at E18 and increased during postnatal development to reach a plateau at P12-P18 (Figure 16C). In the subcellular fractionation, Baiap3 was enriched in the crude synaptic vesicle fraction (LP2). However, unlike Munc13-1 and NMDA R1 (the postsynaptic density component marker), Baiap3 is not enriched in synaptic plasma membrane (SPM) (Figure 16C).

Among the Munc13 family members, Munc13-4 is the isoform most closely related to Baiap3 (Koch et al., 2000). However, unlike the other Munc13s and Baiap3, Munc13-4 is not expressed in neurons. Like Munc13-4, Baiap3 is also expressed in lung and adrenal gland (Figure 16B). Furthermore, we found that Munc13-1, -2, -3 and Baiap3 are expressed in mouse adrenal gland (Figure 17A). We did not detect any alterations in the expression levels of Munc13 isoforms and SNARE core complex components in Baiap3 deficient adrenal glands. The expression level of Chromogranin A, an LDCV marker, was also not changed (Figure 17A). Baiap3 was initially identified as a binding partner BAI1 in a yeast two-hybrid screen (Shiratsuchi et al., 1998). The significance of this interaction has not been determined and we found no alteration of the BAI1 protein expression level in Baiap3 KO brain homogenate (Figure 17A).

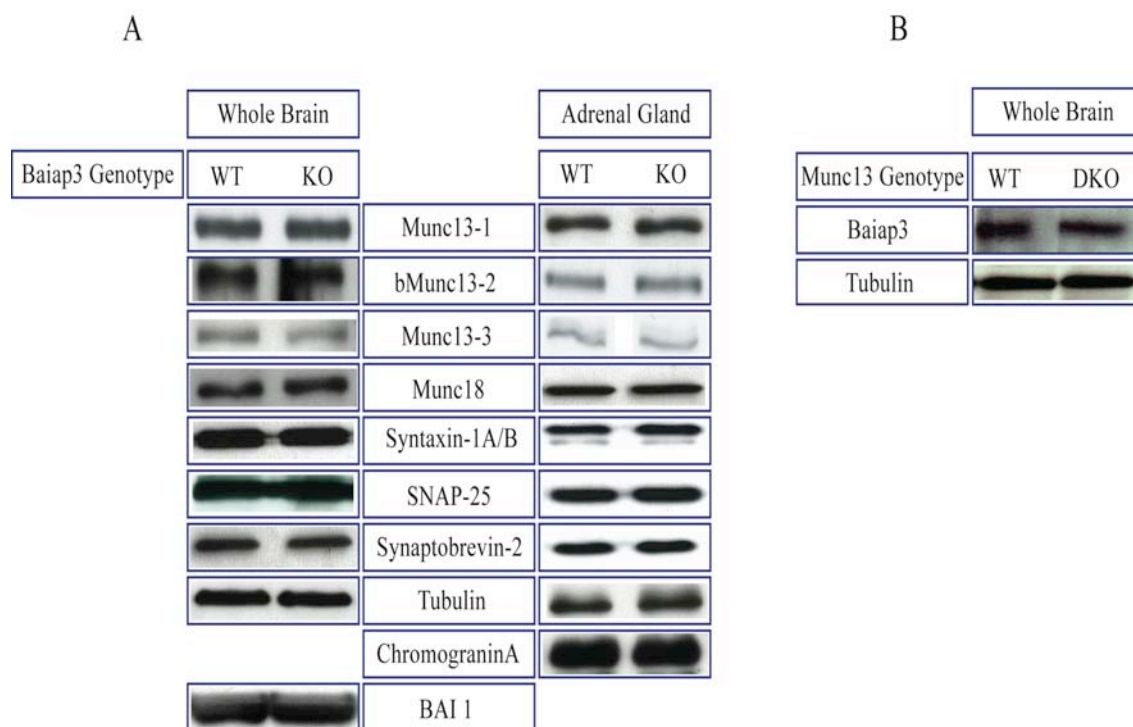


Figure 17. Immunoblot analysis of adult whole brain and adrenal gland.

(A) Expression of SNARE complex components and SNARE regulatory proteins in whole brain and adrenal gland from WT and Baia3 KO mice. (B) Expression of Baia3 protein in whole brain of Munc13 DKO and WT mice. Whole brain and adrenal glands from mice were homogenized, and protein (10 µg for brain, and 20 µg for adrenal gland per lane) was analyzed by SDS-PAGE and immunoblotting with antibodies to the indicated proteins.

We also checked whether Baia3 expression might be altered in the absence of Munc13-1 and -2, but found not differences of Baia3 protein levels between WT and Munc13-1/2 DKO brains (Figure 17B). While Baia3 shows a more restricted expression level in the brain than Munc13-1 and Munc13-2, Baia3 and Munc13-1, -2, and -3 are coexpressed in mouse adrenal gland, and, based on the electrophysiological analysis of the adrenal chromaffin cells, all serve to regulate LDCV exocytosis.

3.2.2 Baiap3 Binds to Both Munc13-1 and Syntaxin 1

Munc13s are essential regulators of SNARE-mediated exocytosis of SVs. Munc13-1 binds not only Syntaxin 1 but also other SNARE core components (Betz et al., 1997). In order to determine whether Baiap3 also bound to SNARE core complex components we performed co-sedimentation assays by using recombinant GST fusion protein constructs. GST-Syntaxin-1A was able to bind not only Munc13-1, but also bound Baiap3 in co-sedimentation assays performed with recombinant Munc13-1 or Baiap3 expressed in HEK 293FT cells (Figure 18A).

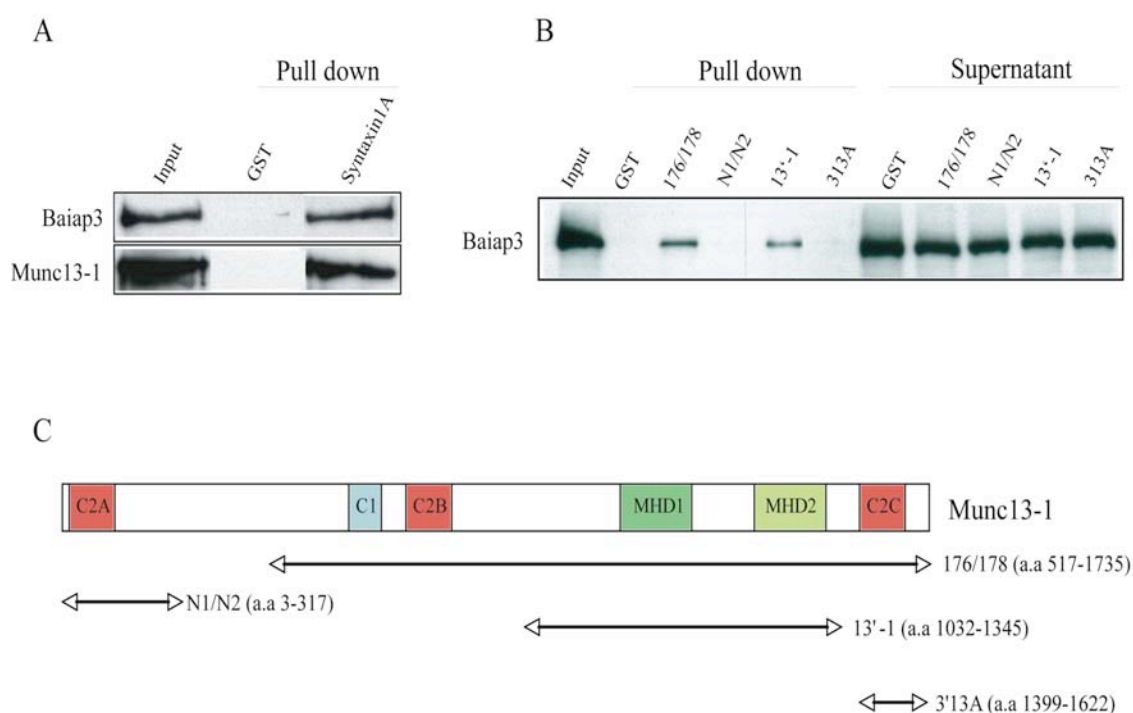


Figure 18. Baiap3 binds to Syntaxin and the MHDs of Munc13-1.

(A) Representative co-sedimentation assays of GST-fused-Syntaxin 1A (a.a.1-276) and of GST alone with Baiap3 or Munc13-1 produced in HEK293FT cells. Munc13-1 was used as a positive control for Syntaxin binding and HEK 293FT cells were transfected with either MYC-Baiap3 or EGFP-Munc13-1. (B) Representative co-sedimentation assays of several GST-fused Munc13-1 fragments and of GST alone with Baiap3 produced in HEK293FT cells. (C) Domain structure of Munc13-1 and representation of GST-Munc13-1 fusion constructs; pGEX-Munc13-1-176/178 (a.a 517-1735), pGEX-Munc13-1-N1/N2 (a.a 3-317), pGEX-Munc13-1-13'1 (a.a 1032-1345), and pGEX-Munc13-1-3'13A (a.a 1399-1622).

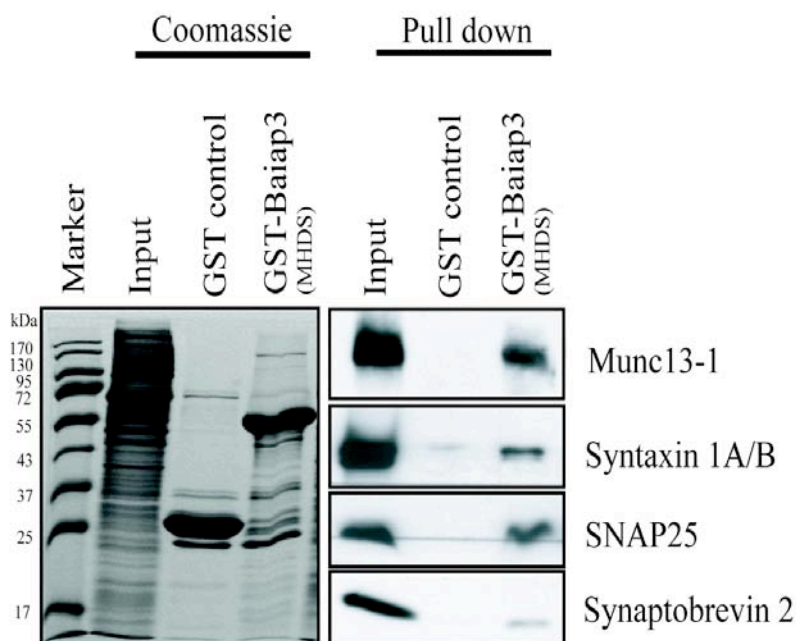


Figure 19. Binding of SNARE complex core components and Munc13-1 to a recombinant Baiap3 fragment encompassing the MHDs.

GST-Baiap3-MHDs-fusion protein and GST alone as a control were used for cosedimentation assays. Binding of Syntaxin 1A/B, SNAP-25, Synaptobrevin 2 and Munc13-1 was assayed by SDS-PAGE, and immunoblotting.

To determine whether Baiap3 also interacts with Munc13-1, we used recombinant protein fragments of Munc13-1. Recombinant GST-Munc13-1 fusion fragments (Betz et al., 1997; Figure 18C) were used in co-sedimentation assays with cell lysate from HEK293FT cells expressing Baiap3, and bound material was assayed for by immunoblotting. Two Munc13-1 constructs, pGEX-Munc13-1-176/178 (a.a 517-1735) and pGEX-Munc13-1-13'1 (a.a 1032-1345), were capable of binding to Baiap3 (Figure 18B). The overlapping regions of the two constructs contain the MHDs of Munc13-1, a region that is also involved in binding Syntaxin 1A.

To test whether Baiap3 is also able to bind Syntaxin and Munc13-1 in a more native context, we used a GST-Baiap3-MHDs fusion protein in a co-sedimentation assay with mouse whole brain homogenate. The GST-Baiap3-MHDs construct pulled down not only Munc13-1 but also SNARE core complex components (Syntaxin 1A/B, SNAP-25 and Synaptobrevin 2) (Figure 19).

These data indicate that Baiap3 interacts with Syntaxin 1 and Munc13-1, and may be associated with the SNARE core complex by binding to Syntaxin 1 and/or Munc13-1. In these experiments, we attempted to use recombinant soluble Baiap3. However, Baiap3 fragments containing the MHD domains are highly insoluble when expressed in *E. coli*, and Baiap3 expressed in HEK293FT cells was mostly recovered in the detergent insoluble membrane fraction and we could not obtain a soluble sample of Baiap3. We do not know whether the detergent insolubility of Baiap3 overexpressed in cells was due to the formation of insoluble aggregates or its association with cytoskeletal elements.

4. Discussion

This is the first study to systematically investigate the role of the Munc13 protein family in LDCV exocytosis. We found that Munc13-1, Munc13-2, which were known to be essential positive regulators of SNARE-mediated exocytosis of neuronal SVs, also control LDCV exocytosis in chromaffin cells. Remarkably, one member of this protein family, Baiap3, seems to suppress LDCV exocytosis in chromaffin cells, making Baiap3 the first Munc13 homologue for which a negative regulatory function in exocytosis has been described.

4.1 Munc13s are Positive Regulators of LDCV Exocytosis

Munc13s are essential for the exocytosis of neuronal SVs in invertebrates as well as in mammals (Augustin et al., 1999b; Varoqueaux et al., 2002; Richmond et al., 1999; Aravamudan et al., 1999). However, their physiological role in mammalian LDCV exocytosis had previously only been examined by overexpression of either Munc13-1 or Munc13-2 in WT chromaffin cells (Ashery et al., 2000; Stevens et al., 2005; Zikich et al., 2008). The three Munc13 isoforms whose role in neuronal SV exocytosis has been established, Munc13-1, -2 and -3, are also found in bovine chromaffin cells (Ashery et al., 2000; Zikich et al., 2008) and in mouse adrenal gland (Figure 17). To examine the role of endogenous Munc13s in Ca^{2+} triggered LDCV exocytosis, we studied exocytosis in chromaffin cells taken from Munc13-1, -2, -3 and Baiap 3 deficient mice, using flash photolysis of caged Ca^{2+} . Flash photolysis protocols cause a sudden uniform increase in the concentration of intracellular Ca^{2+} throughout the cell, triggering an exocytotic burst of LDCV release that is followed by a slower, sustained component of release. The

burst component consists of those vesicles that were already in a fusion competent, i.e. docked and primed state, at the time of the stimulus, whereas the sustained component consists of vesicles that undergo Ca^{2+} -dependent docking, priming and release while Ca^{2+} levels remain high (Neher, 2006). However, the pool of vesicles released in the burst phase and those released during the sustained phase are a continuous pool of vesicles in the sense that they need to go through the same maturation steps, i.e. docking and priming prior to release.

Among the four mouse lines studied, the most drastic reduction of release seen in the absence of a single Munc13 isoform, was detected in the Munc13-1 deficient chromaffin cells. Without Munc13-1, the secretory burst was reduced by 40% and the sustained component by 50% (Figure 6, Figure 20). In Munc13-2 deficient chromaffin cells, the reduction of the burst phase and the sustained phase was only 30% and 40%, respectively, which was statistically not significant (Figure 7, Figure 20). However, in chromaffin cells lacking both Munc13-1 and -2, the reduction in burst and sustained release was greater than in both single knockouts, indicating that Munc13-2 also functions to regulate LDCV exocytosis (Figure 8, Figure 20). The absence of Munc13-3 on the other hand, had no significant effect on either the burst or sustained phase of release (Figure 10, Figure 20). In addition to the distinction between the burst phase of release and the sustained phase, analysis of the kinetics of release during the burst phase reveals the presence of a slow and a fast burst components, which is thought to represent different states of the fusion machinery that translate into differences in the “readiness” of docked and primed vesicles to fuse (Neher, 2006). The state of the fusion machinery that is responsible for the slow burst seems to be a precursor of the configuration that mediates the fast burst (Voets et al. 1999). Since Munc13s are thought to function in the docking/priming of vesicles, their absence should affect both

the fast and the slow burst components, as is the case for most manipulations of the size of the burst pool (Neher 2006). In line with this assumption, in Munc13-1 and Munc13-1/2 DKO cells, i.e. those genotypes with a significant reduction in the exocytotic burst, both the slow and the fast burst component were reduced, without any significant change in the time constants (Figure 6D,E and Figure 8D,E).

Our study is the first report of a deficit in LDCV exocytosis from chromaffin cells in Munc13 deficient animals, and establishes that endogenous Munc13-1 and Munc13-2 regulate LDCV exocytosis in chromaffin cells. Since both the burst and the sustained component of release were reduced, without any change in their kinetics (Figures 6-8) our data are best explained by a model in which Munc13-1 and -2, in principle, have equivalent roles as docking/priming factors in establishing the pool of release ready vesicles (vesicles released during the burst phase) and in the Ca^{2+} -dependent docking/priming of new LDCVs during the sustained phase of release. Munc13-1 may be more efficient in mediating the docking/priming process, its absence thus having the greatest effect. However, the apparent differences in priming efficiency between Munc13-1, -2 and -3 could of course also be due to differences in the level of protein present in chromaffin cells. Unfortunately, we were not able to compare proteins levels directly, because the amount of protein that could be obtained from cultured chromaffin cells was too low, and whole adrenal glands also contain synapses, presumably with unknown amounts of different Munc13 isoforms. Somewhat surprisingly, while deletion of Munc13-1 and -2 completely eliminates SV exocytosis in cultured hippocampal neurons (Augustin et al., 1999b; Varoqueaux et al., 2002), LDCV exocytosis was not completely abolished even in the absence of Munc13-1 -2 and -3 (Figure 10D-F). Munc13-independent neurotransmitter release has however been described for the neuromuscular junction (Varoqueaux et al., 2005). In chromaffin cells, docking and

priming of LDCVs therefore appears to involve other regulatory proteins, whose identity and function of remains to be investigated. Potentially Caps proteins, which are involved in SVs exocytosis in mammalian neurons (Jockusch et al., 2007) as well in LDCV exocytosis in chromaffin cells (Elhamadani et al., 1999; Liu et al., 2008) and in *C. elegans* (Speese et al., 2007, Zhou et al., 2007) could be responsible for the residual LDCV release in the absence of Munc13s. Yet, Caps and Munc13 do not perform the same function in the docking/priming reaction, since overexpression of one does not rescue the phenotype seen in the absence of the other (Jockusch et al., 2007), which argues against this theory. Two other obvious candidates that might be responsible for LDCV exocytosis in the Munc13-1, -2, -3 TKOs, would be the two remaining members of the Munc13 protein family, Munc13-4 and Baiap3. However, we were unable to detect Munc13-4 in adrenal gland by Western blotting (data not shown), and based on our analysis of the role of Baiap3 in chromaffin cells, Baiap3 is a negative rather than a positive regulator of LDCV exocytosis.

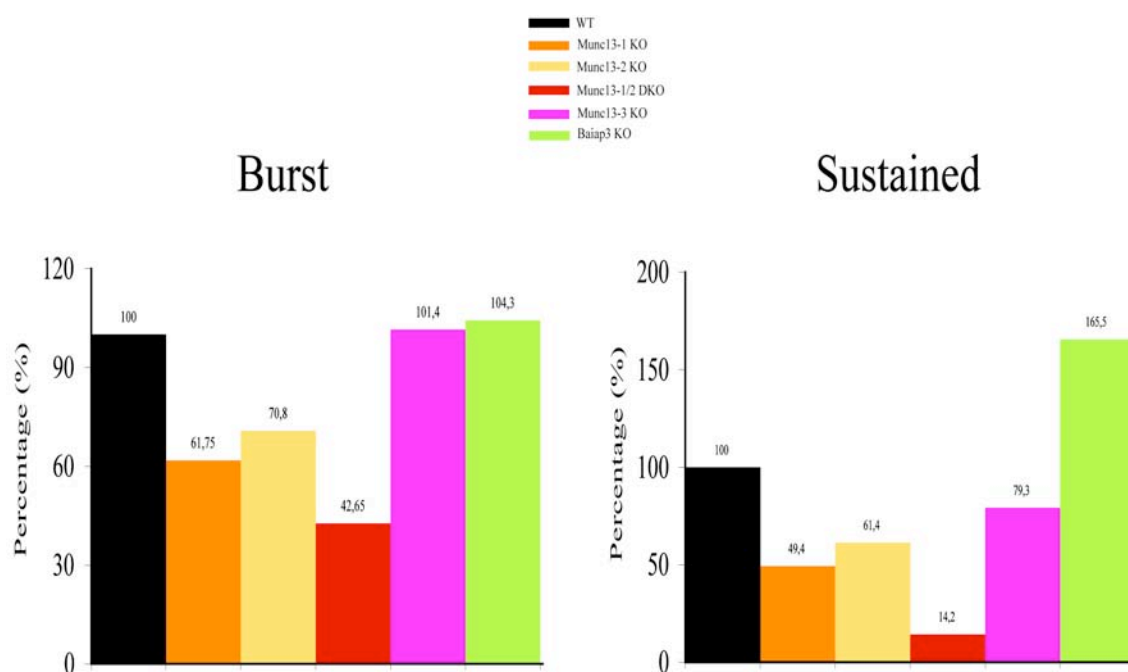


Figure 20. Relative amplitude sizes of the burst and sustained phases of LDCV exocytosis in the absence of Munc13-1, Munc13-2, Munc13-1/2, Munc13-3 and Baiap3.

4.2 Baiap3/Bap3 is a Negative Regulator of LDCV Exocytosis.

Baiap3 was first identified and named as a binding partner of the brain specific angiogenesis inhibitor I (BAI1), which encodes a seven span transmembrane protein, which belongs to the adhesion-type G-protein-coupled receptor family (Shiratsuchi et al., 1998). Evolutionarily, Baiap3 appears to be related to Munc13s, its domain structure is homologous to the Munc13 C-terminal half which features two Munc-homology-domains (MHDs) flanked by C2 domains (Shiratsuchi et al., 1998; Koch et al., 2000). Based on sequence similarity, the closest relative of Baiap3 is the non-neuronal isoform Munc13-4 (Figure 21; Table 2; Koch et al., 2000), which is essential for exocytosis of secretory granules from cells of the hematopoietic lineage (Feldmann et al., 2003; Neeft et al., 2005).

Because all Munc13 isoforms whose function had been analyzed previously were found to be positive regulators of SNARE-mediated exocytosis, we were surprised to discover that LDCV exocytosis was in fact enhanced, rather than reduced in the absence of Baiap3 (Figure 11). Conversely, when we overexpressed Baiap3 in WT chromaffin cells, LDCV exocytosis was dampened, indicating that Baiap3 negatively regulates LDCV exocytosis (Figure 13). In flash photolysis experiments using Baiap3 KO chromaffin cells, only the sustained component was increased, whereas overexpression suppressed both the burst and the sustained component of release. This suggests that Baiap3 suppresses both the pre-burst docking/priming of vesicles and the recruitment of new vesicles at elevated Ca^{2+} levels.



Figure 21. Protein Sequence Comparison of the C2 domains and the MHDs of Munc13 isoforms and Baiap3.

	VS	Munc13-2	Munc13-3	Munc13-4	Bap3
Munc13-1	C2B	100% (109/109)	90.8% (99/109)	31.2% (34/109)	15.6% (17/109)
	MHD1	81.3% (117/144)	79.9% (115/144)	13.2% (19/144)	14.6% (21/144)
	MHD2	70.8% (119/168)	64.9% (109/168)	13.7% (23/168)	17.3% (29/168)
	C2C	99.2% (129/130)	66.2% (86/130)	23.1% (30/130)	21.5% (28/130)

Table 2. Percent identity of the domain structure of Munc13s and Baiap3.

To further analyze the effect of Munc13-1/2 and Baiap3 on the release-ready vesicle pool, we also stimulated Munc13-1/2 DKO and Baiap3 KO cells by depolarization. Depolarization protocols do not lead to the sudden uniform increase in the intracellular Ca^{2+} concentration achieved by flash photolysis, because the Ca^{2+} enters the cell via voltage gated Ca^{2+} channels, allowing the experimental distinction between vesicles docked in the vicinity of Ca^{2+} channels and those docked at a greater distance based on their release kinetics (Schneggenburger and Neher, 2005). The immediately releasable pool (IRP) seen with depolarization is thought to represent those vesicles docked/primed closest to the Ca^{2+} channels, they are also released during the fast burst in flash photolysis experiments, but due to the uniform increase in intracellular Ca^{2+} do not show up as a separate pool (Voets et al., 1999). According to the model of LDCV exocytosis refined by Voets and colleagues (1999), the relationship between the vesicle pools mobilized by depolarization and by those release after flash photolysis is as follows: The IRP and the readily releasable pool (RRP) of vesicles released by depolarization together correspond to the fast burst pool of flash photolysis experiments

(Figure 22), whereas the vesicles of the slow burst component and those of the sustained component are not released in response to our depolarization protocol.

Baiap3 KO cells, which showed no reduction in the fast or slow burst component after flash photolysis, also showed no deficit in the IRP or RRP released in response to depolarization (Figure 12E-H). Munc13-1/2 deficient cells on the other hand, which did have a deficit in the slow and the fast burst phase in responses to flash photolysis, also showed a deficit in the IRP and RRP exocytosis elicited by depolarization (Figure 12A-D). Thus, neither Baiap3 nor Munc13-1 and Munc13-2 appear to be essential for selective docking/priming of vesicles in close vicinity of Ca^{2+} channels.

Taken together, our analyses of Munc13 and Baiap3 deficient chromaffin cells suggest that Baiap3 functions as a negative regulator of the same steps in LDCV exocytosis that are facilitated by Munc13-1 and Munc13-2. The fact that the exocytotic burst was not affected in Baiap3 KO cells, but suppressed when Baiap3 was overexpressed, can be explained if endogenous Baiap3 levels are not high enough to interfere with the establishment, i.e. docking and priming, of a WT-sized pool of vesicles when the cell has not been stimulated, but sufficiently high to impair the recruitment of new vesicles at times of high demand, i.e. during ongoing release. We therefore propose a model in which Baiap3 acts as an antagonist in the docking/priming reaction that requires Munc13-1 and Munc13-2 and is necessary to establish the release ready pool of vesicles as well as their Ca^{2+} stimulated re-supply (Figure 22).

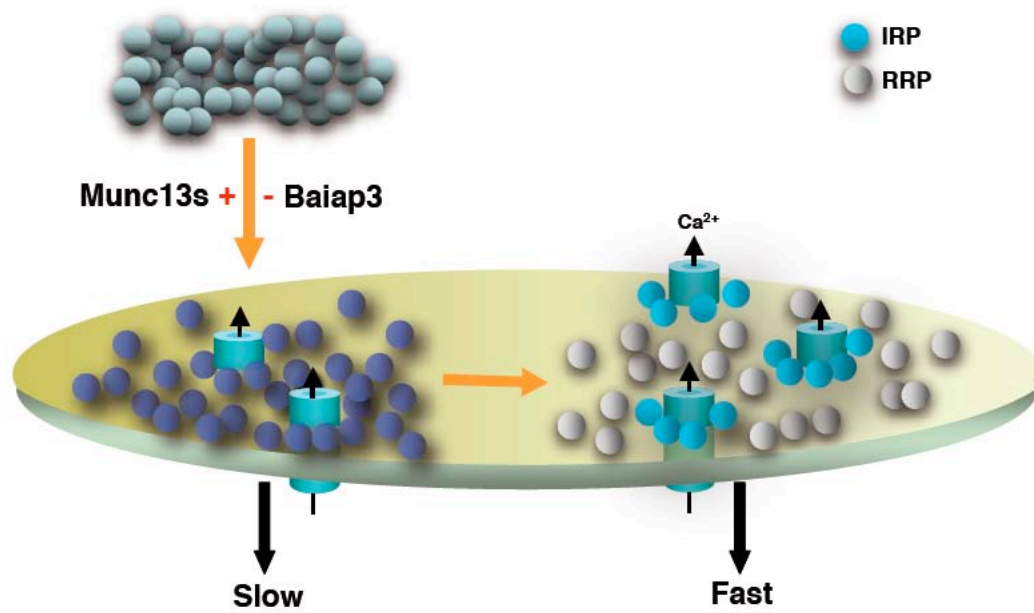


Figure 22. Munc13s and Baiap3 control LDCV exocytosis. Munc13s are positive regulators and Baiap3 a negative regulator in recruiting LDCVs for release and thus function upstream of both the slow and the fast pool of release-ready vesicles.

4.3 Munc13s and Baiap3 as Regulators of SNARE-Mediated Exocytosis

The docking and priming reactions that occur before a vesicle reaches fusion competence require SNARE proteins and SNARE regulatory proteins like Munc13 and Munc18 (Augustin et al., 1999b; Jahn and Scheller, 2006; Varoqueaux et al., 2002; Verhage et al., 2000; Voets et al., 2001; Weimer et al., 2003). Munc13s are thought to facilitate SNARE complex formation by keeping Syntaxin in an open conformation (Betz et al., 1997; Brose et al., 2000; Richmond et al., 2001). Although SNARE complex formation was originally thought occur downstream of a separate vesicle

docking step (Broadie et al., 1995; Hunt et al., 1994; Sørensen et al., 2003; Voets et al. 2001; Washbourne et al., 2002), more recent evidence indicates that at least in *C. elegans* both Syntaxin and Unc-13 are required for vesicle docking. Docking defects in *unc-13* mutant worms are rescued by the open form of Syntaxin, which indicates that SNARE complex formation may equal vesicle docking, with Unc-13 acting upstream of SNARE assembly (Hammerlund et al., 2007). In *C. elegans*, docking and exocytosis of SVs appears to require Unc-13 and Syntaxin, whereas docking and exocytosis of large dense core vesicles involves Caps and Syntaxin (Hammarlund et al., 2007; Hammarlund et al., 2008; Speese et al., 2007; Zhou et al., 2007), with Unc-13 playing a potential auxiliary role (Zhou et al., 2007; Hammarlund et al., 2008). By contrast, a clear division of labor between Munc-13 and Caps proteins in the regulation of SV and LDCV exocytosis does not appear to be a feature of the mammalian system. In mouse neurons, effective excitation-secretion coupling of SVs requires both Munc13 and Caps proteins (Jockusch et al. 2007), and our study shows that LDCV exocytosis, which has previously been shown to require Caps (Elhamadani et al., 1999; Liu et al., 2008), is also regulated by Munc13-1 and -2. Since physical docking of LDCVs in chromaffin cells also requires Syntaxin (de Wit et al., 2006), we propose that Munc13-1 and Munc13-2 regulate LDCV exocytosis by acting upstream of SNARE complex assembly, which does however not exclude the possibility that they have additional functions within the fusion machinery.

Our electrophysiological analysis of the role of Baiap3 in LDCV exocytosis suggests that Baiap3 acts as a negative regulator at the same step that requires Munc13-1 and -2. This notion is also supported by our biochemical data, which show that Baiap3 can bind to Syntaxin1 as well as to Munc13-1. It is therefore conceivable that Baiap3 and other Munc13 isoforms compete for binding to Syntaxin and other SNARE complex

components. Although we were unable to show that Baiap3 interferes with the binding of Munc13-1 to Syntaxin1, this may be an experimental limitation due to the fact that Munc13 does not interact with purified Syntaxin in solution (Basu et al., 2005) and the interaction therefore most likely requires additional factors. Because of the limited sequence similarity of Munc13-1 and Baiap3 (Table 2), they are unlikely to share all interaction partners, and binding of Baiap3 to Syntaxin may thus result in a configuration that is unfavorable to SNARE complex assembly

Other components of the fusion machinery for which a negative regulatory function in LDCV exocytosis has been reported are Amysin, Tomosyn (Yizhar et al., 2004; Constable et al., 2005) and Complexins (Archer et al., 2002; Itakura et al., 1999). Amysin and Tomosyn are a Syntaxin binding proteins with a C-terminal SNARE motif able form a fusion-incompetent SNARE complex with Syntaxin and SNAP-25 (Fujita et al., 1998; Scales et al., 2002; Pobbati et al., 2004; Groffen et al., 2005;). In *C. elegans*, Tomosyn antagonizes Unc-13-dependent release (Gracheva et al., 2006; McEwen et al., 2006) and also negatively regulates CAPS-dependent peptide release from dense core vesicles (Gracheva et al., 2007). By comparison, the evidence that Complexins are negative regulators of exocytosis is weak, because although overexpression impairs exocytosis (Archer et al., 2002; Itakura et al., 1999), their deletion does the same (Reim et al., 2001), suggesting that their in vivo function is not an inhibitory one. In our case, the overexpression and deletion of Baiap3 resulted in compatible data sets, i.e. overexpression reduced LDCV exocytosis and deletion enhanced it. Since the effect of overexpression was greater than the effect of deletion, the efficacy of Baiap3 in interfering with Munc13-dependent docking/priming appears to be sensitive to the relative protein levels of Baiap3 and the other Munc13s. High levels of Baiap3 could

potentially sequester Syntaxin or Munc13, or both, thereby lowering the rate at which productive SNARE complexes are formed. However, the question remains, whether inhibition of LDCV exocytosis is the “true” function of Baiap3, or whether it is also a docking/priming factor, albeit a less efficient one.

To answer the open questions with respect to the mechanism of Baiap3 function it will also be necessary to determine its function in neurons. In the brain, Baiap3 has a more restricted expression pattern than Munc13-1 and Munc13-2, with prominent expression seen in hypothalamus, amygdala, periaqueductal grey, septum and several brainstem nuclei. We did not find obvious alterations in synaptic release of glutamate or GABA from cultured hypothalamic neurons, arguing against a function of Baiap3 in suppressing SV exocytosis. However, we were unable to reliably detect Baiap3 expression by staining cultured neurons (data not shown), and it remains to be investigated whether those neurons that express Baiap3 in the intact brain survived in our cultures. Potentially, Baiap3 could also function as a regulator of LDCV exocytosis in neurons, and/or be involved in the vesicular release of neurotransmitters other than GABA and glutamate.

4.4 Conclusions

I set out to determine whether mammalian LDCV exocytosis requires the same Munc13 isoforms that are essential for SV exocytosis, or whether the Munc13 relative Baiap3 might be more important for LDCV release. Two of the three neuronal Munc13 isoforms, Munc13-1 and Munc13-2, do indeed regulate LDCV exocytosis from mouse

chromaffin cells, and thus play a more significant role in LDCV exocytosis than their *C.elegans* counterpart Unc-13. I found that Baiap3 is also a regulator of LDCV exocytosis, but against all expectations, it functions to suppress LDCV exocytosis, making it the first member of the Munc13 protein family for which a negative regulation of SNARE-mediated exocytosis has been described.

4.5 Future Studies

Future experiments to further delineate the role of Munc13s and Baiap3 in mammalian LDCV exocytosis will include ultrastructural analysis of possible LDCV docking defects in Munc13-1/2 and Baiap3 deficient chromaffin cells by electron microscopy. Docking defects in the in Munc13 deficient neurons have not been described (Varoqueaux et al. 2002), however, it is possible that such docking defects were missed due to fixation artifacts (Hammerlund et al. 2008). In *C.elegans*, the Unc-13 docking deficit, as well as the functional release deficit was rescued if Tomosyn was deleted as well, implying that Unc-13 and Tomosyn are true functional antagonists (Gracheva et al., 2006; McEwen et al., 2006). Comparison of the number of docked vesicles in Munc13-1/2 KO and Baiap3 KO cells, combined with functional analysis of LDCV exocytosis in Munc13-1/2/Baiap3 triple deficient cells, may thus answer the question whether the same is true for Baiap3 and Munc13s.

5. References

- Allersma, M.W., Wang, L., Axelrod, D., and Holz, R.W. Visualization of regulated exocytosis with a granule-membrane probe using total internal reflection microscopy (2004). *Mol Biol Cell* 15, 4658-4668.
- Andrew-Zwilling, YS., Kawabe, H., Reim, K., Varoqueaux, F., and Brose, N. Binding to Rab3a-interacting-molecule RIM regulates the presynaptic recruitment of Munc13-1 and ubMunc13-2 (2006). *J Biol Chem* 281, 19720-19731.
- Aravamudan, B., Fergested, T., Davis, WS., Rodesch, CK., and Broadie, K. *Drosophila* Unc-13 is essential for synaptic transmission (1999). *Nat Neurosci* 2, 965-971.
- Archer, DA., Graham, ME., and Burgoyne, RD. Complexin regulates the closure of the fusion pore during regulated vesicle exocytosis (2002). *J Biol Chem* 277, 18249-18252.
- Ashery, U., Betz, A., Xu, T., Brose, N., and Rettig, J. An efficient method for infection of adrenal chromaffin cells using the semliki Forest virus gene expression system (1999). *Eur J Cell Biol* 78, 525-32.
- Ashery, U., Varoqueaux, F., Voets, T., Betz, A., Thakur, P., Koch, H., Neher, E., Brose, N., and Rettig, J. Munc13-1 acts as a priming factor for large dense-core vesicles in bovine chromaffin cells (2000). *EMBO J* 19, 3586-3596.
- Augustin, I., Betz, A., Herrmann, C., Jo, T., and Brose, N. Differential expression of two novel Munc13 proteins in rat brain (1999a). *Biochem J* 337, 363-371.
- Augustin, I., Rosenmund, C., Südhof, TC., and Brose, N. Munc13-1 is essential for fusion competence of glutamatergic synaptic vesicles (1999b). *Nature* 400, 457-461.
- Augustin, I., Korte, S., Rickmann, M., Kretschmar, H.A., Südhof, T.C., Herms, J.W., and Brose, N. The Cerebellum-specific Munc13 isoform Munc13-3 regulates cerebellar synaptic transmission and motor learning in Mice (2001). *J Neurosci* 21, 10-17.

- Bai, J., and Chapman, ER. The C2 domains of Synaptotagmin partners in exocytosis (2004). *Trends Biochem Sci* 29, 143-151.
- Bai, J., Wang, CT., Richards, DA., Jackson, MB., and Chapman, ER. Fusion pore dynamics are regulated by synaptotagmin t-SNARE interactions (2004). *Neuron* 41, 929-942.
- Basu, J., Shen, N., Dulubova, I., Lu, J., Guan, R., Guryev, O., Grishin, N.V., Rosenmund, C., and Rizo, J. A minimal domain responsible for Munc13 activity (2005). *Nat Struct Mol Biol* 12, 1017-1018.
- Becherer, U., and Rettig, J. Vesicle pools, docking, priming, and release (2006). *Cell Tissue Res* 326, 393-407.
- Betz, A., Ashery, U., Rickmann, M., Augustin, I., Neher, E., Südhof, TC., Rettig, J., and Brose, N. Munc13-1 is a presynaptic phorbol ester receptor that enhances neurotransmitter release (1998). *Neuron* 21, 123-136.
- Betz, A., Okamoto, M., Benseler, F., and Brose, N. Direct interaction of the Rat unc-13 homologue Munc13-1 with the N terminus of Syntaxin (1997). *J Biol Chem* 272, 2520-2526.
- Betz, A., Thakur, P., Junge, H.J., Ashery, U., Rhee, JS., Scheuss, V., Rosenmund, C., Rettig, J., and Brose, N. Functional interaction of the active zone proteins Munc13-1 and RIM1 in synaptic vesicle priming (2001). *Neuron* 30, 183-196.
- Bollmann, JH., Sakmann, B., and Borst, JG. Calcium sensitivity of glutamate release in a calyx-type terminal (2000). *Science* 289, 953-957.
- Brenner, S. The genetics of *Caenorhabditis elegans* (1974). *Genetics* 77, 71-94.
- Broadie, K., Prokop, A., Bellen, HJ., O'Kane, CJ., Schulze, KL., and Sweeney, ST. Syntaxin and synaptobrevin function downstream of vesicle docking in *Drosophila* (1995). *Neuron* 15, 663-73.

- Brose, N. For better or for worse: Complexins regulates SNARE function and vesicle fusion (2008). *Traffic* 9, 1403-1413.
- Brose, N., Hofmann, K., Hata, Y., and Südhof, T.C. Mammalian homologues of *Caenorhabditis elegans* unc-13 gene define novel family of C2-domain proteins (1995). *J Biol Chem* 270, 25273-25280.
- Brose, N., Petrenko, AG., Südhof, TC., and Jahn, R. Synaptotamin: a calcium sensor on the synaptic vesicle surface (1992). *Science* 256, 1021-1025.
- Brose, N., Rosenmund, C., and Rettig, J. Regulation of transmitter release by Unc-13 and its homologues (2000). *Curr Opin Neurobiol* 10, 303-311.
- Burgoyne, RD., and Morgan, A. Secretory granule exocytosis (2003). *Physiol Rev* 83, 581-632.
- Carmichael, SW., and Winkler, H. The adrenal chromaffin cell (1985). *Scientific American* 253, 40-49.
- Cases-Langhoff, C., Voss, B., Garner, AM., Appeltau, U., Takei, K., Kindler, S., Veh, RW., De Camilli, P., Gundelfinger, ED., and Garner, CC. Piccolo, a novel 420 kDa protein associated with the presynaptic cytomatrix (1996). *Eur J Cell Biol* 69, 214-223.
- Chan, AM., and Weber, T. A putative link between exocytosis and tumor development (2002). *Cancer Cell* 2, 427-8.
- Chapman, ER., Hanson, PI., An, S., and Jahn, R. Ca^{2+} regulates the interaction between synaptotagmin and syntaxin 1 (1995). *J Biol Chem* 270, 23667-23671.
- Constable, JRL., Graham, ME., Morgan, A., and Burgoyne, RD. Amisyn regulates exocytosis and fusion pore stability by both syntaxin-dependent and syntaxin-independent mechanisms (2005). *J Biol Chem* 280, 31615-31623.

- Craxton, M. Synaptotamin gene content of the sequenced genomes (2004). *BMC Genomics* 5, 43.
- Dai, H., Tomchick, DR., García, J., Südhof, TC., Machius, M., and Rizo, J. Crystal structure of the RIM2 C2A-domain at 1.4 Å resolution (2005). *Biochemistry* 44, 13533-13542.
- de Wit, H., Cornelisse, LN., Toonen, RF., and Verhage, M. Docking of secretory vesicles is syntaxin dependent (2006). *PLoS ONE* 27, e126.
- Dietrich, D., Kirschstein, T., Kukley, M., Pereverzec, A., von der Brelie, C., Schneider, T., and Beck, H. Functional specialization of presynaptic Cav2.3 Ca²⁺ channels (2003). *Neuron* 39, 483-496.
- Dikeakos, JD., and Reudelhuber, TL. Sending proteins to dense core secretory granules: still a lot to sort out (2007). *J Cell Biol* 177, 191-196.
- Elhamdani, A., Martin, TF., Kowalchuk, JA., and Artalejo, CR. Ca²⁺-dependent activator protein for secretion is critical for the fusion of dense-core vesicles with the membrane in calf adrenal chromaffin cells (1999). *J Neurosci* 19, 7375-83.
- Feldmann, J., Callebaut, I., Raposo, G., Certain, S., Bacq, D., Dumont, C., Lambert, N., Chardin, M.O., Chedeville, G., Tamary, H., Minard-Colin, V., Vilmer, E., Blanche, S., Le Deist, F., Fisher, A., and de Saint Basile, G. Munc13-4 is essential for cytolytic granules fusion and is mutated in a form of familial hemophagocytic lymphohistiocytosis (FHL3) (2003). *Cell* 115, 461-473.
- Fujita, Y., Shirataki, H., Sakisaka, T., Asakura, T., Ohya, T., Kotani, H., Yokoyama, S., Nishioka, H., Matsuura, Y., Mizoguchi, A., Scheller, RH., and Takai, Y. Tomosyn: a syntaxin-1-binding protein that forms a novel complex in the neurotransmitter release process (1998). *Neuron* 20, 905-915.
- Gillis, KD., Mossner, R., and Neher, E. Protein kinase C enhances exocytosis from chromaffin cells by increasing the size of the readily releasable pool of secretory

granules (1996). *Neuron* 16, 1209-20.

Gracheva, EO., Burdina, AO., Holgado, AM., Berthelot-Grosjean, M., Ackley, BD., Hadwiger, G., Nonet, ML., Weimer, RM., and Richmond, JE. Tomosyn inhibits synaptic vesicle priming in *C. elegans* (2006). *PLoS Biol* 4, 1426-1437.

Gracheva, EO., Burdina, AO., Touroutine, D., Berthelot-Grosjean, M., Parekh, H., and Richmond, JE. Tomosyn negatively regulates CAPS-dependent peptide release at *C.elegans* synapses (2007). *J Neurosci* 27, 10176-10184.

Grynkiewicz, G., Poenie, M., and Tsien, RY. A new generation of Ca^{2+} indicators with greatly improved fluorescence properties (1985). *J Biol Chem* 260, 3440-3450.

Groffen, AJ., Friedrich, R., Brian, EC., Ashery, U., and Verhage, M. DOC2A and DOC2B are sensors for neuronal activity with unique calcium-dependent and kinetic properties (2006). *J Neurochem* 97, 818-33.

Guan, R., Dai, H., and Rizo, J. Binding of the Munc13-1 MUN domain to membrane-anchored SNARE complexes (2008). *Biochemistry* 47, 1474-1481.

Hammarlund, M., Palfreyman, MT., Watanabe, S., Olsen, S., and Jorgensen, EM. Open syntaxin docks synaptic vesicles (2007). *PLoS Biol* 5, 1695-1711.

Hammarlund, M., Watanabe, S., Schuske, K., and Jorgensen, EM. CAPS and syntaxin dock dense core vesicles to the plasma membrane in neurons (2008). *J Cell Biol* 180, 483-491.

Hayashi, T., Yamasaki, S., Nauenburg, S., Binz, T., and Niemann, H. Disassembly of the reconstituted synaptic vesicle membrane fusion complex in vitro (1995). *EMBO J* 14, 2317-2325.

Hosono, R., and Kamiya, Y. Additional genes which result in an elevation of acetylcholine levels by mutations in *Caenorhabditis elegans* (1991). *Neurosci Lett* 128, 243-244.

- Hunt, JM., Bommert, K., Charlton, MP., Kistner, A., Habermann, E., Augustine, GJ., and Betz, H. A post-docking role for synaptobrevin in synaptic vesicle fusion (1994). *Neuron* 12, 1269-1279.
- Itakura, M., Misawa, H., Sekiguchi, M., Takahashi, S., and Takahashi, M. Transfection analysis of functional roles of complexin I and II in the exocytosis of two different types of secretory vesicles (1999). *Biochem Biophys Res Commun* 265, 691-696.
- Jahn, R., Lang, T., and Südhof, TC. Membrane fusion (2003). *Cell* 112, 519-33.
- Jahn, R., and Scheller, RH. SNAREs-engines for membrane fusion (2006). *Nat Rev Mol Cell Biol* 7, 631-643.
- Jockusch, WJ., Speidel, D., Sigler, A., Sørensen, JB., Varoqueaux, F., Rhee, JS., and Brose, N. CAPS-1 and CAPS-2 are essential synaptic vesicle priming proteins (2007). *Cell* 131, 796-808.
- Junge, H.J., Rhee, J.S., Jahn, O., Varoqueaux, F., Spiess, J., Waxham, M.N., Rosenmund, C., and Brose, N. Calmodulin and Munc13 form a Ca^{2+} sensor/effector complex that controls short-term synaptic plasticity (2004). *Cell* 118, 389-401.
- Kee, Y., and Scheller, RH. Localization of synaptotagmin-binding domains on syntaxin. *J Neurosci* 16, 1975-1981.
- Kim, TY., Gondre-Lewis, MC., Arnaoutova, I., and Loh, YP. Dense-core secretory granule biogenesis (2006). *Physiology* 21, 124-133.
- Koch, H., Hofmann, K., and Brose, N. Definition of Munc13-homology-domains and characterization of a novel ubiquitously expressed Munc13 isoform (2000). *Biochem J* 349, 247-253.
- Krasnoperov, VG., Bittner, MA., Beavis, R., Kuang, Y., Salnikow, KV., Chepurny, OG., Little, AR., Plotnikov, AN., Wu, D., Holz, RW., and Petrenko, AG. α -Latrotoxin

- stimulates exocytosis by the interaction with a neuronal G-protein-coupled receptor (1997). *Neuron* 18, 925-937.
- Lelianova, VG., Davletov, BA., Sterling, A., Rahman, MA., Grishin, EV., Totty, NF., and Ushkayov, YA. α -Latrotoxin receptor, latrophilin, is a novel member of the secretion family of G-protein-coupled receptors (1997). *J Biol Chem* 272, 21504-21508.
- Li, C., Ullrich, B., Zhang, JZ., Anderson, RG., Brose, N., and Südhof, TC. Ca^{2+} dependent and independent activities of neuronal and non-neuronal synaptotagmins (1995). *Nature* 375, 594-599.
- Liu, Y., Schirra, C., Stevens, DR., Matti, U., Speidel, D., Hof, D., Bruns, D., Brose, N., and Rettig, J. CAPS facilitates filling of the rapidly releasable pool of large dense core vesicles (2008). *J Neurosci* 28, 5594-5601.
- Lu, J., Machius, M., Dulubova, I., Dai, H., Südhof, TC., Tomchick, DR., and Rizo, J. Structural basis for a Munc13-1 homodimer to Munc13-1/RIM heterodimer switch (2006). *PLoS Biol* 4, e192.
- Martin, TFJ. The molecular machinery for fast and slow neurosecretion (1994). *Curr Opin Neurobiol* 4, 626-632.
- McEwen, JM., Madison, JM., Dybbs, M., and Kaplan, JM. Antagonistic regulation of synaptic vesicle priming by Tomosyn and UNC-13 (2006). *Neuron* 51, 303-315.
- Neeft, M., Wieffer, M., de Jong, AS., Negroju, G., Metz, CHG., van Loon, A., Griffith, J., Krijgsveld, J., Wulffraat, N., Koch, H., Heck, A., Brose, N., Kleijmeer, M., and van der Sluijs, P. Munc13-4 is an effector of Rab27a and controls secretion of lysosomes in hematopoietic cells (2005). *Mol Biol Cell* 16, 731-741.
- Neher, E. A comparison between exocytotic control mechanisms in adrenal chromaffin cells and a glutamatergic synapse (2006). *Pflugers Arch* 453, 261-268.

- Nonet, ML., Saifee, O., Zzhao, H., Rand, JB., and Wie, L. Synaptic transmission deficits in *C.elegans* synaptobrevin mutants (1998). *J Neurosci* 18, 70-80.
- Olofsson, CS., Gopel, SO., Barg, S., Galvanovski, J., Ma, X., Salehi, A., Rorsman, P., and Eliasson, L., Fast insulin secretion reflects exocytosis of docked granules in mouse pancreatic β -cells (2002). *Pflugers Arch* 444, 43-51.
- Palmer, R., Lee, S.B., Wong, J.C., Reynolds, P.A., Zhang, H., Truong, V., Oliner, J.D., Gerald, W.L., and Haber, D.A. Induction of BAIAP3 by the EWS-WT1 chimeric fusion implicates regulated exocytosis in tumorigenesis (2002). *Cancer Cell* 2, 497-505.
- Parsons, TD., Coorssen, JR., Horstmann, H., and Almers, W. Docked granules, the exocytotic burst, and the need for ATP hydrolysis in endocrine cells (1995). *Neuron* 15, 1085-1096.
- Pobbati, AV., Razeto, A., Böddener, M., Becker, S., Fasshauer, D. Structural basis for the inhibitory role of tomosyn in exocytosis (2004). *J Biol Chem* 279, 47192-47200.
- Reim, K., Mansour, M., Varoqueaux, F., McMahon, HT., Südhof, TC., Brose, N., and Rosenmund, C. Complexins regulate a late step in Ca^{2+} -dependent neurotransmitter release (2001). *Cell* 104, 71-81.
- Rhee, J.S., Betz, A., Pyott, S., Reim, K., Varoqueaux, F., Augustin, I., Hesse, D., Südhof, T.C., Takahashi, M., Rosenmund, C., and Brose, N. β -phorbol ester- and diacylglycerol-induced augmentation of transmitter release is mediated by Munc13s and not by PKCs (2002). *Cell* 108, 121-133.
- Richmond, JE., Davis, WS., and Jorgensen, EM. UNC-13 is required for synaptic vesicle fusion in *C.elegans* (1999). *Nat Neurosci* 2, 959-964.
- Richmond, JE., Weimer, RM., and Jorgensen, EM. An open form of syntaxin bypasses the requirement for UNC-13 in vesicle priming (2001). *Nature* 412, 338-41.

- Rickman, C., and Davletov, B. Mechanisms of calcium-independent synaptotagmin binding to target SNAREs (2003). *J Biol Chem* 278, 5501-5504.
- Rizo, J., Rosenmund, C. Synaptic vesicle fusion (2008). *Nat Struct Mol Biol* 15, 665-74.
- Rupnik, M., Kreft, M., Sikdar, SK., Grile, S., Romih, R., Zupancic, G., Martin, TF., and Zorec, R. Rapid regulated dense-core vesicle exocytosis requires the CAPS protein (2000). *Proc Natl Acad Sci U S A* 97, 5627-32.
- Rutter GA, Hill EV. Insulin vesicle release: walk, kiss, pause ... then run (2006). *Physiology (Bethesda)* 21, 189-96.
- Sadakata T., Kakegawa, W., Mizoguchi, A., Washida, M., Katoh-Semba, R., Shutoh, F., Okamoto, T., Nakashima, H., Kimura, K., Tanaka, M., Sekine, Y., Itohara, S., Yuzaki, M., Nagao, S., and Furuichi, T. Impaired cerebellar development and function in mice lacking CAPS2, a protein involved in neurotrophin release (2007). *J Neurosci* 27, 2472-2482.
- Sadakata, T., Mizoguchi, A., Sato, Y., Katoh-Semba, R., Fukuda, M., Mikoshiba, K., and Furuichi, T. The secretory granule-associated protein CAPS2 regulates neurotrophin release and cell survival (2004). *J Neurosci* 24, 43-52.
- Scales, SJ., Hesser, BA., Masuda, ES., and Scheller, RH. Amisyn, a novel syntaxin-binding protein that may regulate SNARE complex assembly (2002). *J Biol Chem* 277, 28271-28279.
- Schneggenburger, R., and Neher, E. Presynaptic calcium and control of vesicle fusion (2005). *Curr Opin Neurobiol* 15, 266-74.
- Schoch, S., Castillo PE., Jo, T., Mukherjee, K., Geppert, M., Wang, Y., Schmitz, F., Malenka, RC., and Südhof, TC. RIM 1 α forms a protein scaffold for regulating neurotransmitter release at the active zone (2002). *Nature* 415, 321-326.

- Schoch, S., Deak, F., Königstorfer, A., Mozhayeva, M., Sara, Y., Südhof, TC., and Kavalali, ET. SNARE function analyzed in synaptobrevin/VAMP knockout mice (2001). *Science* 294, 1117-1122.
- Schulze, KL., Broadie, K., Perin, MS., and Bellen, HJ. Genetic and electrophysiological studies of *Drosophila* syntaxin-1A demonstrate its role in nonneuronal secretion and neurotransmission (1995). *Cell* 80, 311-320.
- Serra-Pages, C., Medley, QG., Tang, M., Hart, A., and Streuli, M. Liprins, a family LAR transmembrane protein-tyrosine phosphatase-interacting proteins (1998). *J Biol Chem* 273, 15611-15620.
- Shiratsuchi, T., Oda, K., Nishimori, H., Suzuki, M., Takahashi, E., Tokino, T., and Nakamura, Y. Cloning and Characterization of Baiap3 (BAI-Associated Protein 3), a C2 domain-containing protein that interacts with BAI1 (1998). *Biochem Biophys Res Commun* 251, 158-165.
- Söllner, T., Whiteheart, SW., Brunner, W., Erdjument-Bromage, N., Geromanos, S., Tempst, P., and Rothman, JE. SNAP receptors implicated in vesicle targeting and fusion (1993). *Nature* 362, 318-324.
- Sørensen, JB., Nagy, G., Varoqueaux, F., Nehring, RB., Brose, N., Wilson, MC., and Neher, E. Differential control of the releasable vesicle pools by SNAP-25 splice variants and SNAP-23 (2003). *Cell* 114, 75-86.
- Speese, S., Petrie, M., Schuske, Kim., Ailion, M., Ann, K., Iwasaki, K., Jorgensen, EM., and Martin, TFJ. UNC-31 (CAPS) is required for dense core vesicle but not synaptic vesicle exocytosis in *C. elegans* (2007). *J Neurosci* 27, 6150-6162.
- Stevens, DR., Wu, ZX., Matti, U., Junge, H.J., Schirra, C., Becherer, U., Wojcik, S.M., Brose, N., and Rettig, J. Identification of the Minimal Protein Domain Required for Priming Activity of Munc13-1 (2005). *Curr Biol* 15, 1-6.

- Südhof, TC. The Synaptic Vesicle Cycle: a cascade of protein-protein interactions (1995). *Nature* 375, 645-653.
- Südhof, TC. The Synaptic Vesicle Cycle (2004). *Annu Rev Neurosci* 27, 509-547.
- Tandon, A., Bannykh, S., Kowalchuk, JA., Banerjee, A., Martin, TF., and Balch, WE. Differential regulation of exocytosis by calcium and CAPS in semi-intact synaptosomes (1998). *Neuron* 21, 147-54.
- tom Dieck, S., Sanmarti-Vila, L., Langnaese, K., Richter, K., Kindler, S., Soyke, A., Wex, H., Smalla, KH., Kämpf, U., Fränzer, JT., Stumm, M., Garner, CC., and Gundelfinger ED. Bassoon, a novel zinc-finger CAG/glutamine-repeat protein selectively localized at the active zone of presynaptic nerve terminals (1998). *J Cell Biol* 142, 499-509.
- Trifaro, JM. Molecular biology of the chromaffin cells (2002). *Ann N Y Acad Sci* 971, 11-18.
- Varoqueaux, F., Sigler, A., Rhee, JS., Brose, N., Enk, C., Reim, K., and Rosenmund, C. Total arrest of spontaneous and evoked synaptic transmission but normal synaptogenesis in the absence of Munc13-mediated vesicle priming (2002). *Proc Natl Acad Sci U S A* 99, 9037-9042.
- Varoqueaux, F., Sons, M.S., Plomp, J.J., and Brose, N. Aberrant Morphology and residual transmitter release at the Munc13-deficient mouse neuromuscular synapse (2005). *Mol Cell Biol* 25, 5973-5984.
- Verhage, M., Maia, AS., Plomp, JJ., Brussaard, AB., Heeroma, JH., Vermeer, H., Toonen, RF., Hammer, RE., van den Berg, TK., Missler, M. Synaptic assembly of the brain in the absence of neurotransmitter secretion (2000). *Science* 287, 864-869.
- Voets, T. Dissection of three Ca^{2+} - dependent steps leading to secretion in chromaffin cells from mouse adrenal slices (2000). *Neuron* 28, 537-545.

- Voets, T., Neher, E., and Moser, T. Mechanisms underlying phasic and sustained secretion in chromaffin cells from mouse adrenal slices (1999). *Neuron* 23, 607-615.
- Voets, T., Toonen, RF., Brian, EC., de Wit, H., Moser, T., Rettig, J., Südhof, TC., Neher, E., and Verhage, M. Munc18-1 promotes large dense-core vesicle docking (2001). *Neuron* 31, 581-591.
- Wang, Y., Liu, X., Biederer, T., and Südhof, TC. A family of RIM-binding proteins regulated by alternative splicing: implications for the genesis of synaptic active zones (2002). *Proc Natl Acad Sci U S A* 99, 14464-14469.
- Wang, Y., Okamoto, M., Schmitz, F., Hofman, K., and Südhof, TC. RIM: a putative Rab3-effector in regulating synaptic vesicle fusion (1997). *Nature* 388, 593-598.
- Wang, Y., Sugita, S., and Südhof, TC. The RIM/NIM family of neuronal C2 domain proteins. Interactions with Rab3 and a new class of Src homology 3 domain proteins (2000). *J Biol Chem* 275, 20033-20044.
- Washbourne, P., Thompson, PM., Carta, M., Costa, ET., Mathews, JR., Lopez-Bendito, G., Molnar, Z., Becher, MW., Valenzuela, CF., Partridge, LD., and Wilson, MC. Genetic ablation of the t-SNARE SNAP-25 distinguishes mechanisms of neuroexocytosis (2002). *Nat Neurosci* 5, 19-26.
- Weimer, RM., Richmond, JE., Davis, WS., Hadwiger, G., Nonet, ML., and Jorgensen, EM. Defects in synaptic vesicle docking in unc-18 mutants (2003). *Nat Neurosci.* 6, 1023-1030.
- Wojcik, SM., and Brose, N. Regulation of membrane fusion in synaptic excitation-secretion coupling: speed and accuracy matter (2007). *Neuron* 55, 11-24.
- Xu, T., Binz, T., Niemann, H., and Neher, E. Multiple kinetic components of exocytosis distinguished by neurotoxin sensitivity (1998). *Nature* 1, 192-200.

Yizhar, O., Matti, U., Melamed, R., Hagalili, Y., Bruns, D., Rettig, J., and Ashery, U. Tomosyn inhibits priming of large dense-core vesicles in a calcium-dependent manner (2004). *Proc Natl Acad Sci U S A* *101*, 2578-2583.

Zhou, KM., Dong, YM., Ge, Q., Zhu, Dan., Zhou, W., Lin, XG., Liang, T., Wu, ZX., and Xu, T. PKA activation bypasses the requirement for UNC-31 in the docking of dense core vesicles from *C.elegans* neurons (2007). *Neuron* *56*, 657-669.

Zikich, D., Meser, A., Varoqueaux, F., Sheinin, A., Junge, H.J., Nachliel, E., Melamed, R., Brose, N., Gutman, M., and Ashery, U. Vesicle priming and recruitment by ubMunc13-2 are differentially regulated by calcium and calmodulin (2008). *J Neurosci* *28*, 1949-1960.

Zucker RS. Exocytosis: A Molecular and Physiological Perspective (1996). *Neuron* *17*, 1049-1055.

6. Summary

Members of mammalian uncoordinated 13 protein family (Munc13s) are essential for SV exocytosis in neurons and have also been implicated in LDCV exocytosis in chromaffin cells. However, the *C.elegans* ortholog Unc-13 appears to be dispensable for LDCV exocytosis, raising the question whether SNARE-mediated exocytosis of SVs and LDCVs is controlled by distinct regulatory proteins. We therefore analyzed LDCV exocytosis in cultured chromaffin cells taken from knockout mouse lines of four members of the Munc13 protein family, Munc13-1, Munc13-2, Munc13-3 and Baiap3. Baiap3/Bap3 (brain specific angiogenesis inhibitor 1 associated protein 3), was identified and named as an interaction partner of BAI 1 (brain specific angiogenesis inhibitor-1), and is a Munc13 homologue of unknown function. Its closest known relative, the non-neuronal Munc13-4, has been shown to be essential for the secretion of lymphocyte cytolytic granule content. Unlike Munc13-4, Baiap3 expression is largely restricted to brain and adrenal gland, with low levels also present in lung. To determine whether LDCV exocytosis is impaired in the absence of Munc13-1, Munc13-2, Munc13-3 or Baiap3, we combined flash photolysis of caged Ca^{2+} and membrane capacitance measurements in cultured chromaffin cells. Our analysis of exocytosis in chromaffin cells shows that Munc13-1 and Munc13-2 act as positive regulators of LDCV exocytosis and play a more critical role in the release of this vesicle type than their *C.elegans* ortholog Unc-13. Based on sequence similarity, Baiap3 is a member of the Munc13 protein family. However, unlike Munc13-1, -2, -3 and -4, which function as essential positive regulators of SNARE-mediated exocytosis, our data indicate that Baiap3 negatively regulates exocytosis, at least in chromaffin cells. In this study, we found that exocytosis in chromaffin cells from Munc13-1 deficient mice and mice lacking both Munc13-1 and Munc13-2, showed a dramatic reduction in LDCV

exocytosis. In contrast to this, chromaffin cells deficient for Baiap3 showed increased exocytosis and Baiap3 overexpression in WT cells suppressed LDCV release. The exact molecular mechanism by which Munc13s regulate SNARE-mediated exocytosis remains to be elucidated. However, we found that Baiap3 interacted with both Munc13-1 and Syntaxin in co-sedimentation assays, which indicates that competition for binding to SNARE complex components is a possible explanation for the opposing functions of Munc13-1/2 and Baiap3 LDCV exocytosis.

Acknowledgments

I would like to express my appreciation to God for his guidance throughout my life and research. I would also like to thank many people who were willing to assist in all things (research and living, etc) during my Ph.D course. Although it's so difficult to express my gratitude to them in words, it's a way of showing my appreciation to them. Firstly, I am indebted to Dr. Sonja M. Wojcik, who is my perfect supervisor. When I started living abroad, she helped me greatly in organizing my residence in Germany and with the language, experiments, etc... Moreover, despite some failed experiments during my Ph.D. course, she always, through encouragement, patience, and motivation, led me back on course to a successful Ph.D. I'm really honored have met and worked with Prof. Dr. Nils Brose, who is also a perfect director. I am really indebted to Nils for giving me an opportunity to join as a member of his fantastic laboratory. I am grateful to Dr. Jeong-seop Rhee, who is a smart adviser. I often consulted with him about all things in Korean (life, research, etc...). He advised me about them based on his own know-how. Many thanks to all colleagues from Department of Molecular Neurobiology at the Max Planck Institute for Experimental Medicine for creating a pleasant work atmosphere. Especially, thanks to Dr. Wolf J. Jockusch for his technical support of physiological experiments and Dr. Benjamin Cooper, Dr. Andrea Betz, Dr. Andrea Burgalossi, Dr. Alexandros Pouloupoulos, Friederike Wolk and Ramya Nair for their support with official things and for interesting conversations. I would like to express my sincere gratitude to Prof. Dr. Ernst A. Wimmer, Prof. Dr. Ralf Heinrich, PD. Dr. Michael Hoppert, Prof. Dr. Dieter. Heineke, and Prof. Dr. Stefan Treue for agreeing to be in my thesis committee. I am grateful to the members of the Koreanische Ev. Kirchengemeinde in Goettingen, for making my life in Goettingen happy and enjoyable. I thank MinKyu Cho and Hai-Young Kim, who as friends and advisers, shared

problems, ambitions, the pleasures of life, science and each other. I am really grateful to my whole family; Parents (Shin, Bong-Rae and Kim, Chang-Soon), Parents in law (Kim, Tae-Kwon and Kang, Yun-Hee), Elder sisters (Shin, Eun-Hye and Shin, Eun-Hee), Brothers in law (Kim, Seung-Eon and Jung, Hak-Jae and Kim, Chi-Eon), Sisters in law (Kim, Mi-Kyung and Kim, Geum-Jung), Nieces (Kim, Hyeon-Gyeong and Kim, Do-Gyeong and Jung, Da-Yeon and Jung, Da-Vin), for their support and prayers towards the successful completion of my Ph.D course. Finally and importantly, I would like to express my gratitude to Kim, EunJung, who is my lovely wife, for her encouragement and assistance during our life abroad and in science. Moreover, she always takes care of our beloved daughter, Shin, ChaeWon, so I could concentrate on my research during the Ph. D course.

About the Author

Personal Data

Name: Yong Shin
Birth: 01.02.1977 in Seoul
Nationality: Republic of Korea
Marital Status: Married, one daughter

Education

03/83-02/89 Kwan-ack Elementary School, Korea
03/89-02/92 Bong-Lim Middle school, Korea
03/92-02/95 Young Nak high school, Korea
03/95-02/02 Korea University (Bachelor Degree), Korea
03/03-02/05 Seoul National University (Master Degree), Korea
03/05-11/08 Georg-August-Universität (Biology), Germany

Research

09/01-02/05 National Cancer Center, Korea
(Center for Colorectal Cancer)
03/05- 11/08 Pre-doctoral training at Max Planck Institute for
Experimental Medicine, Göttingen, Germany
(Prof. Dr. Nils Brose's Laboratory)

List of Publications

Shin Y, Rhee JS, Augustin I, Jockusch WJ, Brose N, and Wojcik SM. Large dense core vesicle exocytosis in mouse chromaffin cells is regulated by Munc13s and Baiap3. In Preparation.

Lim SB, Jeong SY, Kim IJ, Kim DY, Jung KH, Chang HJ, Choi HS, Sohn DK, Kang HC, Shin Y, Jang SG, Park JH and Park JG. Analysis of microsatellite instability in stool DNA of patients with colorectal cancer using denaturing high performance liquid chromatography (2006). *World. J. Gastroenterol* 12, 6689-92.

Kang HC, Kim IJ, Park JH, Shin Y, Jang SG, An SA, Park HW, Lim SB, Oh SK, Kim DJ, Lee KW, Choi YJ, Park YJ, Lee MR, Kim DW and Park JG. Three novel VHL germline mutations in Korean patients with von Hippel-Lindau disease and pheochromocytomas (2005). *Oncol Rep.* 14, 879-883.

Kim DW, Kim IJ, Kang HC, Park HW, Shin Y, Park JH, Jang SG, Yoo BC, Lee MR, Hong CW, Park KJ, Oh NG, Kim NK, Sung MK, Lee BW, Kim YJ, Lee HS and Park JG. Mutation Spectrum of the APC gene in 83 Korean FAP Families (2005). *Hum Mutation* 26, 281-286.

Kim IJ, Kang HC, Shin Y, Yoo BC, Yang HK and Park JG. Familial gastric cancers with Li-Fraumeni syndrome: A case repast (2005). *World J. Gastroenterol* 14, 4124-4126.

Kim IJ, Ku JL, Kang HC, Park JH, Yoon KA, Shin Y, Park HW, Jang SG, Lim SK, Han SY, Shin YK, Lee MR, Jeong SY, Shin HR, Lee JS, Kim WH and Park JG. Mutational analysis of OGG1, MYH, MTH1 In FAP, HNPCC and sporadic colorectal cancer patients: R154H OGG1 polymorphism is associated with colorectal cancer patients (2004). *Hum Genet* 115, 498-503.

Kim IJ, Kang HC, Shin Y, Park HW, Jang SG, Han SY, Lim SK, Lee MR, Chang HJ, Ku JL, Yang HK and Park JG. A TP53-truncating germline mutation (E287X) in a family with characteristics of both Hereditary diffuse gastric cancer and Li-Fraumeni

syndrome (2004). *J Hum Genet* 49, 591-595.

Shin Y, Kim IJ, Kang HC, Park JH, Park HW, Jang SG, Lee MR, Chang HJ, Jeong SY, Ku JL and Park JG. A functional polymorphism -347G/GA of *E-cadherin* gene is associated with colorectal cancer (2004). *Carcinogenesis* 25, 2173-2176.

Shin Y, Kim IJ, Kang HC, Park JH, Park HR, Park HW, Park MA, Lee JS, Yoon KA, Ku JL and Park JG. The *E-cadherin* -347G/GA promoter polymorphism and its effect on transcriptional regulation (2004). *Carcinogenesis* 25, 895-899.

Park JH, Kim IJ, Kang HC, Shin Y, Park HW, Jang SG, Ku JL, Lim SB, Jeong SY and Park JG. Oligonucleotide microarray-based mutation detection of the K-ras gene in colorectal cancers using Competitive DNA Hybridization (CDH) (2004). *Clinical Chemistry* 50, 1688-91.

Kang HC, Kim IJ, Park JH, Shin Y, Park HW, Ku JL, Yang HK, Lee KU, Choe KJ and Park JG. Promoter hypermethylation and silencing of CHFR mitotic stress checkpoint gene in human gastric cancers (2004). *Oncology Reports* 12, 129-133.

Kang HC, Kim IJ, Park JH, Shin Y, Jung MS, Yoo BC, Kim HK and Park JG. Differentially expressed genes in acquired drug-resistant gastric cancer cells by oligonucleotide microarrays (2004). *Clinical Cancer Research* 10, 272-284.

Kim IJ, Shin Y, Kang HC, Park JH, Ku JL, Park HW, Park HR, Lim SB, Jeong SY, Kim WH and Park JG. Robust microsatellite instability (MSI) analysis by denaturing high-performance liquid chromatography (DHPLC) (2003). *J Hum Genet* 48, 525-530.

Kim IJ, Park JH, Kang HC, Shin Y, Park HW, Park HR, Ku JL, Lim SB and Park JG. Mutational analysis of BRAF and K-ras in gastric cancers: absence of BRAF mutations in gastric cancers (2003). *Hum Genet* 114, 118-120.

Kim IJ, Park JH, Kang HC, Shin Y, Lim SB, Ku JL, Yang HK, Lee KU and Park JG. A novel germline mutation in the MET extracellular domain in a Korean patient with the diffuse type of familial gastric cancer (2003). *J Med Genet* 40, e97.

Kim IJ, Kang HC, Park JH, Shin Y, Ku JL, Lim SB, Park SY, Jung SY., Kim HK and Park JG. Development and applications of a β -catenin oligonucleotide microarray: β -catenin mutations are dominantly found in the proximal colon cancers with microsatellite instability (2003). Clin. Cancer Res 9, 2920-2925.

Park JH, Kim IJ, Kang HC, Lee SH, Shin Y, Kim KH, Lim SB, Kang SB, Lee KU, Kim SY, Lee MS, Lee MK, Park JH, Moon SD and Park JG. Germline mutations of the *MEN1* gene in Korean families with multiple endocrine neoplasia type 1 (MEN1) or MEN1-related disorders (2003). Clin Genet 64, 48-53.

Kang HC, Kim IJ, Park JH, Kwon HJ, Won YJ, Heo SC, Lee SY, Kim KH, Shin Y, Noh DY, Yang DH, Choe KJ, Lee BH, King SB and Park JG. Germline mutations of BRCA1 and BRCA2 in Korean breast and/or ovarian cancer families (2002). Hum Mutat 64, 48-53.

